N76-19400

REPORT NO. FAA–RD–76-11
TM X–64988

PROPERTY OF U.S. AIR FORCE
AEDC TECHNICAL LIBRARY
ARNOLD AFB, TN 37389

540500-75-C-0001

LASER DOPPLER VELOCIMETER WAKE VORTEX TESTS

March 1976

FINAL REPORT

Prepared for

NATIONAL AERONAUTICS AND
SPACE ADMINISTRATION
GEORGE C. MARSHALL SPACE FLIGHT CENTER
Marshall Space Flight Center, Alabama 35812

U.S. DEPARTMENT OF TRANSPORTATION
FEDERAL AVIATION ADMINISTRATION
Systems Research & Development Service
Washington, D.C. 20590

NOTICE

Because of the Federal Aviation Administration's preference, the English units of measurements are used as the primary units throughout the body of this report, followed by the corresponding metric units in parentheses. Conversion factors are given on appropriate figures and tables.

EDITOR'S NOTE

Use of trade names or names of manufacturers in this report does not constitute an official endorsement of such products or manufacturers, either expressed or implied, by the National Aeronautics and Space Administration or any other agnecy of the United States Government.

TECHNICAL REPORT STANDARD TITLE PAGE

1. REPORT NO.	2. GOVERNMENT ACCESSION NO.	3. RECIPIENT'S CATALOG NO.
NASA TM X-64988		

4 TITLE AND SUBTITLE	5. REPORT DATE
Laser Doppler Velocimeter Wake Vortex Tests	March 1976
	6. PERFORMING ORGANIZATION CODE

7. AUTHOR(S)	8. PERFORMING ORGANIZATION REPORT #
J. W. Bilbro, H. B. Jeffreys, E. A. Weaver, R. M. Huffaker, G. D. Craig, R. W. George, and P. J. Marrero	

9. PERFORMING ORGANIZATION NAME AND ADDRESS	10. WORK UNIT, NO.
George C. Marshall Space Flight Center Marshall Space Flight Center, Alabama 35812	11. CONTRACT OR GRANT NO.

12. SPONSORING AGENCY NAME AND ADDRESS		13. TYPE OF REPORT & PERIOD COVERED
National Aeronautics and Space Administration Washington, D.C. 20546	U.S. Department of Transportation Federal Aviation Administration Washington, D.C. 20590	Final Report Technical Memorandum
		14. SPONSORING AGENCY CODE

15. SUPPLEMENTARY NOTES

Prepared by Electronics and Control Laboratory, Science and Engineering

16. ABSTRACT

A Scanning Laser Doppler Velocimeter (SLDV) has been developed by the Marshall Space Flight Center (MSFC) under a program sponsored jointly by the National Aeronautics and Space Administration (NASA) and the Federal Aviation Administration (FAA). The SLDV was installed at John F. Kennedy (JFK) International Airport as part of the FAA's Wake Vortex Avoidance System (WVAS) and was operated for six months collecting data on vortices gengerated by landing aircraft. This report contains a description of the SLDV system, a summary of the JFK test operations, an analysis of selected portions of the data, and recommendations for improvements to the SLDV. The vortex information, including track and velocity data, on over 1600 aircraft landings is contained in the appendices of this report.

1. Airplanes -- Vortices
2. Vortices -- Measurement
5. Velocimeters

17. KEY WORDS	18. DISTRIBUTION STATEMENT
	James W. Bilbro Unclassified — Unlimited

19. SECURITY CLASSIF. (of this report)	20. SECURITY CLASSIF. (of this page)	21. NO. OF PAGES	22. PRICE
Unclassified	Unclassified	152	NTIS

For sale by National Technical Information Service, Springfield, Virginia 22151

PREFACE

The Scanning Laser Doppler Velocimeter is an optical radar system which represents the first practical application of the laser Doppler technology in other than an experimental environment. The information presented here, and in the major references, provides a detailed report on the design, development, and operation of the system as used in measuring the velocity and associated position of aircraft wake vortices. It was anticipated that the design and development of this system would require from 3 to 5 years. However, because of the urgent need for the vortex data, an accelerated program was initiated which resulted in the completion of the development phase in less than a year and a half. Following this development, data were collected at John F. Kennedy International Airport for 6 months. This collection of data together with the information obtained in the development phase represents the state-of the-art for laser Doppler technology. This technology can now be used to provide a unique operational and/or research tool for the scientific and industrial communities.

ACKNOWLEDGMENT

The Scanning Laser Doppler Velocimeter was the result of a program sponsored jointly by National Aeronautics and Space Administration (NASA) and the Federal Aviations Administration (FAA). A complex development and test program such as this requires the talent and effort of many people. While it is impossible to recognize every individual who contributed, the authors would like to identify those people that were directly responsible for its success.

Overall coordination of the program between agencies included Ken Hodge, Jack Enders, Bill McGowan, and Harry Verstynen of NASA, and Karl Bierach and Larry Taubenkibel of the FAA. The efforts of the Transportation Systems Center in support of the FAA were managed by Bill Wood who was assisted by Jim Hallock and Ed Spitzer.

The system design, analysis, integration, evaluation, and data handling were primarily in-house MSFC activities. The MSFC people contributing to this work were Dudley Belton, Herb Bush, Werner Dahm, Alan Dunkin, Andy Ellner, George Fichtl, Carl Hall, Clyde Jones, Ira Jones, Jack Jones, Gene McClard, Bill Murphree, Homer Powers, Joe Randall, Jim Reinbolt, Gray Settle, John Shirey, Joe Sloan, Wayne Wagnon, Terry West, Herb Wright, and Tom Yarbrough. They were assisted by Ron Fletcher, Barry Gregory, Bill Keenum, and Jerry Vickers from the Computer Science Corporation.

Lockheed's Huntsville Research and Engineering Center was responsible for the telescope, the servo scan controls, and the integration and system tests. This work was managed by T. R. Lawrence, Dave Wilson, and Mike Krause. Those contributing to this effort were Ed Coffee, Charles Craven, Bob Edwards, Ed Gorzinski, C. C. Huang, Jim Jetton, Nelson Logan, Larry Morrison, and Ken Shrider.

The graphics capability of the system was developed by M&S Computing Inc. This effort was led by Earle Easton and contributors were Ray Conway, Tom Dunn, Gary Matuck, Jim Roe, Judy Taylor, Bob Thurber, and A. Turner.

The system modeling concepts and portions of the conceptual design and data analysis techniques were provided by Physical Dynamics Inc.; Alex Thompson and Jim Meng were the contributors in this area.

The Raytheon Company was responsible for the laser, frequency translator, detector, interferometer, and signal processor developments. They were also responsible for part of the data analysis and algorithm design. This effort was under the direction of Sandy Campbell and Al Jelalian. Clark Harris, Wayne Keene, Chuck Sonnenschein, and John Zimmer assisted in the management of the project. Assisting in this work were Bill Bomberger, Bob Chandler, Dorothy Clippinger, Don Delgrego, Chuck DeMarzio, Ron Evett, Roger Goff, Bob Hamm, Tony Jagodnik, Derek Lentz, Chris Miller, Dick Schaaf, Dick Seavey, John Shabeck, and Ron VanderKruik.

The National Aviation Facilities Experiment center provided valuable assistance during the test period at John F. Kennedy Airport. The onsite management was provided by Roman Spangler and Nick Rasch. Considerable assistance, particularly in the initial installation was provided by Joe Walaconis.

The outstanding efforts of these people led to the successful deployment and operation of a highly complex system. It is with deep appreciation that these individuals are acknowledged.

TABLE OF CONTENTS

		Page
1.0	INTRODUCTION	1-1
	1.1 Wake Vortex Program	1-1
	1.2 SLDV Development	1-2
	1.3 NASA-FAA Interagency Agreement	1-5
2.0	SUMMARY	2-1
	2.1 Introduction	2-1
	2.2 System Description	2-1
	2.3 Data Processing Techniques	2-4
	2.4 Test Operation	2-4
	2.5 Data/System Analysis	2-4
	2.6 Recommendations	2-7
	2.7 Conclusions	2-7
3.0	SYSTEM DESCRIPTION	3-1
	3.1 Introduction	3-1
	3.2 System Operational Description	3-1
	3.3 Component Description	3-8
	3.3.1 Laser	3-8
	3.3.2 Interferometer	3-9
	3.3.3 Translator	3-10
	3.3.4 Telescope	3-11
	3.3.5 Detector	3-11
	3.3.6 Scanner	3-12
	3.3.7 Receiver Electronics	3-16
	3.3.8 Signal Processor	3-17
	3.3.9 Data Recording	3-21
	3.3.10 Data Algorithm Processor and Display System	3-22
4.0	DATA PROCESSING TECHNIQUES AND DATA DISPLAYS	4-1
	4.1 Introduction	4-1
	4.2 Onsite Data Processing and Display	4-1

TABLE OF CONTENTS (Continued)

		Page
	4.2.1 Real Time Data Processing and Displays	4-3
	4.2.2 Post Data Processing and Display Algorithms	4-7
	4.3 Offsite Data Processing and Displays	4-16
	4.3.1 High Speed Data Processing	4-20
	4.3.2 Low Speed Data Processing	4-28
5.0	TEST OPERATION	5-1
	5.1 Introduction	5-1
	5.2 Installation	5-1
	5.2.1 Test Site Description	5-1
	5.2.2 Site Preparations	5-1
	5.2.3 Instrument Van Transportation	5-4
	5.2.4 Optics/Electronics Transportation	5-4
	5.2.5 System Layout	5-4
	5.2.6 Safety	5-4
	5.2.7 System Support	5-9
	5.3 Calibration	5-9
	5.3.1 Component Calibration	5-9
	5.3.2 System Performance Calibration	5-10
	5.4 Operation	5-10
	5.5 Data Handling	5-11
	5.6 Test Summary	5-12
	5.7 Hardware Evaluation	5-12
	5.7.1 Laser	5-12
	5.7.2 Interferometer	5-14
	5.7.3 Telescope	5-14
	5.7.4 Detector	5-14
	5.7.5 Receiver	5-14
	5.7.6 Scanner	5-14
	5.7.7 Signal Processor	5-15
	5.7.8 Recorders	5-15
	5.7.9 Data Algorithm Processor	5-15
	5.7.10 Vans	5-15

TABLE OF CONTENTS (Continued)

		Page
6.0	DATA/SYSTEM ANALYSIS	6-1
	6.1 Phase I Airport Tests	6-1
	6.1.1 Hard Target Analysis	6-1
	6.1.2 Wind Measurements	6-3
	6.1.3 Vortex Transport Analysis	6-6
	6.1.4 Vortex Flow Fields	6-8
	6.1.5 Data Verification	6-14
	6.1.6 Thresholds and Algorithm Parameters	6-16
	6.2 Phase II Airport Tests	6-17
	6.2.1 High Speed Tape Analysis	6-17
	6.2.2 Statistical Analysis of Data	6-18
	6.2.3 High Altitude Flyby	6-37
7.0	RECOMMENDATIONS DIRECTED TOWARD MORE OPERATIONAL SLDV SYSTEMS	7-1
	7.1 Introduction	7-1
	7.2 Hardware Considerations	7-1
	7.2.1 Laser	7-1
	7.2.2 Optics	7-3
	7.2.3 Detector	7-4
	7.2.4 Scanner	7-4
	7.2.5 Signal Processor	7-5
	7.2.6 Data Reduction	7-5
	7.3 Software	7-6
8.0	CONCLUSION	8-1
9.0	REFERENCES	9-1
	DATA CROSS REFERENCE AND INDEX	APPENDIX A
	DATA LOG SHEETS	APPENDIX B
	B-707 DATA	APPENDIX C

TABLE OF CONTENTS (Concluded)

Page

B-727 DATA . . . . . APPENDIX D

B-747 DATA . . . . . APPENDIX E

DC-8 DATA . . . . . APPENDIX F

DC-9 DATA . . . . . APPENDIX G

DC-10 DATA . . . . . APPENDIX H

L10-11 DATA . . . . . APPENDIX J

B-737 AND MISCELLANEOUS AIRCRAFT DATA . . . . APPENDIX K

LIST OF ILLUSTRATIONS

Figure	Title	Page
1-1.	Smoke entrained vortex of a DC-3 aircraft	1-3
1-2.	Artists concept of SLDV airport testing	1-4
1-3.	Flow chart	1-7
1-4.	SLDV program time schedule	1-8
2-1.	Laser-Doppler principle	2-2
2-2.	System composite	2-3
2-3.	Aerial view of JFK Test Site	2-5
2-4.	SLDV scan plane	2-6
3-1.	SLDV overall block diagram	3-2
3-2.	Optical block diagram	3-3
3-3.	Laser Doppler line-of-sight velocity detection	3-5
3-4.	One-half power range resolution for a 12 in. (30.48 cm) CO_2 Laser optical heterodyne system as a function of range to target	3-7
3-5.	Scanner block diagram	3-13
3-6.	Signal processor block diagram	3-18
3-7.	Data/ algorithm processor block diagram	3-23
4-1.	VIDS flow chart	4-2
4-2.	Sample spectrum output	4-3
4-3.	Vortex location algorithm outline	4-5

LIST OF ILLUSTRATIONS (Continued)

Figure	Title	Page
4-4.	Sample time-based data plot	4-8
4-5.	Sample x, y data plot	4-9
4-6.	Sample tabular data output	4-10
4-7.	Sample calibration data output	4-11
4-8.	Sample V_{pk} scatter plot	4-13
4-9.	Sample I_{pk} scatter plot	4-14
4-10.	Sample DBUG output	4-15
4-11.	Sample wind profile plot	4-17
4-12.	Sample least-square-fit vortex transport plot	4-18
4-13.	High-speed data processing flow chart	4-19
4-14.	Sample cell output data tabulation	4-22
4-15.	Split gate method of determining angle turn-around	4-24
4-16.	Sample vortex flow-field plot	4-29
5-1.	Test site layout	5-2
5-2.	Instrument van pad and transformer	5-3
5-3.	Van installation	5-5
5-4.	Van layout	5-6
5-5.	System layout	5-7
5-6.	JFK test site	5-8

LIST OF ILLUSTRATIONS (Continued)

Figure	Title	Page
6-1.	Integrated intensities from a hard target as a function of range	6-4
6-2.	I_{pk} from the wind as a function of range	6-5
6-3.	Vortex time history	6-9
6-4.	V_{pk} versus θ for a B-707 vortex Day 310, Run 1029, scan 1 vortex 1 range = 100 ± 20 m	6-11
6-5.	Smallest detectable target size as a function of wind amplitude above threshold	6-12
6-6.	Interaction of vortex and wind vortex V_{max} = 100 ft/sec (30.48 m/s)	6-13
6-7.	Vortex circulation versus time	6-15
6-8.	Transport of near (x) and far (0) vortices	6-19
6-9.	Vortex circulation versus time	6-20
6-10.	Vortex time history; horizontal transport	6-21
6-11.	Vortex time history; vertical transport	6-22
6-12.	Vortex time history; circulation versus time	6-23
6-13.	Wind rose for runway 31R JFK Airport	6-24
6-14.	Aircraft mix on runway 31R — numbers in parentheses indicate total landings of each aircraft type	6-27
6-15.	Sample number of runs versus wind speed and direction all aircraft, both vans	6-29
6-16.	Aircraft mix	6-30

LIST OF ILLUSTRATIONS (Concluded)

Figure	Title	Page
6-17.	Average time of vortex tracks, B-707 and DC-8	6-31
6-18.	Average time of vortex tracks, B-727	6-32
6-19.	Average time of vortex tracks, B-747	6-33
6-20.	Sample data runs indicating data quality	6-35
6-21.	Average data quality versus wind speed and direction	6-36
6-22.	Average data quality versus aircraft type	6-38
6-23.	Percentage of runs producing usable data versus aircraft	6-39
6-24.	Descent rate versus wind speed and direction (all aircraft)	6-40
6-25.	Average vortex descent rate versus headwind	6-41
6-26.	Average vortex descent rate	6-43
6-27.	Intensity scatter plot for high altitude flyby	6-44

LIST OF TABLES

Table	Title	Page
3-1.	Characteristics of LDV Detectors	3-12
5-1.	Data Summary	5-13
6-1.	System Efficiency from Lab Measurements	6-2
6-2.	Signal to Noise Calculations	6-3
6-3.	Signal to Noise Calculations	6-7
6-4.	Signal to Noise Calculations	6-7
6-5.	Sensor Correlation	6-10
6-6.	Sensor Correlation	6-10
6-7.	Width Integration Test	6-16
6-8.	Default Parameters	6-17
6-9.	Number of Landings with Various Aircraft Types on Each Day of Test	6-26
6-10.	Data Statistics (Runway 31R, JFK Airport, Phase II)	6-28
6-11.	Subjective Evaluations	6-34
6-12.	Descent Rates of Various Vortices	6-42
7-1.	System Comparison	7-2

TECHNICAL MEMORANDUM X-64988

LASER DOPPLER VELOCIMETER WAKE VORTEX TESTS

1.0 INTRODUCTION

The Scanning Laser Doppler Velocimeter (SLDV) System was installed at John F. Kennedy (JFK) International Airport in September 1974. The SLDV, together with several other systems, was put into operation at JFK as part of the Federal Aviation Administration's (FAA) Wake Vortex Avoidance System (WVAS) test program. This report includes a summary description of the SLDV and covers the collection, processing, presentation, and analysis of data collected during the test operations at JFK Airport. The development of the SLDV for vortex applications is covered in FAA report FAA-RD-74-213 [1] dated March 1975. A brief discussion of the FAA vortex program and the program management for the SLDV development, testing, and the Interagency Agreement are presented in this section.

1.1 Wake Vortex Program

While wake vortices have been in existence since aircraft were first flown, the advent of the "jumbo jet," together with the increased traffic load at major airports, has resulted in the wake vortex becoming a significant safety hazard during landing and takeoff. At present this hazard is minimized by requiring increased separation between aircraft on landing and takeoff, thereby necessarily decreasing the capacity of the airport. This decreased capacity, in itself, becomes a problem due to the increased traffic load which is being placed on major airports. The FAA objective is to increase airport capacity by a factor of two by 1980 and a factor of five by 1995. This increase in capacity must in part come from a reduced separation between aircraft which can be accomplished only when the wake vortex problem is resolved.

Two solutions to this problem are being actively pursued by the FAA: the first being to reduce the hazard using techniques to quickly dissipate the vortices, and the second is to develop a WVAS. The WVAS would be capable of determining aircraft separation criteria based on aircraft type and airport

weather conditions far enough in advance to establish minimum safe landing and takeoff patterns. The avoidance system is based on the fact that (1) vortices often move quickly out of the flight path, (2) the important parameters of the vortices can be predicted, and (3) vortices can be detected and tracked with existing technology [2]. The National Aeronautics and Space Administration (NASA) is working with the FAA on the wake vortex problem by providing research measurements on vortex behavior, elimination, and their dissipation in addition to the development of the SLDV for the detection and tracking of vortices [3].

1.2 SLDV Development

In 1969, Marshall Space Flight Center (MSFC), at the request of NASA Headquarters, performed a series of tests at the Redstone Arsenal Airstrip which showed that a Laser Doppler System could be used successfully to detect aircraft wake vortices. For visual confirmation, smoke from a tower was injected into the vortex downstream from the laser system. An example of the DC-3 type vortex which was successfully detected is shown in Figure 1-1. Development of experimental Laser Doppler sensors for measuring atmospheric winds and turbulence continued after these initial detection tests. In 1972, FAA and NASA entered into discussions to determine what was required to upgrade the basic existing laser system capable of measuring three wind velocity components to a system that would be capable of detecting, tracking, and measuring the velocity structure of wake vortices. Once the requirements were determined, an interagency agreement was implemented between NASA and the FAA (Section 1.3). This agreement provided for the acceleration of research into the Laser Doppler Systems to develop a SLDV which would be deployed at JFK Airport for testing (Fig. 1-2). Three major objectives were established for this program:

a. The first and primary objective was to detect and track the vortices in the landing corridor and provide their positions with time, and to use the SLDV as a standard against which other vortex sensors could be compared.

b. The second objective was to evaluate the SLDV for use in an operational mode at airports.

c. The third objective was to measure the vortex velocity fields and their transport and decay characteristics.

The responsibility for implementing this agreement was given to MSFC.

Figure 1-1. Smoke entrained vortex of a DC-3 aircraft.

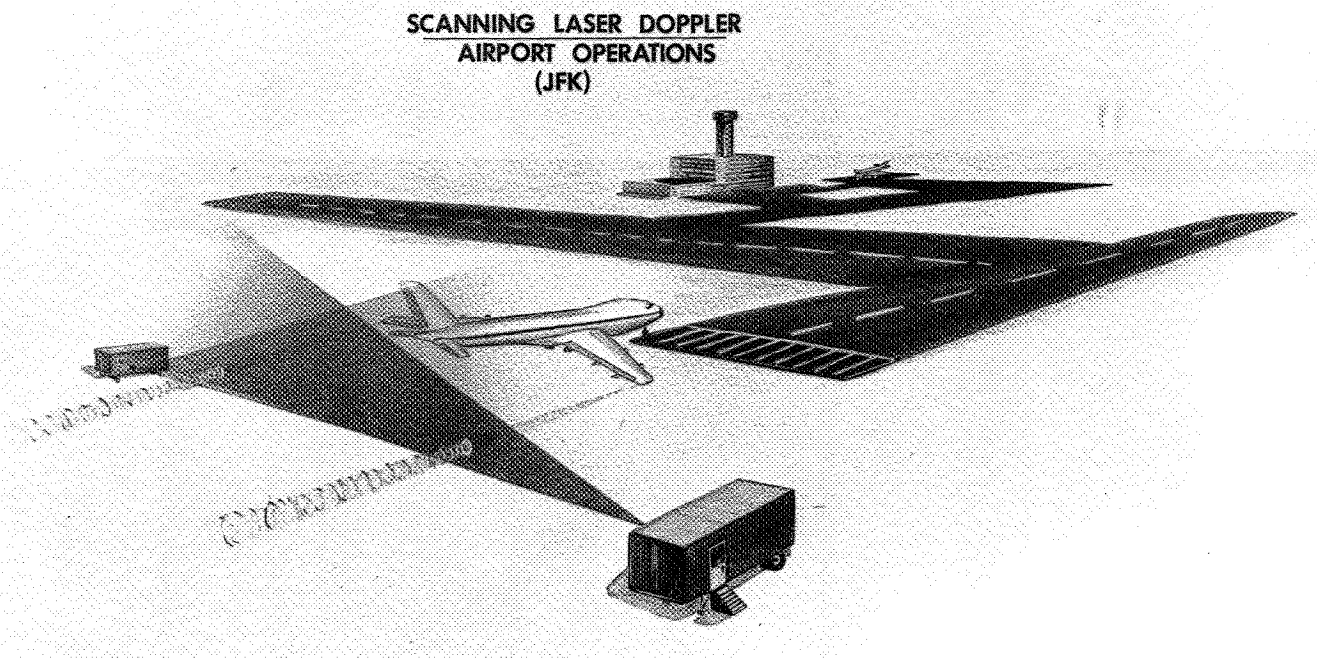

Figure 1-2. Artists concept of SLDV airport testing.

The SLDV program combined an in-house MSFC effort with the work of four companies: Lockheed Missiles and Space Company' s Huntsville Research and Engineering Center; M&S Computing, Inc., of Huntsville, Alabama; Physical Dynamics of Berkeley, California; and Raytheon Company' s Equipment Division at Sudbury, Massachusetts. When the interagency agreement was signed, program management responsibility was delegated to MSFC' s Aerophysics Division under the direction of Werner K. Dahm. A working team was established, consisting of personnel from the Aerophysics Division, the Instrumentation and Communications Division, and the Technology Division. In June 1974, this program was transferred to the Optical and RF Systems Division at MSFC directed by Dr. J. L. Randall. This reorganization brought the personnel who were primarily involved in the program into one group. At this time, the Simulation Division was asked to assist in providing the computer graphics capability necessary to meet the recently established vortex location goals.

The MSFC in-house effort was primarily concentrated on systems-related activities. This included engineering design, analysis, integration, test data handling, data program design, and site activation. Lockheed' s Huntsville Research and Engineering Center designed and built the telescope and the servo scan controls. This company was also responsible for system verification testing and the vortex data collection test program at JFK Airport. M&S Computing, Inc., provided the computer graphics hardware and software. Physical Dynamics, Inc., was responsible for system modeling concepts, part of the specific data analyses, and real-time algorithm design. The Raytheon Company was responsible for the hardware and software components of the program which included CO_2 lasers, signal processor, interferometer, receiver electronics, and data and systems analysis.

The development was initiated with contracts in April 1973 and was completed in September 1974. The system was then set up at the JFK Airport and used to measure and track vortices until June 1975. This concluded the primary data collection activity for FAA. The specific requirements for FAA are discussed later in this section.

1.3 NASA-FAA Interagency Agreement

An interagency agreement, DOT-FA73-WAI-373, between NASA and FAA was signed in March 1973 and called for the development of a Laser Doppler System to detect, track, and measure aircraft wake vortices. It

specified the development of a three-van experimental system that would operate in two modes: vortex tracking and three-dimensional line scanning. The three-dimensional mode was eliminated from the FAA requirements in December 1973 in favor of a two-van test at JFK Airport. The following 10 tasks were specified by the FAA for developing the SLDV system:

a. MSFC will perform the system engineering, including the model studies of the sensor and the atmosphere, and preliminary design to provide the real-time displays of the data essential to meet the vortex tracking objectives.

b. A delay-line-type signal processor will be developed for handling the Doppler data received by the sensor.

c. A real-time display for observing the vortices and their tracks will be developed using the data from the signal processor.

d. All the necessary hardware for a three-van system will be fabricated, assembled, integrated, and tested.

e. System test plans and procedures will be prepared.

f. Data reduction and evaluation programs will be developed.

g. Verification tests of the system performance, including aircraft flybys, will be performed.

h. The manuals necessary for operating the components, subsystems, and the system will be prepared.

i. A two-van system will be prepared for shipment.

j. A two-van system will be operated at JFK International Airport.

In addition to these tasks, in April 1974, the FAA established a real-time vortex location and tracking goal for the SLDV. This goal was ±10 ft (3 m) at a range of 500 ft (152 m) from the van.

A program flow chart for the development of the SLDV is shown in Figure 1-3. Included in the chart are computer simulation studies and data analysis program development. The simulation program was the tool that formed the basis for the data analysis efforts and it provided the initial programs required in the graphics capability. A time breakdown of the key program events is shown on the schedule in Figure 1-4.

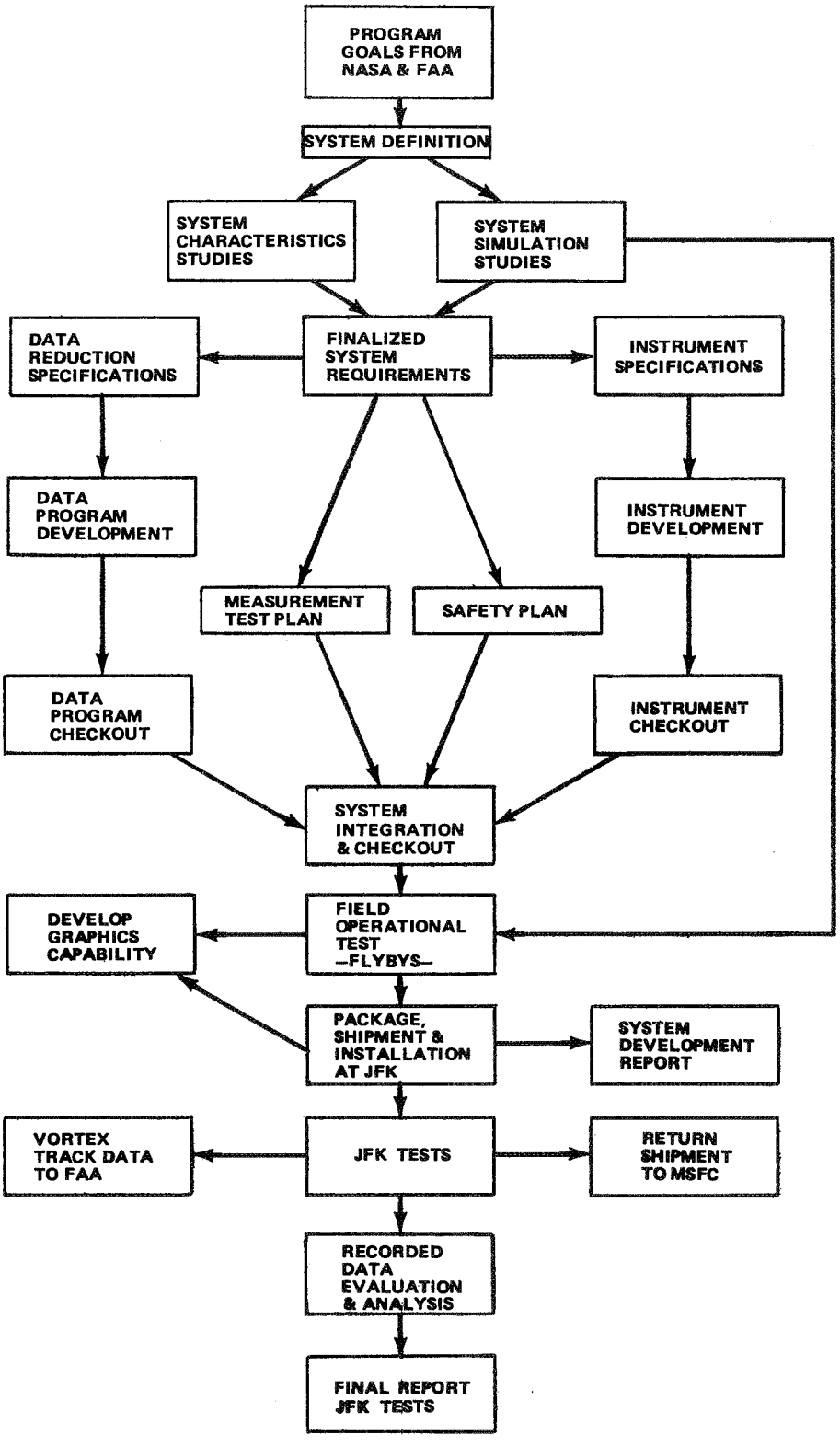

Figure 1-3. Flow chart.

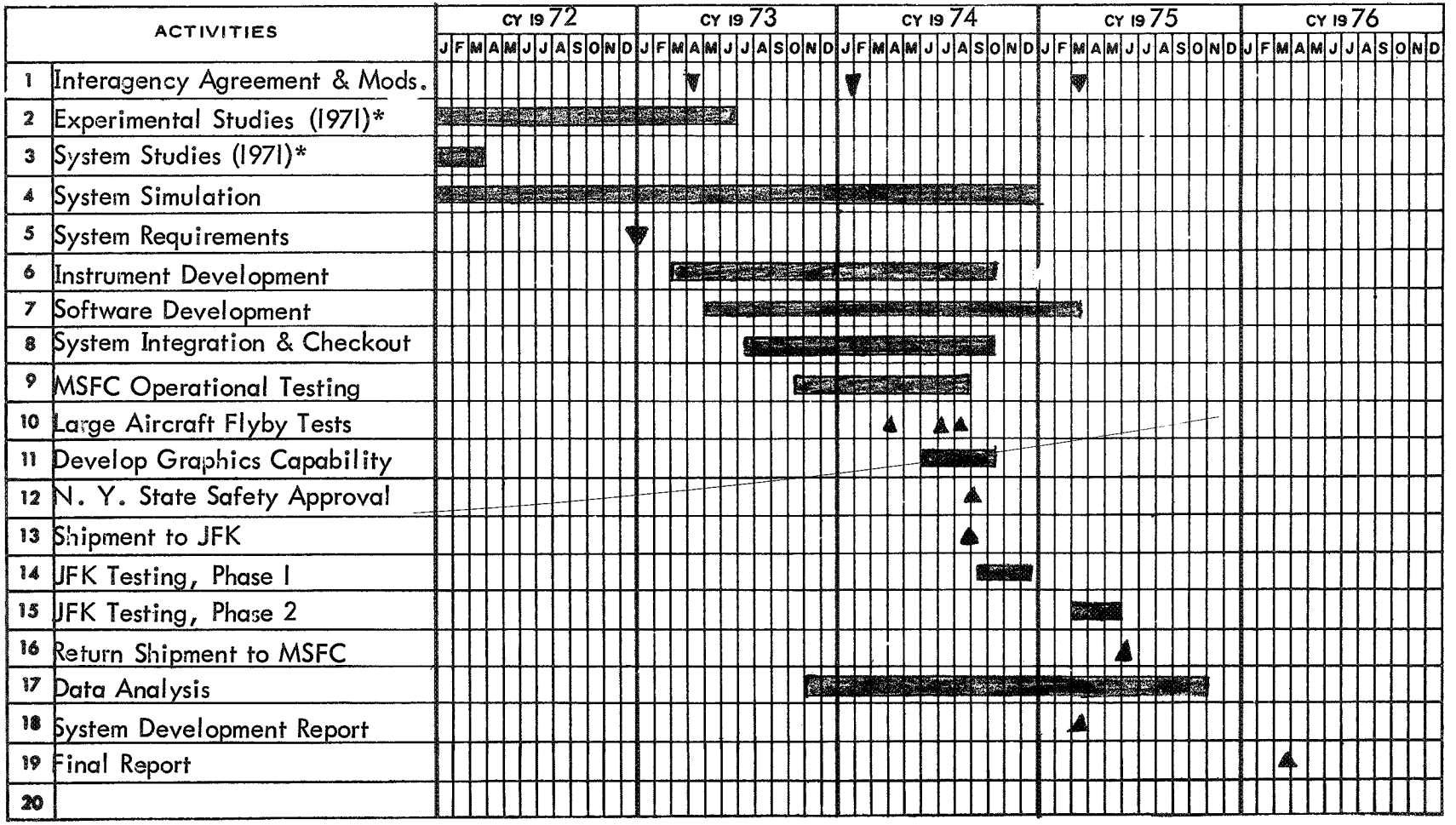
ACTIVITIES
CY 1972
CY 1973
CY 1974
CY 1975
CY 1976
J F M A M J J A S O N D J F M A M J J A S O N D J F M A M J J A S O N D J F M A M J J A S O N D J F M A M J J A S O N D
1 Interagency Agreement & Mods.
2 Experimental Studies (1971)*
3 System Studies (1971)*
4 System Simulation
5 System Requirements
6 Instrument Development
7 Software Development
8 System Integration & Checkout
9 MSFC Operational Testing
10 Large Aircraft Flyby Tests
11 Develop Graphics Capability
12 N. Y. State Safety Approval
13 Shipment to JFK
14 JFK Testing, Phase I
15 JFK Testing, Phase 2
16 Return Shipment to MSFC
17 Data Analysis
18 System Development Report
19 Final Report
20

* THIS WORK WAS STARTED IN 1971.

Figure 1-4. SLDV program time schedule.

2.0 SUMMARY

2.1 Introduction

MSFC has developed a SLDV which is capable of detecting, tracking, and measuring aircraft wake vortices. This system is the result of a MSFC prototype Laser Doppler System modified according to a 1973 NASA-FAA Interagency Agreement. This agreement was aimed at developing a breadboard system for use in testing at an operational airport.

The SLDV system was installed at JFK Airport in September 1974. It was involved in testing at the JFK Airport until December 1974 when it was placed in a standby condition. In March 1975, testing with the SLDV resumed and continued through June 1975, when the system was returned to MSFC. During these two test periods, vortex track data were collected on over 1600 aircraft landings. In addition, successful tests were performed using the SLDV to measure wind profiles at JFK Airport.

2.2 System Description

The principle of the SLDV is the same as conventional Doppler radars; the primary difference is in the wavelength. The wavelength of conventional radars is on the order of centimeters, whereas the SLDV laser wavelength is 10.6 μm. Conventional radar can detect scattering from large objects (tens of centimeters), and the SLDV can detect scattering from objects of 1μm in size (i.e., dust or pollen). As is shown in Figure 2-1, the laser beam from the SLDV is directed and focused optically at a given point in space. The aerosol particles scatter the transmitted radiation in all directions. Some of the radiation is back-scattered along the same optical path as the transmitted beam. This back-scattered radiation is collected by the receiving optics and is combined with a portion of the transmitted beam used as a local oscillator and imaged on an infrared detector. The back-scattered radiation has been Doppler shifted in frequency by the motion of the atmospheric particles and, as a result of this, the heterodyning of the back-scattered signal with the local oscillator signal by the detector results in an output signal which is proportional to the Doppler shift created by the particles and hence by the wind.

The SLDV system, shown in Figure 2-2, consists of a very stable, single frequency, CO_2 laser; a modified Mach-Zehnder interferometer; a Bragg cell translator; transmit-receive optics; an infrared detector; a versatile range-angle scanner; a signal processor; a data-algorithm processor; displays; and recorders. A summary description of these components is presented in Section 3.0.

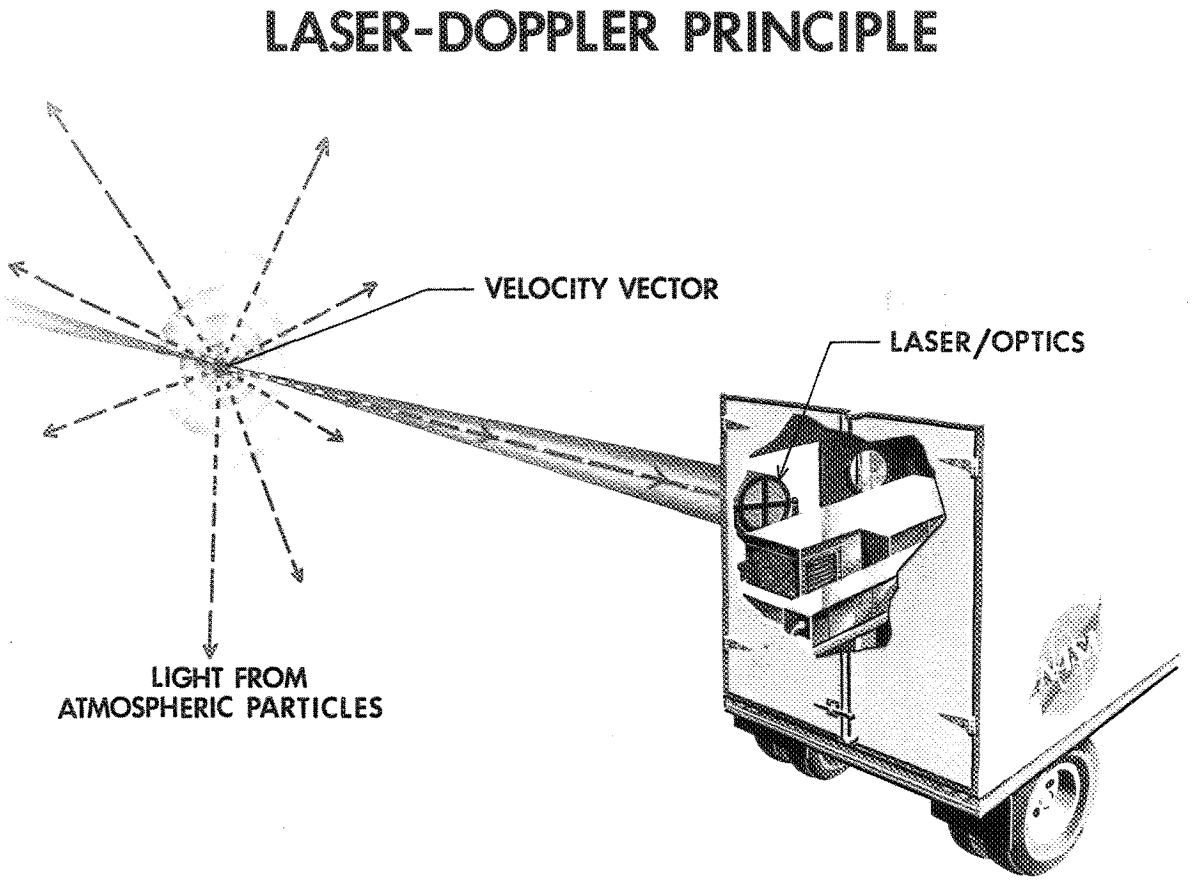

Figure 2-1. Laser-Doppler principle.

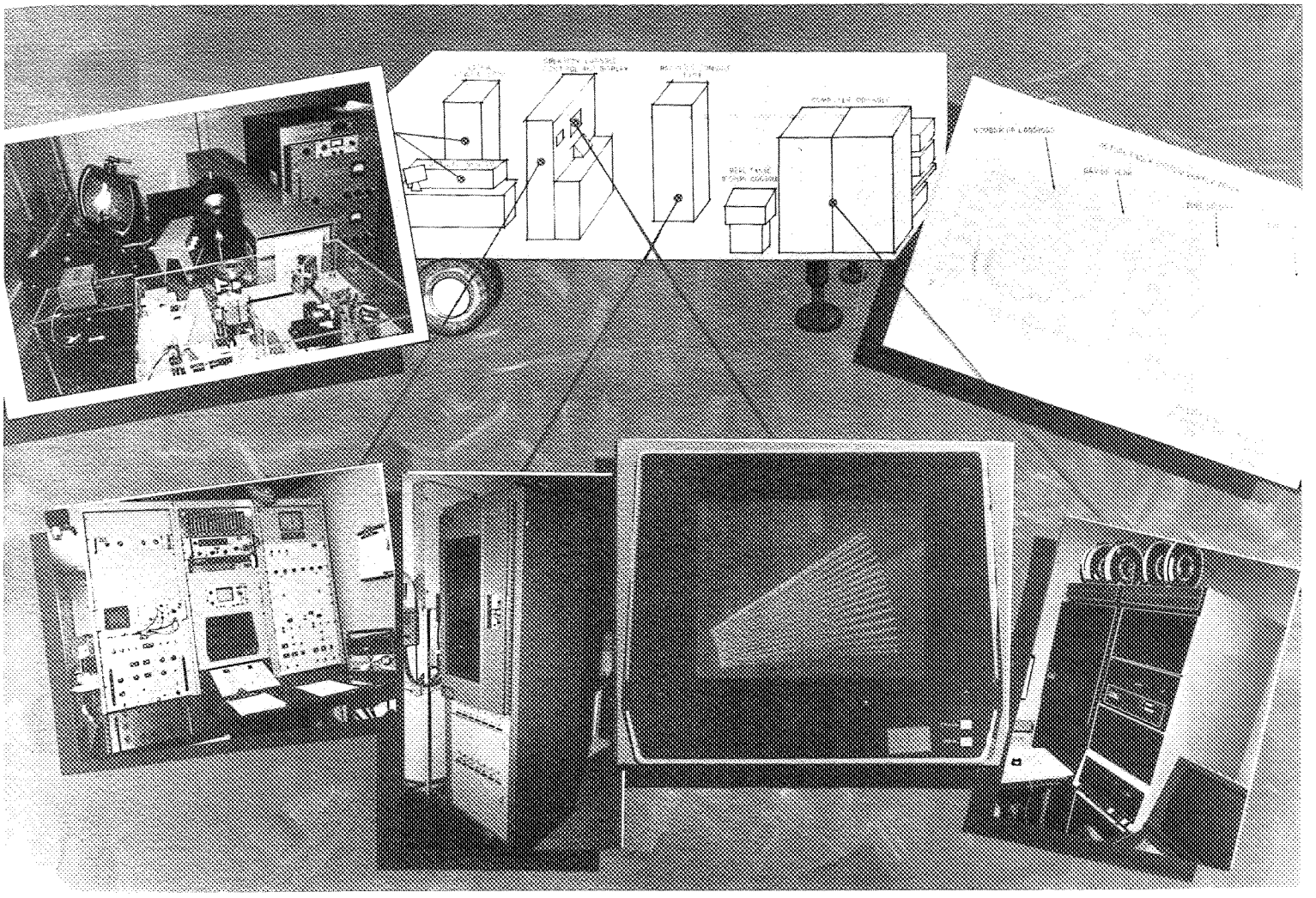

Figure 2-2. System composite.

2.3 Data Processing Techniques

The processing and displaying of data from the SLDV system is accomplished in real time and post analysis through the Vortex Information Display System. The data which are received from two asynchronous SLDV systems include position, velocity, and intensity information. This information is recorded on magnetic tape for post analysis and at the same time processed for real time display. Post analysis can be performed either on-site using the PDP-11 computer or offsite using a variety of available computer facilities. The onsite real time processing makes use of three basic algorithm programs: the V_{pk} algorithm, I_{pk} algorithm, and the range-elevation calibration algorithm. Onsite post data processing algorithms include: V_{pk} scatter, I_{pk} scatter, DBUG, wind profile, and least-square curve fit. Offsite data processing employs high speed data tapes and low speed data tapes. High speed data tape processing programs are cell output, calibration run analysis, vortex location, graphing, least square fit, and vortex flow field analysis. Low speed data tape processing duplicates as closely as possible post processing of high speed data tapes. A complete description of the processing and display techniques together with their associated algorithms is given in Section 4.0.

2.4 Test Operation

The FAA wake vortex test site, shown in Figure 2-3, was located near the middle marker of runway 31 right, JFK Airport. Two SLDV systems were installed at this test site approximately 800 ft (244 m) apart, 400 ft (122 m) on either side of the extended runway center line. The units were located approximately 200 ft (61 m) in front of the middle marker, 2700 ft (823 m) from the end of the runway. In this configuration, a vertical plane is scanned across the approach corridor to determine the tracks of the vortices. This scan plane is illustrated in Figure 2-4. Detailed information concerning the installation, calibration, operation, and data handling is given in Section 5.0. A summary of the test data and an evaluation of the equipment operation are also included.

2.5 Data/System Analysis

Data and system performance analyses have been a continuing activity since the MSFC checkout tests of the SLDV. This report deals with the analysis of the data collected specifically at JFK Airport. Selected runs have been

Figure 2-3. Aerial view of JFK Test Site.

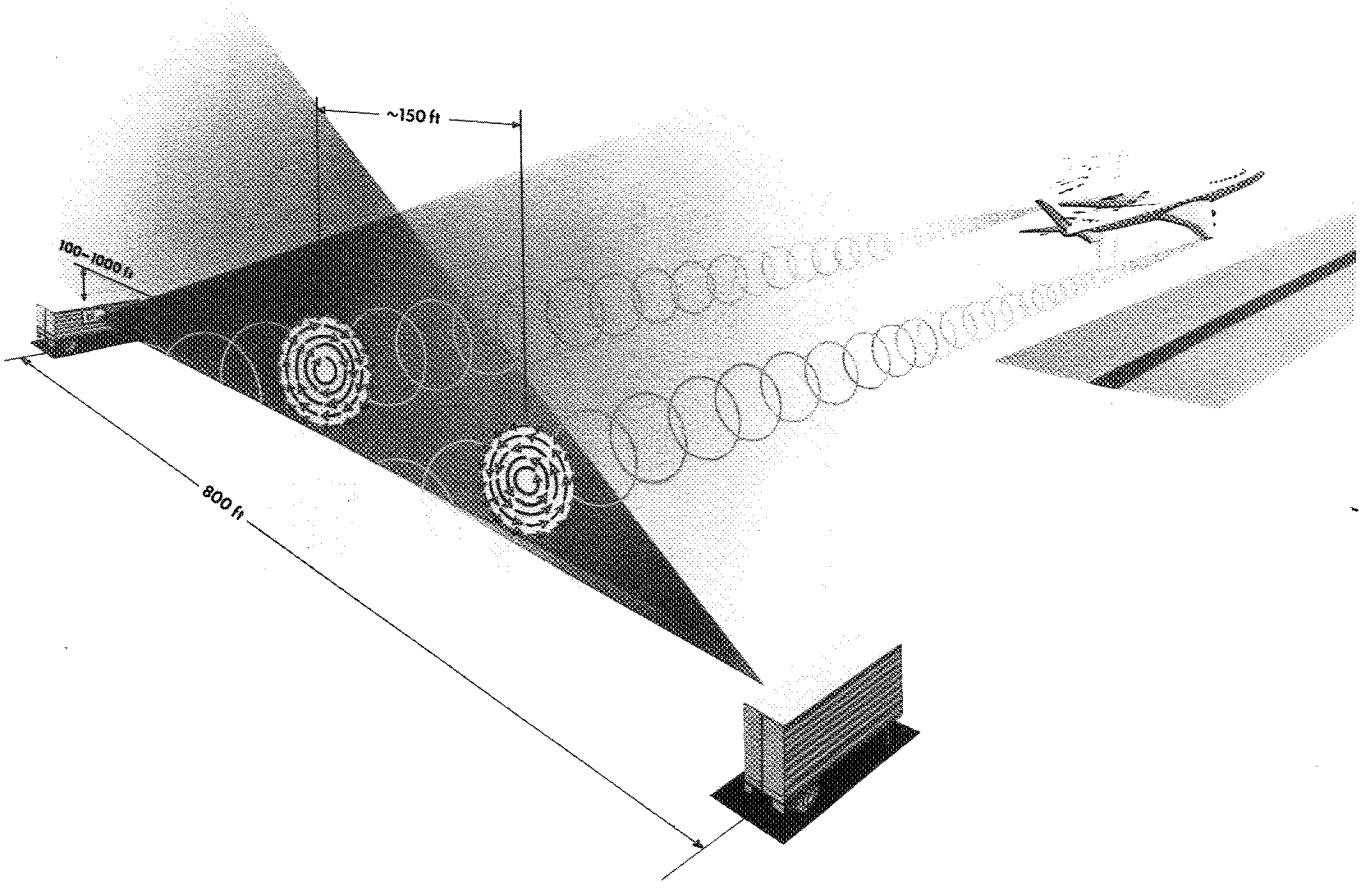

Figure 2-4. SLDV scan plane.

processed to obtain information on vortex transport, vortex circulation, wind signal/noise, calibration results, effectiveness of thresholds and algorithm parameters, and overall system performance. In addition, a verification of the overall data has been performed, and an attempt has been made to establish statistics on aircraft type and wind effect on vortex transport. Analysis has also been performed on the special long range flybys of a Convair 880 at JFK Airport. The detailed analysis information is given in Section 6.0. Copies of the vortex data collected at JFK Airport are located in the appendices.

2.6 Recommendations

As a result of the JFK Airport tests, it has become possible to determine what changes could be implemented in the present system design to improve reliability and at the same time reduce complexity. Section 7.0 of this report deals with the improvement of the SLDV system on a component-by-component basis with the improvements being directed at developing operational systems, one system for monitoring aircraft wake vortices on landing and takeoff, and a second system for research oriented applications.

2.7 Conclusions

The SLDV System as developed by MSFC under a joint NASA-FAA Interagency Agreement has been shown to be a versatile, accurate system which fully meets the original objective of the program. Analysis of the JFK Airport tests has indicated that SLDV systems are capable of determining vortex locations to accuracies of approximately 10 ft (3 m). It also showed that a significant amount of vortex flow field information could be obtained.

Evaluation of the system's operation indicated that while the system operated quite reliably, a number of changes could be implemented which would improve reliability and ease of operation. Since the present SLDV system is a general purpose system, the complexity of the system could be greatly reduced by a special purpose design limited specifically to vortex monitoring.

3.0 SYSTEM DESCRIPTION

3.1 Introduction

The SLDV is basically composed of two main subsystems: optics and signal processing. The optics subsystem is made up of a laser, interferometer, translator, telescope, telescope scan controller, and detector. The signal processing subsystem is comprised of receiver and detector bias electronics, a signal processor, algorithm processor, displays, and recording electronics. A summary description of the entire system as well as each of the components is given in this section. A more detailed description together with performance data can be found in Reference 1 and the references cited for the individual components.

3.2 System Operational Description

The overall block diagram of the SLDV is shown in Figure 3-1. Its operational description can best be communicated by tracing the coherent output radiation from the CO_2 laser transmitter through the optics, to the atmosphere, and back to the data algorithm processor and its displays. As shown in Figure 3-2, the horizontally polarized, collimated 6 mm beam exits from the CO_2 laser and impinges on the first beamsplitter which is oriented at 45° to the beam path. Approximately 10 percent of this beam is passed through the beamsplitter to be used as a local oscillator signal. This portion then passes through either a Bragg cell frequency translator or a series of attenuators. In the translated mode, the Bragg cell shifts the frequency by 24 MHz to create an offset zero frequency for which positive and negative Doppler shifts can be observed. In the nontranslated mode, the beam attenuators reduce the local oscillator power to a level for satisfactory operation of the detector. In this mode, positive and negative Doppler shifts and the direction of the velocity cannot be determined. The local oscillator beam is then reflected 90° by a mirror placed at 45° to the beam path. The beam then passes through a half-wave plate, changing the beam polarization from horizontal to vertical, and a recombining beamsplitter where it is mixed with the return signal onto the detector. The main portion of the exit beam from the laser is reflected 90° by the first beamsplitter and passes through a Brewster window that is aligned such that it transmits horizontally polarized light and reflects vertically polarized light. The exit beam is then reflected 90° and passes through a quarter-wave plate that changes the polarization of the beam to right-hand circular. The direction of polarization is reversed

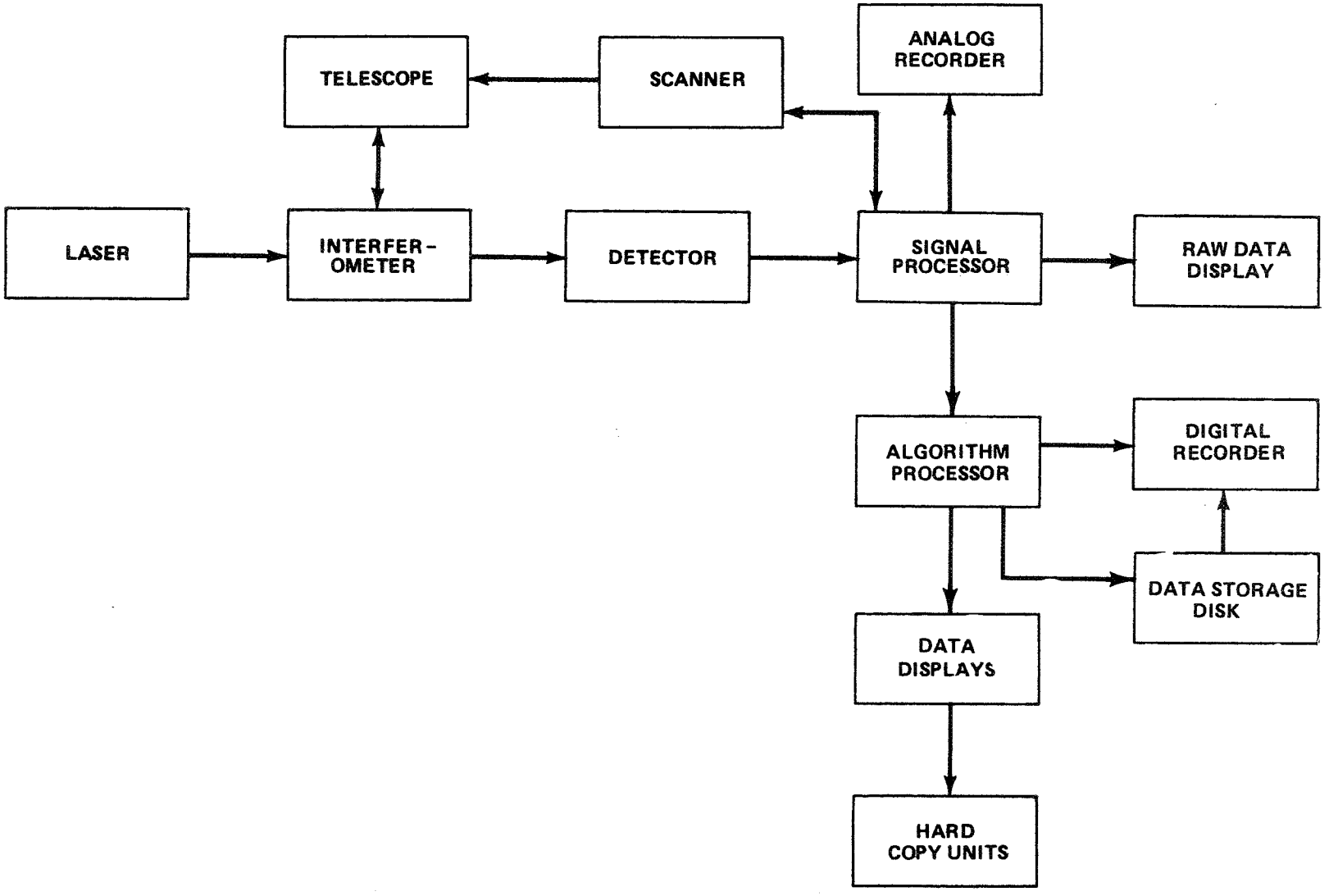

Figure 3-1. SLDV overall block diagram.

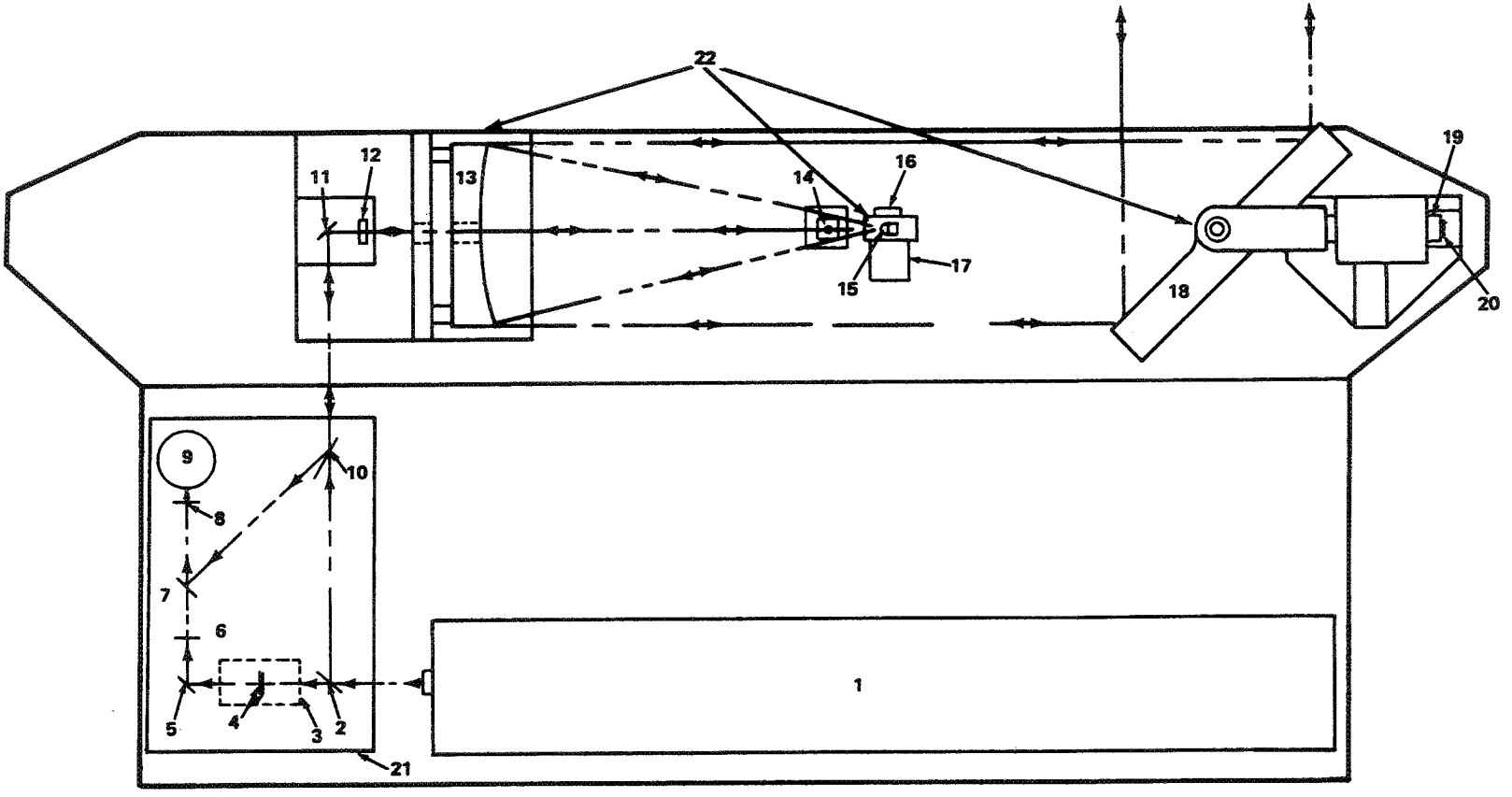

1. LASER
2. BEAM SPLITTER
3. BRAGG CELL
4. ATTENUATOR
5. 45° MIRROR
6. HALF WAVE PLATE
7. BEAM SPLITTER
8. FOCUSSING LENS
9. DETECTOR
10. BREWSTER WINDOW
11. 45° MIRROR
12. QUARTER WAVE PLATE
13. PRIMARY MIRROR
14. SECONDARY BACKSCATTER ATTENUATOR
15. SECONDARY MIRROR
16. SERVO MOTOR
17. SHAFT ENCODER
18. SCANNING MIRROR
19. SERVO MOTOR
20. SINE COSINE POT
21. INTERFEROMETER
22. TELESCOPE

Figure 3-2. Optical block diagram.

at the transmit telescope's secondary mirror and again at the primary mirror, such that the radiation impinging on the scanning flat mirror is again right-hand circularly polarized. Upon reflection from the primary, the beam expands to approximately 10 in. (25.4 cm) in diameter, strikes the scanning mirror at 45°, and focuses at positions in space by movement of the secondary mirror and the scanning flat. The right-hand circularly polarized radiation is reflected by atmospheric aerosols in the focal volume of the system as left-hand circular and at the same time shifts the frequency of the beam by an amount proportional to the velocity of the aerosols along the line of sight (Fig. 3-3). This return signal travels back along the same path as the exit beam until it reaches the quarter-wave plate where, because the direction of polarization has been reversed by the atmospheric backscatter, it is converted to vertical polarization upon passing through. This vertically polarized return signal is then reflected by the Brewster window to the recombining beamsplitter where it is mixed with the local oscillator beam. The mixing of these two beams creates an interference pattern that is imaged by the collector lens onto the face of the detector. This pattern varies with time according to the difference frequency of the two beams. The detector converts the radiation energy to electrical energy, and the result is an electrical beat signal that is proportional to the Doppler shift created by the motion of the atmospheric aerosols. This signal is then amplified by the receiver network to the level required for operation of the signal processor. Upon entering the signal processor, the Doppler signal is mixed with a chirp pulse and fed to a surface acoustic wave delay line. The serial output of the delay line is a continuous, analog spectrum analysis of the Doppler signal where the frequency is proportional to time. The signal is then sent to a sample-and-hold unit, the output of which provides a series of discrete spectrum samples (104 samples in the maximum case). Each sample is representative of a particular Doppler frequency interval approximately 100 kHz [approximately 1.8 ft/sec (0.55 m/s)] wide. Each sample is then A/D converted and incoherently integrated by summation averaging. At the end of a selected integration time (0.5 to 64 ms), a complete Doppler velocity distribution is provided for the aerosols contained in the coherent focal volume of the beam for that time and position in space. The coherent focal volume or range resolving capability of the focused coaxial optical heterodyne systems is expressed in terms of that range element in space that contributes a specified portion of the total backscattered signal at various ranges. The signal-to-noise ratio of coaxial focused systems that heterodyne the scattered return from the atmospheric aerosols is given by

$$S/N = \frac{\eta P_T \beta(\pi) \pi R^2}{2\, Bh\nu} \int_{L_1}^{L_2} \frac{dL}{L^2 \left[1 + \left(\frac{\pi R^2}{\lambda L}\right)^2 \left(1 - \frac{L}{f}\right)^2\right]} ,$$

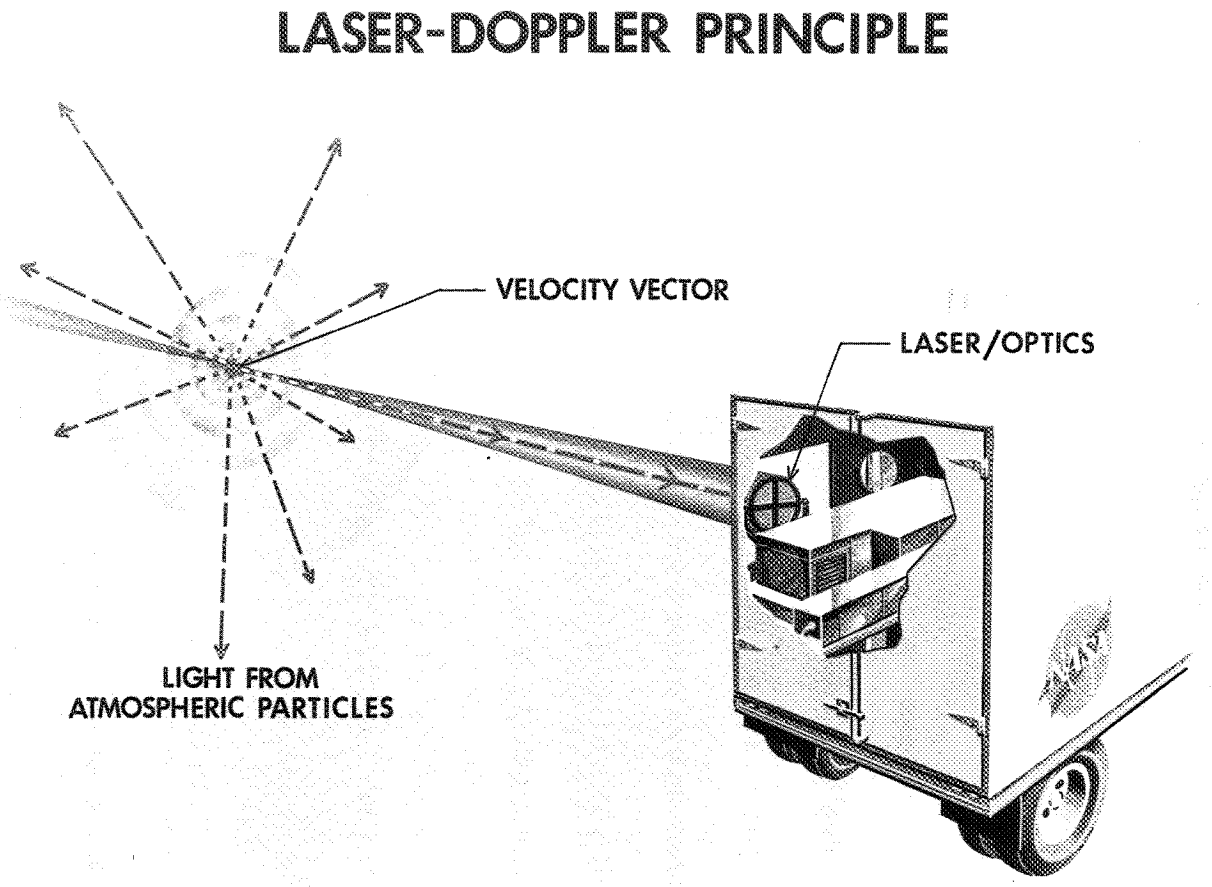

Figure 3-3. Laser Doppler line-of-sight velocity detection.

where

η = detector quantum efficiency

P_T = transmitter power

$\beta(\pi)$ = backscatter coefficient

R = radius of the transmitting optics

B = system bandwidth

L = particle range

h = Planck' s constant

ν = frequency of transmitted radiation

λ = wavelength of transmitted radiation

f = transmitter/ receiver focal length, equivalent to range to focus.

Integration from L_1 to L_2 yields

$$S/N = \frac{\eta P_T \beta(\pi)\lambda}{2\,Bh\nu} \left\{ \tan^{-1}\left[\frac{\lambda L_2}{\pi R^2} - \frac{\pi R^2}{\lambda f}\left(1 - \frac{L_2}{f}\right)\right] - \tan^{-1}\left[\frac{\lambda L_1}{\pi R^2} - \frac{\pi R^2}{\lambda f}\left(1 - \frac{L_1}{f}\right)\right]\right\} .$$

The resolution of the system can be defined by calculating the length of the range element that produces one-half the coherent backscattered signal received from the entire range $L_1 = 0$ to $L_2 = \infty$. Figure 3-4 gives the theoretical one-half power range resolution for a 12 in. (30.48 cm) CO_2 laser optical heterodyne system as a function of range to target. This volume is defined as the volume from which one-half of the coherent backscattered signal is derived.

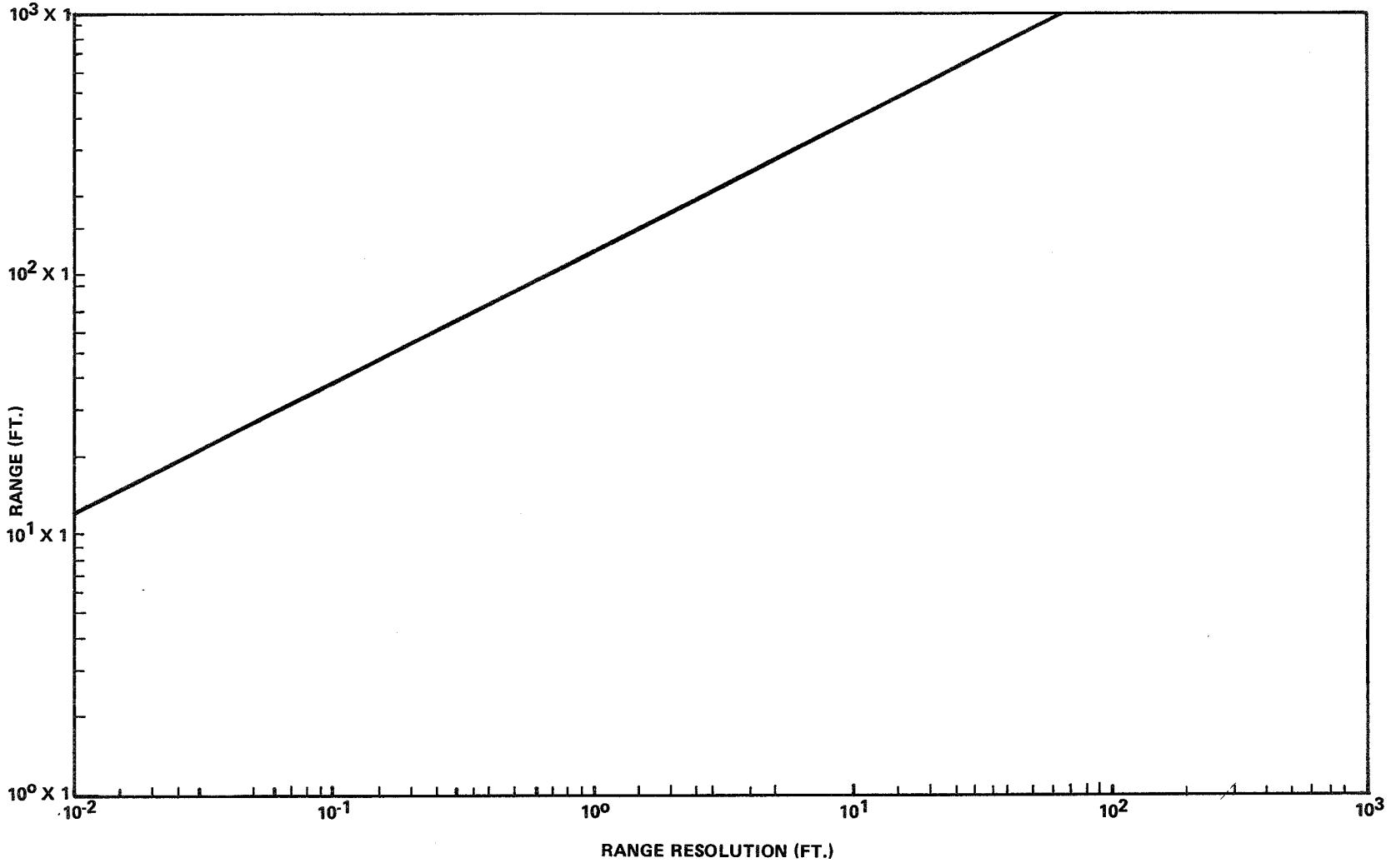

Figure 3-4. One-half power range resolution for a 12 in. (30.48 cm) CO_2 laser optical heterodyne system as a function of range to target (theoretical).

This information, together with the position coordinates, is then recorded on high speed, pulsed-code-modulated (PCM) analog tape at a maximum data rate of approximately 2 megabits. The signal then goes through a velocity and signal amplitude discrimination process in which different velocities and amplitudes of the signal may be eliminated, leaving only a selected portion of the spectrum. This information is further examined by the signal processor and the following information is extracted: V_{max}, the velocity with the highest signal strength; V_{pk}, the highest velocity with signal above the amplitude threshold; I_{pk}, the magnitude of the highest signal amplitude (digital number between 1 and 256); and N, the total number of velocity cells with signal amplitudes above the threshold. This information is sent to the data algorithm processor together with position and time information where it is recorded on tape and/or stored in computer memory for processing on a scan-frame by scan-frame basis in real time. The results of the data algorithm processor are then displayed and automatically hardcopied.

3.3 Component Description

This subsection provides a description of each of the main components involved in the SLDV System. These descriptions are arranged in the order that they are encountered in the operational description of subsection 3.2.

3.3.1 Laser

With reference to Figure 3-2, the laser is a continuous wave CO_2 system operating at 10.6 μm. It is used for the transmission of energy into the atmosphere and to provide a local oscillator to the detector. The laser head contains a split discharge tube closed off with nonhygroscopic zinc selenide windows mounted at Brewster's angle in such a way as to provide horizontal polarization of the output beam. This tube is mounted between a plane output mirror and a 4 m radius of curvature rear reflector. The mirrors and discharge tube are mounted on a frame utilizing four Invar rods for thermal stability. The laser output is in a TEM_{00} mode, single frequency, single wavelength. It has a beam diameter of 6.5 mm with a beam divergence of less than 3 mrad full cone angle.

The laser head is a water cooled, semisealed unit having a nominal output of 17 W. Sealing of the system is through a vacuum valve which permits refilling of the laser in the field if necessary. Refilling is accomplished using the gas bottle and pumping station located in the power unit. This unit also contains the laser power supply, the closed cycle laser cooling system, and a high voltage supply for tuning the laser by piezoelectric control of the cavity length. The laser head is powered by two solid-state, high-voltage supplies which are highly regulated to maintain laser stability. These supplies also produce the drive voltages for the cooling fan and the safety interlock system, which is provided to prevent the operation of the power supplies under potentially dangerous or destructive conditions.

3.3.2 Interferometer

With reference to Figure 3-2, the interferometer [4] is an optical arrangement designed to act as a laser coupler to provide a beam for transmission to the target, a local oscillator beam, and to efficiently recombine the returning signal and local oscillator beams. The local oscillator has the required power to drive the detector into the shot-noise-limited regime. The signal and local oscillator beams are aligned to much less than their diffraction limited divergence angle and the total effect of all optical components in the system is such that they do not degrade the recombining wavefronts.

The configuration of the interferometer is such that a frequency translator can be readily inserted into the local oscillator beam path. This requirement, together with the need to avoid possible feedback paths which exist with the Michelson type of interferometer, has dictated a Mach-Zehnder configuration, modified by using a polarizing output beamsplitter and a quarter-wave plate to achieve approximately 80 percent efficiency of the transmit-receiver coupler.

In operation, the beamsplitter (2) transmits a nominal 10 percent of the incident laser power to be used as a local oscillator. The attenuator (4) consisting of two 10 percent transmitting beamsplitters reduces the power of the local oscillator. The recombining beamsplitter (7) which is also a 10 percent transmitting component, reduces the local oscillator further to a level 10^{-4} times the laser output power or approximately 1.5 to 2.5 mW depending upon the laser power. During assembly, variations of the actual transmission values are used to obtain the local oscillator level most nearly correct for each detector.

The laser beam, after being reflected from beamsplitter (2), is transmitted through the Brewster window (10), which is a germanium flat mounted at Brewster' s angle for a horizontally polarized beam. Essentially the entire beam power is transmitted through this plate. The beam then passes through a CdS quarter-wave plate (12), which is oriented to produce a circularly polarized beam, and enters the telescope.

The returning circularly polarized signal beam is converted to a vertically polarized beam by passing through the quarter-wave plate. Approximately 78 percent of this beam is reflected by Brewster window (10) to the recombining beamsplitter (7), a 90 percent reflector, where it is combined with the local oscillator whose polarization has been rotated 90° by the half-wave plate (6) and focused on the detector (9) by the lens (8). Items (5) and (11) are all fully reflecting mirrors to redirect the beam by 90°.

3.3.3 Translator

With reference to Figure 3-2, a Bragg cell frequency translator (3) [4] is used to generate a local oscillator beam at a frequency different from that of the transmitted beam so that the sense of direction of the Doppler shift from the target may be determined. The specifications of the translator are as follows:

a. Operating wavelength: 10.6 μm

b. Aperture: 8 mm

c. Beam diameter ($1/e^2$): 6 mm

d. Entrance and exit faces are at Brewster' s angle.

e. Cell is water cooled

f. Translation frequency: 24 MHz ± 10 kHz (10 to 40°C)

g. Efficiency ±35 percent when used with driver

h. Flatness: $\lambda/20$ at 10.6 μm over 80 percent of aperture area

i. Parallelism: 3 min

j. Scratch/Dig: 20/10

k. Incident beam polarization horizontal

l. Deflection to be in horizontal plane.

The rf driver is switchable between two ranges. Within these two ranges the following efficiencies are achieved by continuous control:

a. 0.1 to 2 percent,

b. 10 to 50 percent or more.

3.3.4 Telescope

With reference to Figure 3-2, the telescope (22) is an f-2 Coaxial Cassegranian System [4]. As a transmitter, it focuses the laser beam at specific points in space. As a receiver, it collects the backscattered radiation from particles moving through the focal volume.

The telescope consists of a 12 in. (30.48 cm) parabolic primary mirror (13) with a focal length of 24 in. (60.96 cm), a 1/2 in. (1.27 cm) parabolic secondary mirror (15) with a focal length of 0.945 in. (2.4 cm), and a scanning flat measuring 18 by 12 in. (45.72 by 30.48 cm) (18).

All mirrors are coated with aluminum and overcoated with silicon monoxide. Optical quality is $\lambda/10$ at 10.6 μm.

3.3.5 Detector

With reference to Figure 3-2, it is the function of the heterodyne detector (9) to receive the mixed local oscillator and signal beams to generate an electrical signal at the difference frequency. The detector [4] is capable of operating so that the level of shot noise generated by the local oscillator beam exceeds all other noise sources. The detector is a mercury cadium teluride (HgCdTe) photodiode that is a square chip with sides of approximately 250 μm. It is mounted in a stainless steel dewar for operation at the liquid nitrogen temperature of 77 K. Detector characteristics are obtained by measuring the dynamic responsivity, the dynamic reverse impedance, and a heterodyne signal as a function of local oscillator level and bias voltage. Table 3-1 summarizes the range of values of the detectors used in the project. These characteristics are used to determine the optimum bias conditions for operation and to establish the parameters for the bias circuitry.

TABLE 3-1. CHARACTERISTICS OF LDV DETECTORS

Parameter	No. 952	No. 972	No. 1031
Dynamic Resistance (Ω)	300 - 1200	500 - 2500	200 - 400
Responsivity (A/W)	5 - 6	2.5 - 5.5	4.5 - 7.5
Frequency Response (mHz)	> 30	> 30	> 30
Maximum Reverse Voltage/ Current	1.9 V/ 3.5 mA	2.5 V/ 5 mA	1.6 V/ 5 mA
Maximum Power (mW)	4.7	12.5	8

3.3.6 Scanner

With reference to Figure 3-5, the scanner [5] is used to position the mirrors of the telescope to provide the illumination of a desired region in space. Since the optical system illuminates only a very small region concentric with the optical axis, and the system is intended to probe the velocity structure of flow fields (such as vortices) which are neither visible nor accurately located, means must be provided to move the optical axis and the location of the focal region along it in such a way that (1) the coordinates of the focal region are known at all times, (2) a given region of space may be examined in an efficient systematic manner, and (3) the nature of the scan program may be conveniently altered to suit a variety of applications. These capabilities are incorporated in the range-angle scanner. This device consists basically of two servomechanisms [and associated data output (coordinate) devices] which can be programmed in three basic modes:

a. Finger Scan — This mode utilizes a fairly fast, periodic, linear "sawtooth" excursion of the focal volumes simultaneously with a similar but much slower motion of the elevation angle of the optical axis, producing a series of petal-shaped contours, or "fingers" in the x, y space being scanned. This mode is particularly suited to detecting and locating vortices, since a number of closely spaced traverses can be made across the region suspected of containing vortices.

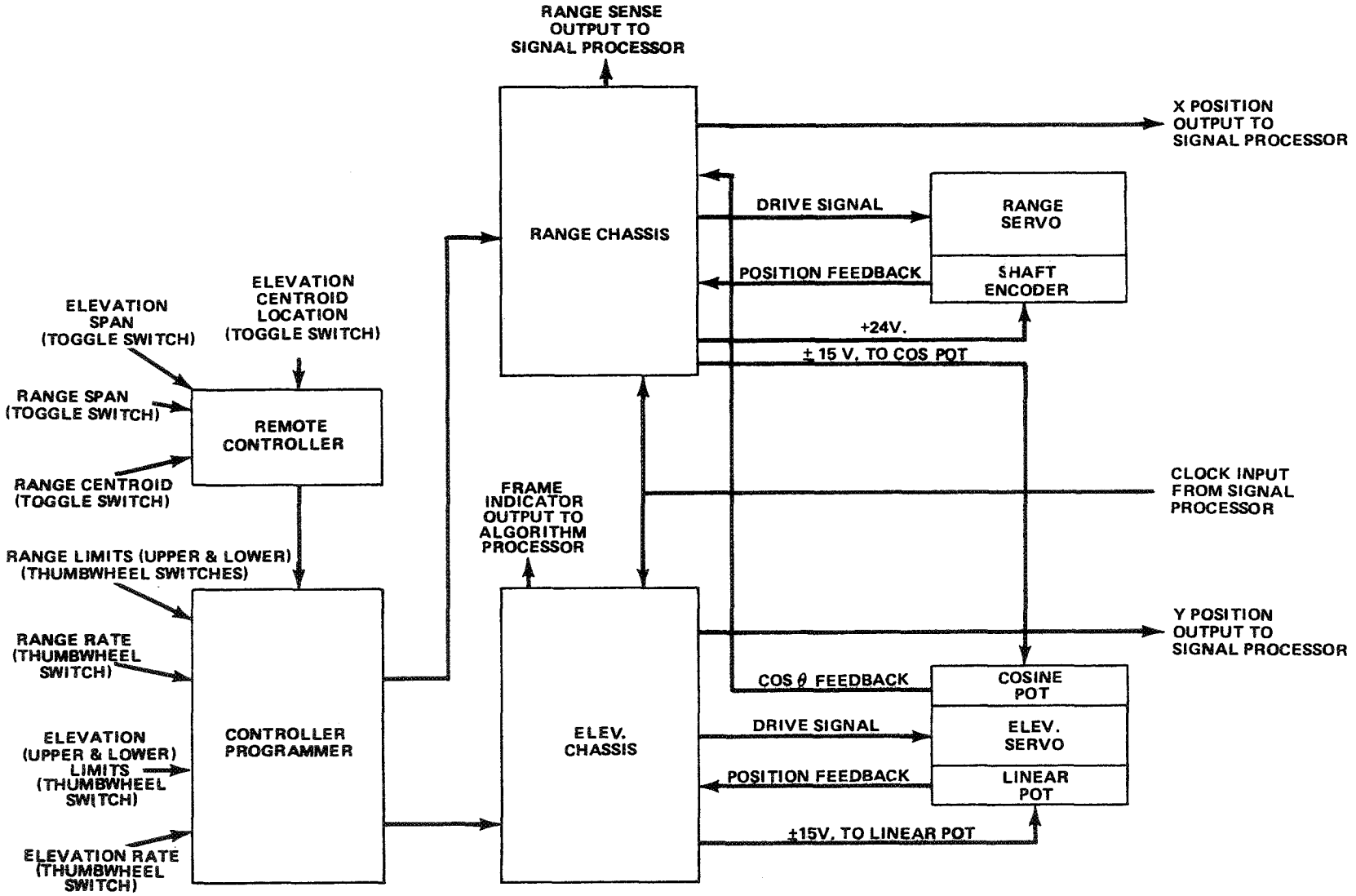

Figure 3-5. Scanner block diagram.

b. Line Scan — This mode causes the focal volume to move vertically at a nearly constant rate along an imaginary line located at any chosen distance from the instrument. By scanning three instruments along the same line and grouping the data, it is possible to obtain the actual three-component velocity vector at all points along the line.

c. Single Axis — For special purposes (e.g., calibration), either degree of freedom may be scanned in the normal mode while the other is stationary, or both may be made to remain stationary at precisely located values.

In addition to the main mode, provisions have been made for a sector scan, which is basically mode (a), but in which the boundaries of the scan pattern can be rapidly enlarged or contracted, and the center of the pattern rapidly translated to specific points in space.

The range-angle scanner provides the means of steering the telescope focal volume to a desired point in space. This implies control over three variables: range, elevation (or angle), and azimuth. In practice, only range and elevation are made variable, with azimuth being fixed normal to the system van. Range is controlled by moving the telescope secondary mirror relative to the primary mirror. Elevation is controlled by rotating a flat mirror upon which the beam is incident at a 45° angle.

The scanner system consists of two independent servocontrolled subsystems and a controller subsystem.

The range angle controller provides the means for setting the desired parameters for a particular set of scan conditions. These parameters include such things as range scan limits, range scan rate, and type of scan. The easiest method of setting these parameters was determined to be by means of thumbwheel switches. The scan limits and rates available are tabulated as follows:

Elevation

a. Upper angle — thumbwheel adjustable from 10 to 59°

b. Lower angle — thumbwheel adjustable from 3 to 59°

c. Scan frequency — thumbwheel adjustable from 0.1 to 1.0 Hz.

Range

a. Maximum range — thumbwheel adjustable from 100 to 599 m

b. Minimum range — thumbwheel adjustable from 32 to 599 m

c. Scan frequency — thumbwheel adjustable from 0.1 to 6.9 Hz.

The elevation servo is of straightforward design. It consists of an error signal amplifier, damping amplifier, power amplifier, and drive motor. Feedback is obtained from a shaft-mounted potentiometer. The motor is a permanent magnet rotor, dc stator, restricted angle type.

The range servo differs from the elevation servo in several respects, the more important of which are the following:

a. For versatility in signal processing, several different integration times are desired. This requires that the signal return be a linear function of range scan. Achieving a linear scan is complicated by the fact that the actual variable being controlled is the location of the point of maximum intensity of a focused laser beam (the focal volume) which is not directly observable and not accessible to provide feedback. The location of this point, however, is related to the position of the secondary mirror by the lens equation of the telescope,

$$\frac{1}{f} + \frac{1}{r} = \frac{1}{F} \quad ,$$

where

f = position of secondary mirror with respect to the focal point of the telescope (object distance)

r = location of point of maximum beam intensity

F = focal length of telescope.

From this equation it is clear that if we have available a voltage proportional to the desired value of f, we must obtain the reciprocal of this to obtain a linear secondary mirror motion (i.e., the servo must "solve" the lens equation). This operation is accomplished by using a precision analog divider.

b. From the lens equation it is evident that when f is small (i.e., when focused at long range), even very small errors in positioning the mirror will lead to very large errors in the position of the focal volume, hence the feedback device which provides a voltage proportional to the mirror position must be extremely accurate. For this reason, the design employs a digital shaft encoder capable of resolving the shaft angle to within ±0.8789°.

c. Anything attached to the secondary mirror will be illuminated by the beam and block part of the energy. Therefore, the drive motor and digital encoder are coupled to the horizontal slider mount of the secondary mirror by means of a flexible cable and pulley arrangement.

The remainder of the circuitry is conventional, consisting of an error amplifier, damping amplifier, power amplifier, and drive motor. The motor is a smaller version of the type used in the elevation servo.

The position of the external focus is required to be in x, y form rather than polar for display purposes. This is accomplished by multiplying r by the sine and cosine of the elevation angle. The trigonometric functions are provided by a sin/cos precision potentiometer on the elevation mirror shaft, and the multiplications performed by precision analog multipliers. This x, y information is provided to the signal processing electronics in digital form.

3.3.7 Receiver Electronics

With reference to Figure 3-6, it is the function of the receiver electronics [4] to supply the proper bias voltage to the detector and to amplify the detected signal to the power level required by the processor. In addition, in the case in which a frequency translator is used, the feedthrough signal at 24 MHz is suppressed by a notch filter.

The receiver was designed to operate in two modes. In one mode, zero velocity signals appear at zero frequency and the directional sense is not available. In this mode, the receiver was designed to have a bandwidth of 12 MHz, but actually goes out to approximately 18 MHz. In the second mode, a translator is incorporated in the interferometer to downshift the local oscillator frequency such that zero velocity signals appear at 24 MHz, with approaching objects appearing at frequencies above 24 MHz, and receding objects appearing at frequencies below 24 MHz. The biasing circuit is designed to bring the detector to the optimum bias point for a variety of local oscillator levels, and to protect the detector againt damage resulting from over voltage, excess current, removal of the local oscillator, or loss of cooling. The baseband mode

circuit is designed to operate in a frequency range of 100 kHz to 12 MHz. The Translate Mode circuit is designed for operation in the 12 to 36 MHz range.

In both modes the receiver chain consists of a low noise first stage preamplifier followed by an amplifier to raise the output level to the processor input requirements and a filter to remove objectionable spurious signals. In the Baseband Mode, a high pass filter is used to remove noise and signals below 100 kHz which comes from the range scan and detector 1/f noise. In the Translate Mode, a notch filter at 24 MHz is used to remove the spurious signal caused by the translator feedthrough and the translated return from the secondary mirror. The effective width of this notch is ±100 kHz. The maximum design output level of the receiver in either mode is 100 mV (rms) into 50 Ω. Typical output noise level is approximately -65 dbm.

3.3.8 Signal Processor

With respect to Figure 3-6, the signal processor [6] converts the signals from the detector to a manageable data form for the processing of desired information. There are five subdivisions in the overall circuitry of the signal processor: spectrum analyzer, spectrum integrator, velocity discriminator, display interface, and formatter. These units function in series: first in analog form to provide frequency resolution; then in digital form to achieve signal-to-noise improvement (video integration), frequency discrimination, and to provide data to the algorithm processor; and finally in analog form again for the purpose of real-time display of the significant velocity data. The formatter collects binary data from various points in the processor and provides a serial output for biphase recording. The signal processor accepts signals from the laser assembly with or without the use of a laser output frequency translator. Without the translator the velocity coverage is either 0 to +170 ft/sec (0 to +52 m/s) or 0 to +100 ft/sec (0 to +30 m/s); with the translator the velocity coverage is either -100 to +100 ft/sec (-30 to +30 m/s), 0 to +170 ft/sec (0 to +52 m/s), 0 to +100 ft/sec (0 to +30 m/s), -120 to +120 ft/sec (-37 to +37 m/s), or +100 to +200 ft/sec (+30 to 61 m/s). Outputs provided for display and recording are range, altitude, and velocity information.

The input level to the signal processor from the laser assembly is 25 mV rms and is in the frequency range from 0 to 10 MHz for operation without the translator; for operation with the translator, it is in a band centered at 24 MHz. With the translator, the spectrum analyzer is capable of accepting a band up to 20 MHz wide. The performance of the spectrum analyzer is highest in the center of the band, providing the 100 kHz resolution over a 6 MHz range.

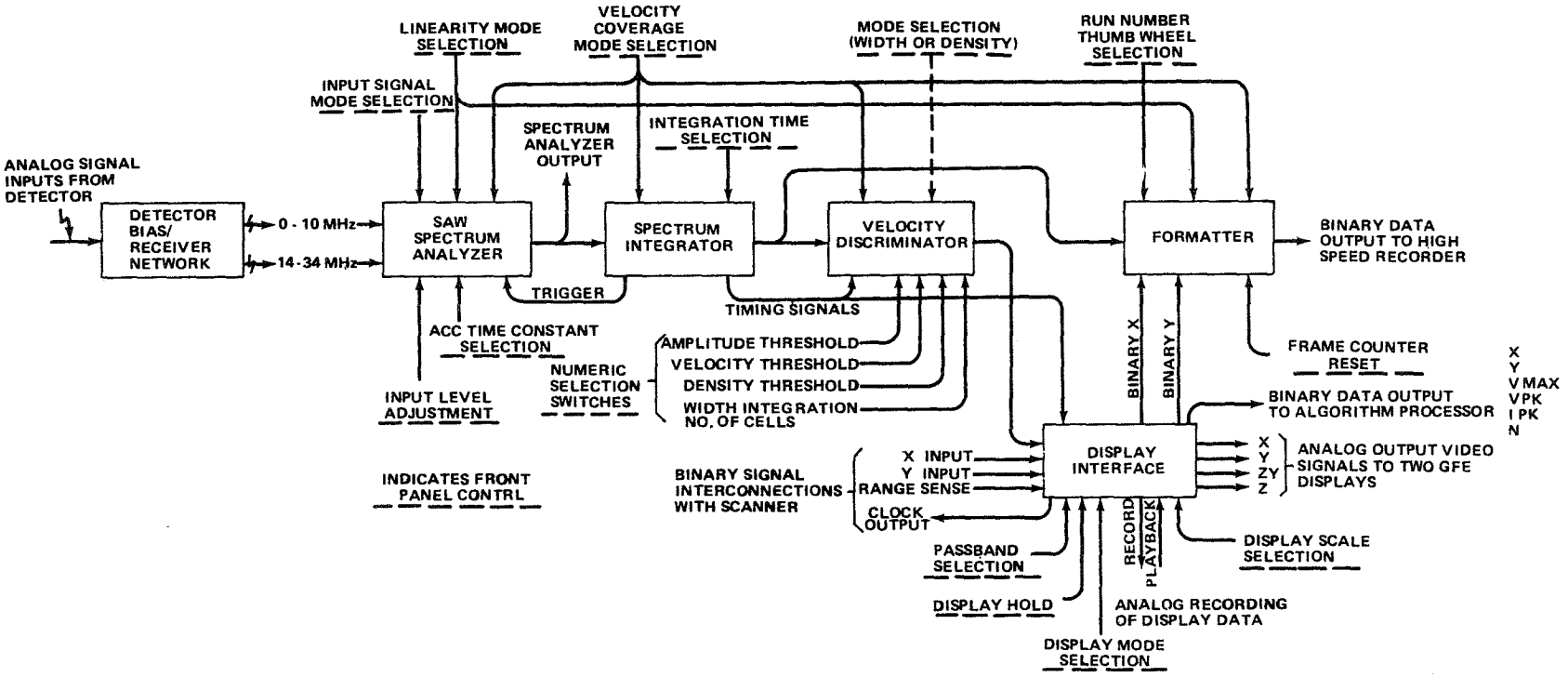

Figure 3-6. Signal processor block diagram.

Beyond this central range, the resolution and sensitivity decrease depending on the bandpass characteristic of the surface acoustic wave dispersive delay line used in the spectrum analyzer.

The spectrum integrator performs integration separately on each resolution cell produced by the analyzer. The output for the complete frequency coverage interval is delivered in binary form to the velocity discriminator where thresholds are applied to extract significant information for display. These thresholds are (a) amplitude to establish the minimum detectable energy level of a spectral component, (b) velocity to establish the minimum velocity to be accepted, and (c) width or density to establish the optimum spectral characteristics of a signal to be detected. The thresholds serve to discriminate against false alarms due to random noise peaks as well as actual signals too low in velocity to be of interest. The false alarm aspect is particularly important because the display system could become cluttered with false velocity indications.

Two operating modes are used with respect to the amplitude range of the signals to be processed. For the most efficient detection of a vortex cell, the "CFAR" mode (Constant False Alarm Rate) is used. This incorporates hard limiting in the spectrum analyzer and results in the normalizing of the background noise to a constant level in the absence of a true signal. The amplitude threshold can be set for a constant false alarm rate in this case. There is negligible loss in signal-to-noise ratio but there is a modification of the spectral distribution of a signal. To perform a true spectrum analysis of a signal, linear operation must be used. For this, a manual gain adjustment is provided to set the input level within the optimum dynamic range of the processor.

The display interface combines the velocity data from the discriminator with horizontal range and altitude inputs to obtain an analog output suitable for display. The display format is compatible with commercially available display equipment and functions by producing brightening of the display face in areas where the scanned laser beams intercept velocities above the velocity threshold.

The display interface also has the capability for analog recoding of the display information and replay/display.

The overall signal processor, with the exception of the display and hard copy unit, is contained in one unit capable of rack mounting in a standard 19 in. relay-rack. The unit contains all necessary power supplies for operation from 115 V, 60 Hz primary power.

All input/output signal interconnections are made at the rear of the unit. All controls necessary for the normal operation of the equipment are located on the panel. Exceptions are any potentiometer type adjustments which are used in initially balancing or calibrating levels within the equipment.

Front panel control includes velocity coverage to select the velocity coverage mode, linearity, input level, integration time, amplitude threshold, velocity threshold, density threshold, velocity discriminator mode, width integration (number of cells), run number, frame counter reset, display mode, scale, velocity passband, normal/hold, normal/playback, AGC time constant, AGC threshold, input signal mode, and power. In addition to these controls, the front panel has two indicator lamps: a green lamp to indicate the power-on condition and a red lamp to indicate a frame counter overflow condition.

The front panel also contains a jack for monitoring the analog signal output of the spectrum analyzer by means of an oscilloscope, plus a jack supplying an appropriate trigger for the scope.

Analog signals are available at the interface output for recording to allow playback directly to the display. The signals included are Display x, Display y, Unblanking, and Analog velocity.

The display coordinate signals are large enough to make full use of the signal-to-noise potential of the recorder. Coordinate noise on playback will be approximately 2 mV rms at 7 1/2 ips and higher. Recording speeds below 7 1/2 ips are not recommended because the recorder bandwidth severely limits display resolution at lower speeds.

Four additional outputs are also provided for use in data analysis. The following outputs are provided in analog form for recording and also in digital form together with x and y to the data algorithm processor. They are:

a. Spectrum Output — The amplitude (serially) of all the cells over the velocity threshold after width integration. This output leads the other analog outputs by one frame.

b. I_{pk} — The highest amplitude in a frame which is higher than the amplitude and velocity thresholds (V_T and I_r).

c. V_{pk} — The highest velocity in a frame for which the amplitude threshold (I_T) is exceeded.

d. N_T — The total number of cells over the amplitude threshold in a frame.

e. V_{max} — The velocity which has the highest amplitude in a given frame.

3.3.9 Data Recording

Tape recording was used in the SLDV field test operations to meet several basic requirements. One was to record the surface acoustic wave spectrum signal for later analysis, a high data rate or high tape speed requirement. A second objective was to record the raw display data in analog form, a lower data rate or slower tape speed requirement. A third requirement was to record the input to the algorithm processor in digital form. The last objective was to record the digital output of the algorithm processor. The recording of the surface acoustic wave spectrum signal (i.e., the processor signal after integration but before any detection logic) allowed a comprehensive analysis via digital computer so that proper detection algorithms could be developed and detailed analysis of the data be performed. These data were recorded using pulse code modulation (PCM) on a direct track of a wide band magnetic tape recorder.

The display data were recorded to allow the recall of displayed data. Wide band FM electronics were used to record the data on the same tape recorder as used for the PCM.

Recording of the input data to the data algorithm processor allows the use of several different algorithms on the same data at the test site location. This was recorded on the 9 track digital recorder contained in the data algorithm processor system.

Recording of the output of the data algorithm processor facilitates handling of the final data. This is recorded on a magnetic disk unit for later transfer to digital tape. In addition hard copy records are obtained from the CRT displays.

3.3.10 Data Algorithm Processor and Display System

Because of the large amount of raw data generated by the two SLDV, the operators cannot easily determine the effectiveness of the system performance. As a result, the Data Algorithm Processor and Display System was developed [7]. This system accepts the raw data from the two SLDV in real-time and processes it, for example, to produce a time event plot of the center of the aircraft vortices on a frame basis. In this manner, the operator can easily observe the actions of the positions of both vortices as a function of time.

The system provides flexible control through system user interaction for collecting wing tip vortex velocity data, processing the data in real-time, displaying the processed data, storing raw data on magnetic tape, and post processing raw data. The data received from the two SLDV include position, velocity, and intensity information. The raw data are written onto magnetic tape for permanent storage and are also processed in real-time. These real-time data are stored on disk and then transferred to tape for a permanent record.

The processor enables the user to make real-time adjustments in processing data and, thereby, provides a better definition of data behavior. Displaying the information in real-time produces a feedback capability to the SLDV system operator, allowing adjustments to be made in the collection of raw data. Therefore, raw data and processing can be continually upgraded during testing to improve data behavior studies. The post-analysis capability permits the analyst to perform indepth studies of test data and to modify vortex behavior models to improve transport predictions.

The Data Algorithm Processor and Display System, (Fig. 3-7) consists of a basic processing mainframe computer with 16 bit words and floating point arithmetic. Also included are 48 K words of memory, two 1.2 million word disks with a transfer rate of 11.08 μs/word and an average access time in the vortex system application of 30 ms, and an industry compatible 9 track, 800 bits/in. tape unit. The terminal equipment includes a standard Display Terminal [19 in. (62 cm) storage tube and alpha-numeric keyboard], Display Monitor [11 in. (36 cm) storage tube], and a Hard Copy unit. A Data Tablet 11 by 11 in. (36 by 36 cm) is used to input information to the computer.

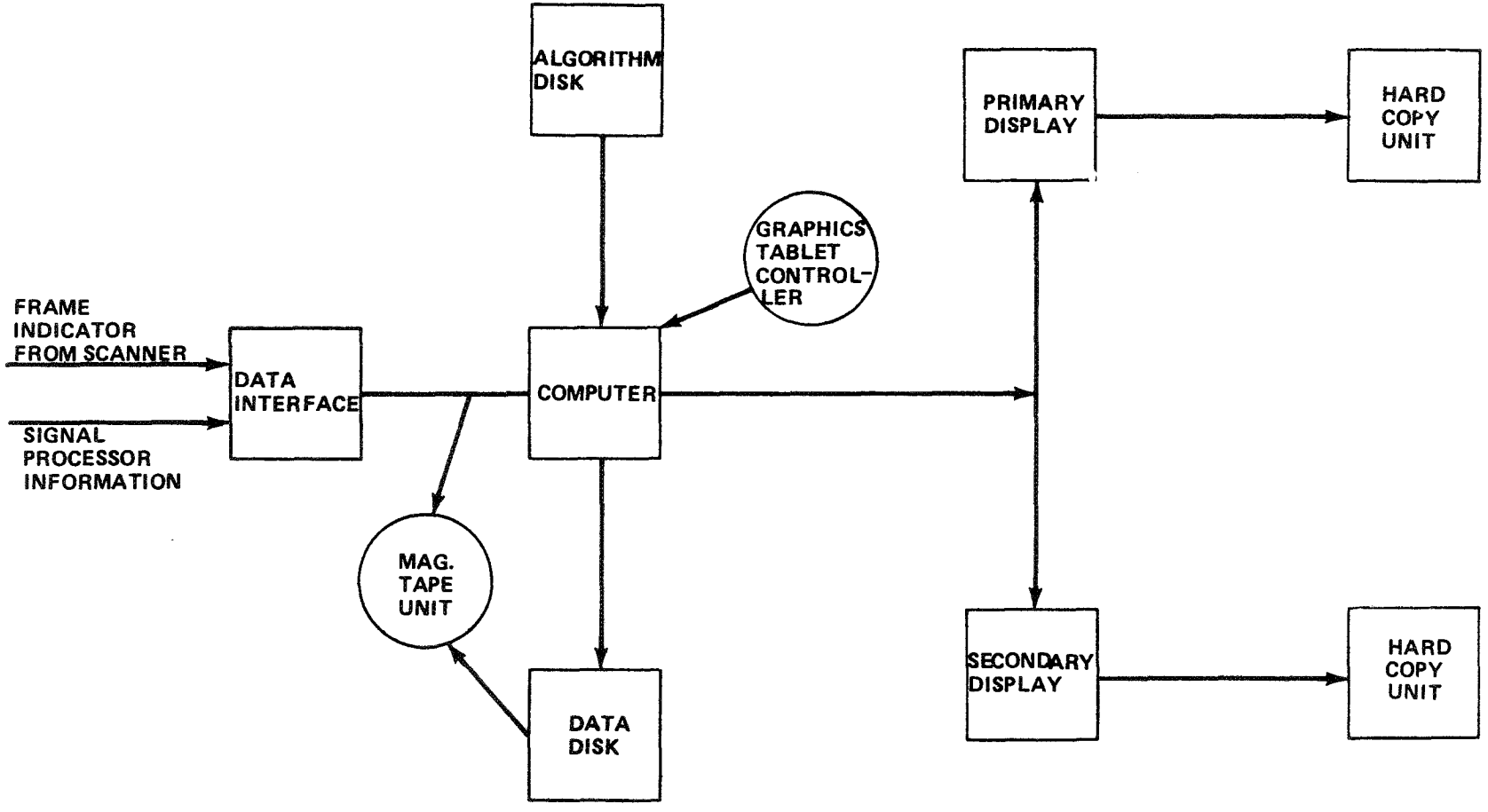

Figure 3-7. Data/algorithm processor block diagram.

In addition to this equipment, an interface unit has been designed and built between the signal processor and computer. This unit serially transfers the position, velocity, and intensity data from the signal processor to the computer at a 300 kHz rate. The computer under software control accepts the data on an interrupt basis from this unit with each interrupt being honored within 300 μs. Another unit was designed and built which provides an interrupt to the computer which signifies the start of a test and also identifies the specific aircraft type. This is used in vortex tracking. Whenever a new aircraft is approaching, the operator simply chooses a switch identifying the aircraft and pushes a start flyby button which causes an interrupt to be sent to the computer. These data are decoded by the data processor and the interrupt starts the data acquisition phase of the system operation.

The software consists of computer support software and application software running under control of the computer operating system.

The application software consists of a real-time interrupt handler written in assembly language and the algorithm control and computation software coded entirely in Fortran to simplify changes to the algorithm. The display software to interface to the graphic displays is a standard software package coded in assembly language.

The raw data from the SLDV are placed in buffers by the interrupt handler. Whenever a buffer becomes full, the buffer is dumped onto the disk. This interrupt-driven software is completely independent of the other application software and executes on a demand basis.

Whenever the first complete frame of data is stored on the disk, those data are read into the processing buffer and stored on magnetic tape. The centroids of the vortices are computed and displayed on the primary and alternate displays in two of the optional formats selected by the operator. In the post-analysis mode, the position, velocity, and intensity data are read from the magnetic tape and processed and displayed. System parameters and algorithm parameters can be easily changed through the interactive capability. Data can be rerun with different system or algorithm parameters.

4.0 DATA PROCESSING TECHNIQUES AND DATA DISPLAYS

4.1 Introduction

The processing and displaying of data from the SLDV system is accomplished in real time and in post analysis through the Vortex Information Display System (VIDS) (Fig. 4-1). The VIDS provides flexible control through system-user interaction for collecting wing-tip-trailing vortex data, processing these data in real time, displaying the processed data, storing raw data and processed data on magnetic tapes, and post processing raw data. The data are received from two asynchronous Laser Doppler Velocimeters and include position, velocity, and intensity information. The raw data are written onto magnetic tapes for permanent storage and are also processed in real time to locate vortices and plot their positions as a function of time. The processed data may be stored on disk and later written to tape using a utility program. Additional post analysis of the SLDV data is performed on the system's high speed PCM data tape using the MSFC-Computer Laboratory's Univac 1108 and Raytheon's Control Data Corporation 6700. This section will describe the data processing algorithms and displays and their applications to the SLDV data in the field and in processing facilities offsite. A more complete description of their operations can be found in References 7 and 8.

4.2 Onsite Data Processing and Display

The onsite processing, real and post time, is performed with the PDP-11 computer system which is described in Section 3.3.10. The onsite processing capability is designed with interactive capabilities to permit system operators and engineers to obtain, in real time, sufficient information to determine vortex characteristics and location, preliminary system performance, and to modify those system operating and data processing parameters when necessary to make system and data collection improvements.

For post analysis the processing capability is designed to provide detailed data information to permit engineers to determine system and subsystem performance. The post-analysis capability naturally serves as a diagnostic tool for troubleshooting the system when problems are detected.

The data available to the computer from the signal processor include position coordinates (x and y), N, I_{pk}, V_{max}, and V_{pk}. Definitions of these data parameters are given in Figure 4-2, which shows a typical velocity-amplitude

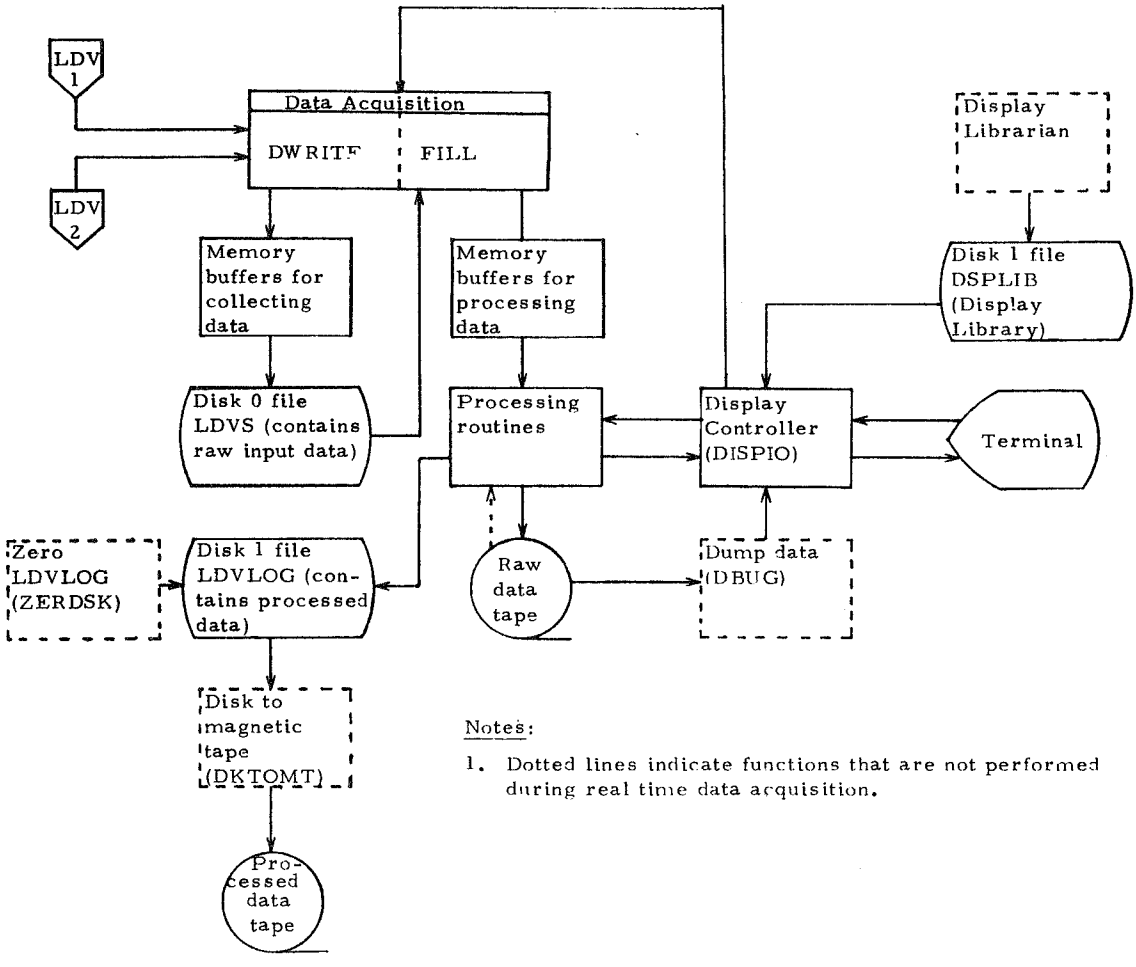

Figure 4-1. VIDS flow chart.

V_{pk} = VELOCITY OF HIGHEST CHANNEL ABOVE AMPLITUDE THRESHOLD

V_{max} = VELOCITY OF THE CHANNEL HAVING THE PEAK SIGNAL

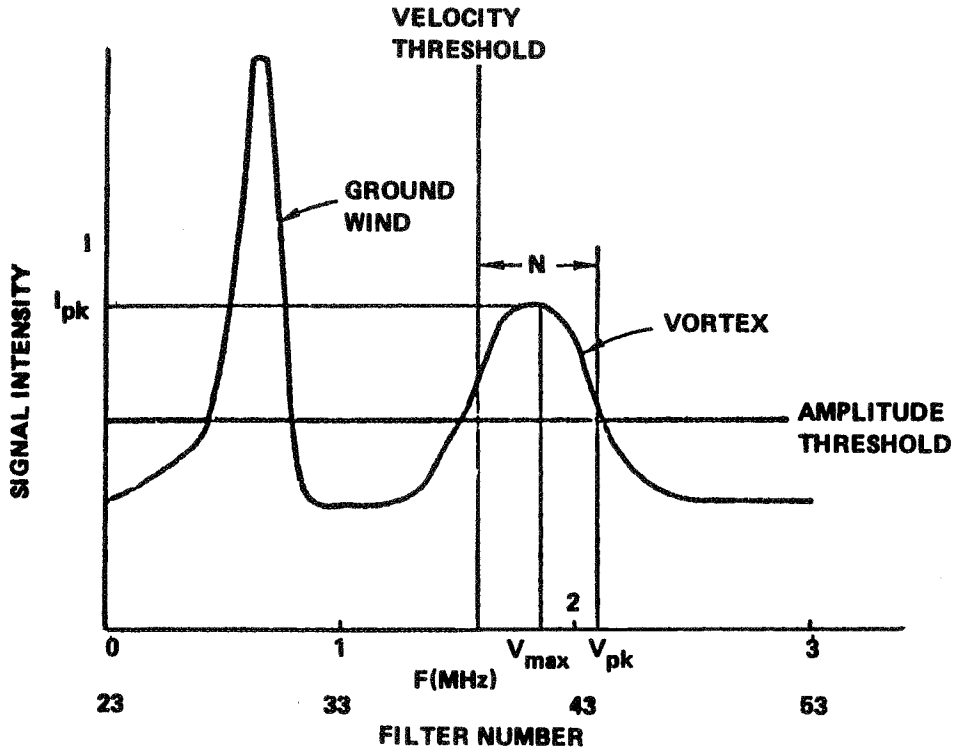

Figure 4-2. Sample spectrum output.

spectrum output. The data processing algorithms used in onsite processing use various combinations of these parameters to determine vortex location, range-elevation calibration, and wind profiles.

4.2.1 Real Time Data Processing and Displays

The original data processing algorithms on the PDP-11 used V_{pk} as an indicator of the presence of a vortex. Good results could be obtained only when thresholds were properly set and low crosswinds were present. As a result of high and low speed data tape analysis, a number of modifications to this program were implemented to improve operation and extend its capability to more adverse weather conditions. First, the analysis suggested that I_{pk} be

used in place of V_{pk} to reduce the algorithm sensitivity to threshold settings. This was accomplished at the end of the first set of airport tests at JFK Airport. Analysis of the early data indicated a need for stronger criteria for determining when only one vortex was present in the scan frame. The data analysis indicated that coefficients should be used in the algorithm in such a manner that for a second vortex to exist B percent of the points in a correlation region must have the parameter I_{pk} or V_{pk} greater than A percent of the highest parameter in vortex one. Previously, it had been required that B percent of the points in a correlation region have a parameter exceeding A percent of the highest parameter in that correlation region itself rather than in that of vortex one. Also, the high speed data analysis showed that the number of points in the correlation region for the second vortex should exceed C percent of the number of points in the correlation region for the first vortex. This avoids the situation where a single vortex is present with a few points outside its correlation region. The I_{pk} and C parameter changes were introduced into the program between the first and second JFK Airport tests.

The data processing algorithms available to the system operators for real time processing include the V_{pk} algorithm, I_{pk} algorithm, and range-elevation calibration algorithms. The V_{pk} algorithm will be discussed in Section 4.2.1.1; the I_{pk} algorithm will be discussed in Section 4.2.1.2; and the range-elevation calibration will be discussed in Section 4.2.1.3.

4.2.1.1 V_{pk} Algorithm

The original vortex location algorithm, developed at MSFC, uses V_{pk} as the most significant parameter. The algorithm checks the number of data points in the scan frame to insure that a sufficient number of data points exist (> 2) to define a vortex. Then it selects the highest V_{pk} in a scan frame and uses the x, y coordinates of this point as the center of a correlation circle of radius R (Fig. 4-3), where R is selected by the system operator based on vortex generation, aircraft type, and previous experience. (A scan frame is defined as a single scan in elevation between the specified upper and lower limits.) Once the correlation circle has been defined, the algorithm requires that at least B percent of the points which lie within the circle have a V_{pk} greater than or equal to A percent of the initially selected V_{pk}. If this criterion is not met, the selected V_{pk} is discarded as a spurious signal and the next

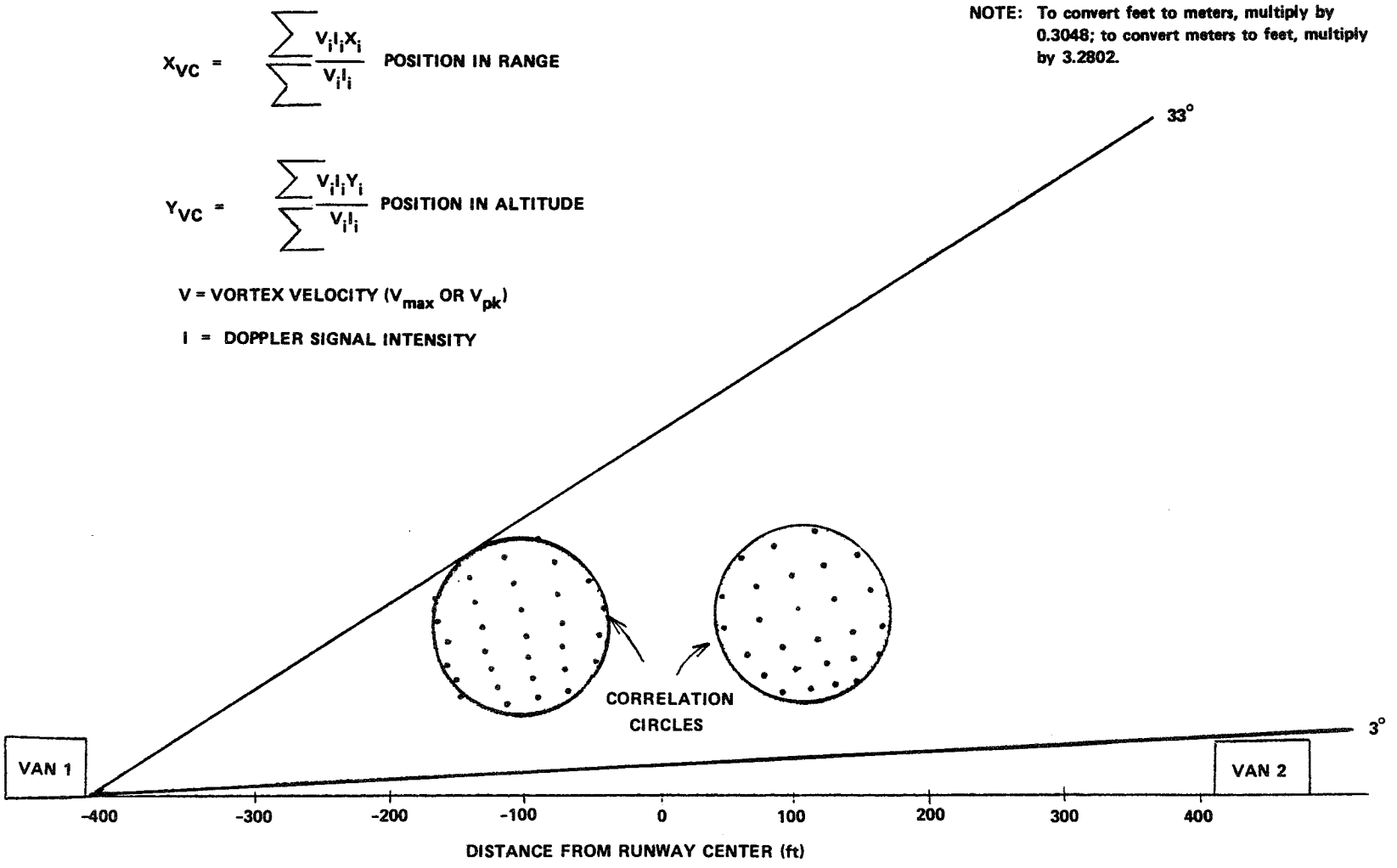

Figure 4-3. Vortex location algorithm outline.

highest V_{pk} is selected until the A and B percentage criterion is met. Once this occurs, a weighted average x and y positions coordinate are computed for all points in the circle using V_{pk}, I_{pk} as the weighting function as shown below:

$$x_{vc} = \frac{\sum V_i I_i x_i}{\sum V_i I_i} \qquad y_{vc} = \frac{\sum V_i I_i y_i}{\sum V_i I_i}$$

where x_{vc} and y_{vc} arc vortex centroid x and y positions, respectively.

Following this calculation, all the data points outside a circle of radius $N_s \cdot R$, centered at the previously calculated vortex center (x_{vc}, y_{vc}), are examined to determine the highest remaining V_{pk}. (N_s is an operator selectable multiplication factor 1, 2, etc.) If this point has C percent of the number of data points in its correlation region that were found in the first vortex' s correlation region and if B percent of the point in its correlation region have V_{pk} greater than A percent of the highest V_{pk} in vortex one, then a second vortex exists in the scan frame. If this criterion is met, then a weighted average is found for its location as described for vortex one.

On a scan frame by scan frame basis, a final validity check is performed between consecutive scans; it is required that the high V_{pk} in a scan be greater than D percent of the V_{pk} for the previous scan.

Parameters A, B, C, D, R, N_s are operator controlled and are selected by the operator based on aircraft type, wind conditions, and previous experience. The value of these input parameters are printed on each real-time data algorithm processor display.

4.2.1.2 I_{pk} Algorithm

The I_{pk} algorithm was implemented in real time due to the high degree of success obtained in a similar algorithm used in post analysis of the high speed data tapes. This algorithm is essentially the same as the V_{pk}

algorithm with the exception that it uses I_{pk} as the key parameter instead of V_{pk}. Analyses have shown that the vortex areas have a higher atmospheric backscatter efficiency than the normal atmosphere and, thus, the I_{pk} signal return from the vortex areas are a good initial indicator of vortex positions. This algorithm appears to give a significant improvement in vortex location over the V_{pk} algorithm. The I_{pk} algorithm was used exclusively in the latter part of the test program. Examples of the displayed data resulting from processing with the I_{pk} algorithm are shown in Figure 4-4, a time history plot of vortex position relative to the runway centerline; Figure 4-5, an x-y plot of vortex position using A, B, C, etc. to denote successive elevation scan frames; and Figure 4-6, a tabular output of key data parameters.

4.2.1.3 Range-Elevation Calibration Algorithm

This algorithm is used with either of the previously mentioned algorithms. It was developed to calibrate the system in range and at zero elevation on a rotating disk fixed at a given point in the field of view of the system. The operation of the algorithm is the same as the I_{pk} and V_{pk} algorithms. However, since the target is fixed at a known location, it now becomes meaningful to calculate a mean location of the target. In operation, the algorithm provides a target location on a scan frame-by-scan frame basis for 30 frames. At the end of 30 frames, the mean and standard deviation of the target locations are displayed (Fig. 4-7).

For calibration and diagnostic purposes, a large error in the calculated mean range and/or elevation to known target indicated range and/or elevation calibration problems, which can be immediately corrected by engineers in the field. A large standard deviation about the mean range and/or elevation to known target indicates scanner malfunctions or processor problems which can be corrected, once identified.

4.2.2 Post Data Processing and Display Algorithms

All the processing algorithms used in real time are also available for post data analysis. In addition to these, four other algorithms are available to the system operator and engineers for more detailed data/system analysis, diagnostics, and wind flow field analysis. These are the V_{pk} scatter plots, I_{pk} scatter plots, DBUG, and wind profile.

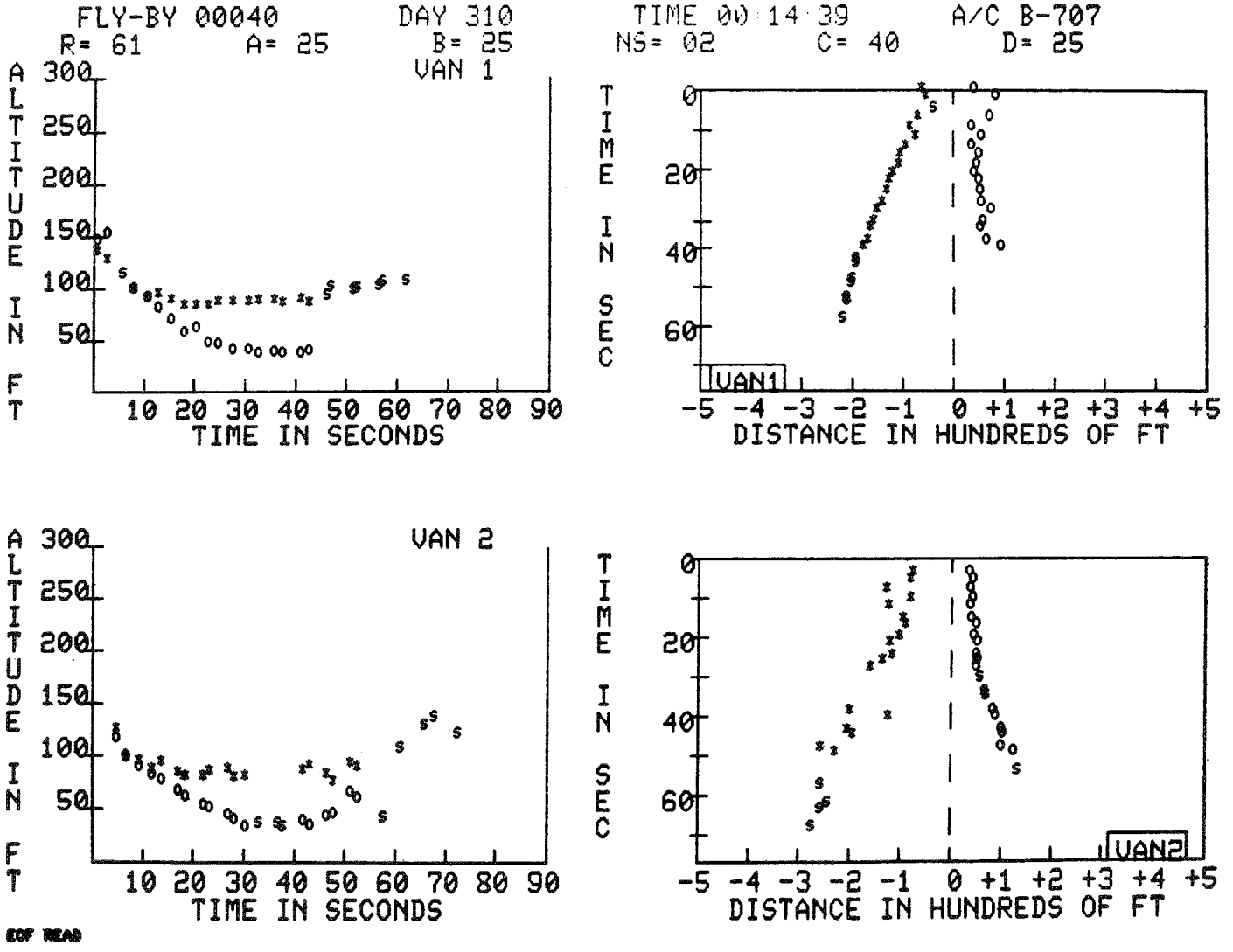

Figure 4-4. Sample time-based data plot.

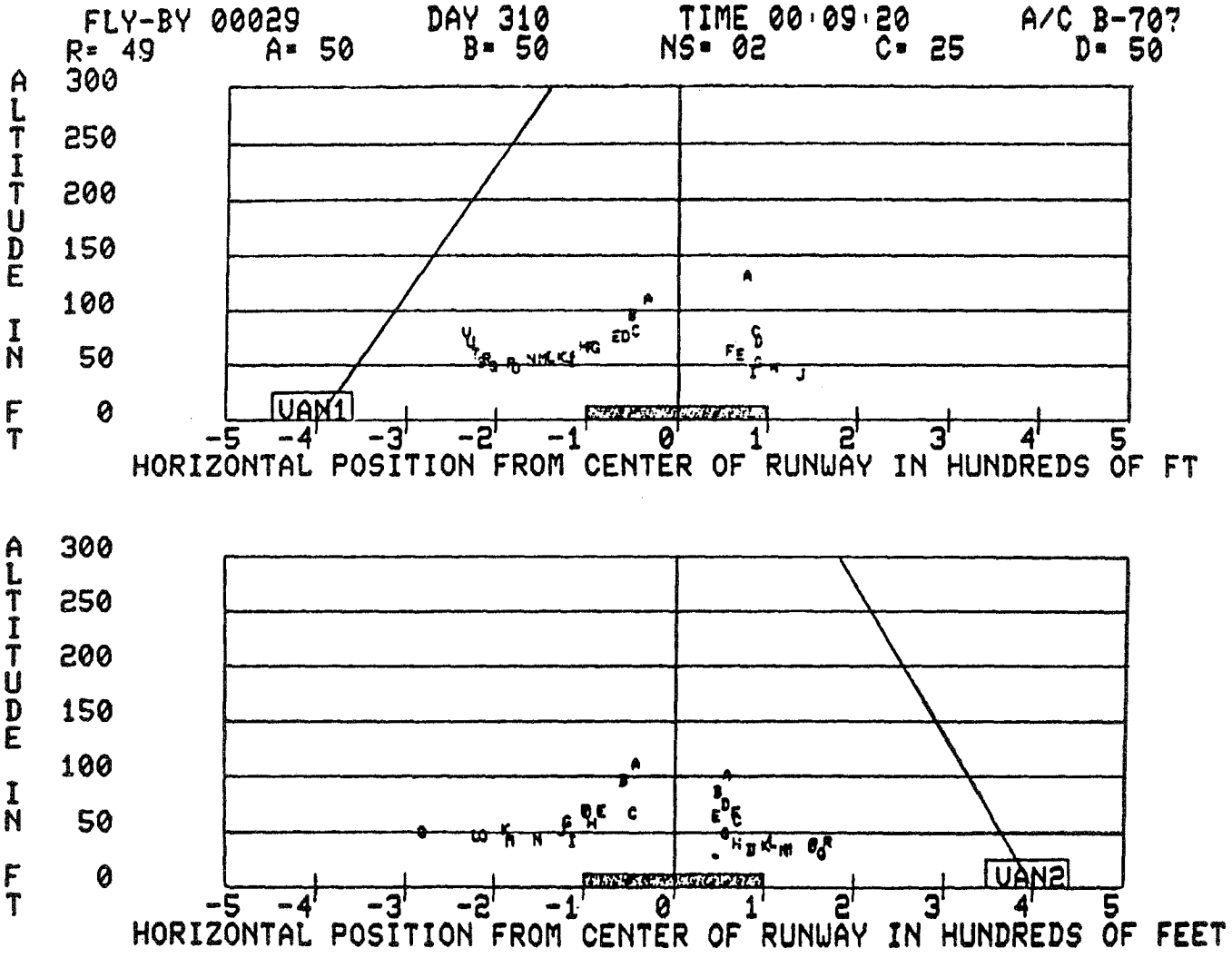

Figure 4-5. Sample x, y data plot.

FLY-BY 00040 DAY 310 TIME 00:15:27 A/C B-707
R= 49 A= 25 B= 25 NS= 02 C= 40 D= 25

FR	DATA PTS	COR PT P	COR PT S	NOISE P	NOISE S	ANGLE MN	ANGLE NX	PK VEL P	PK VEL S	TIME	PORT POS X	PORT POS Y	STARB POS X	STARB POS Y
01	0094	040	031	00	00	15	25	045	054	000 1	-065	132	040	143
02	0076	029	015	00	00	14	24	043	041	002 0	-064	122	085	152
03	0073	043	006	00	05	12	21	046	036	005 1	-045	111		
04	0069	032	012	00	00	09	20	045	043	007 3	-079	095	072	096
05	0046	020	015	00	00	09	18	043	039	010 0	-095	088	035	088
06	0060	026	021	00	00	07	19	043	037	012 3	-076	094	056	080
07	0055	028	014	00	00	07	18	045	037	014 9	-103	085	020	063
08	0051	028	017	00	00	06	19	039	041	017 3	-110	082	053	055
09	0043	019	014	00	00	06	19	041	039	019 9	-116	081	048	060
10	0060	023	015	00	00	04	20	045	045	022 3	-132	078	028	044
11	0054	028	016	00	00	04	20	041	043	024 0	-136	083	041	042
12	0059	034	022	00	00	04	22	043	037	027 1	-135	085	046	037
13	0059	027	025	00	00	04	22	043	039	030 0	-151	083	052	037
14	0039	020	013	00	00	04	23	039	039	032 0	-157	084	076	035
15	0054	027	024	00	00	03	24	043	039	035 1	-164	086	057	035
16	0031	022	008	00	01	04	25	041	036	036 8	-170	083	058	035
17	0039	023	013	00	00	03	25	043	039	040 2	-177	085	056	034
18	0034	021	010	00	00	03	22	041	039	042 0	-185	083	097	037
19	0034	026	000	00	00	04	29	039	000	045 4	-198	089		
20	0020	020	000	00	00	23	29	039	000	046 3	-198	097		
21	0020	020	000	00	00	23	30	041	000	050 7	-205	096		
22	0014	014	000	00	00	25	27	041	000	051 5	-209	096		
23	0013	013	000	00	00	27	29	039	000	055 8	-219	099		
24	0013	013	000	00	00	28	29	041	000	056 5	-215	102		
25	0004	004	000	00	00	30	30	034	000	061 1	-225	103		

FR	DATA PTS	COR PT P	COR PT S	NOISE P	NOISE S	ANGLE MN	ANGLE MX	PK P	PK VEL S	TIME	PORT POS X	PORT POS Y	STARB POS X	STARB POS Y
02	0067	021	027	00	00	11	21	032	034	004 1	-075	125	035	113
03	0060	019	021	00	00	08	18	030	037	006 1	-056	095	045	096
04	0071	018	023	00	00	08	16	032	036	008 6	-139	094	033	087
05	0043	014	014	00	00	08	15	032	028	011 3	-092	086	040	076
06	0048	013	016	01	00	07	18	030	030	013 1	-135	090	037	073
07	0030	014	010	00	00	07	12	030	028	016 4	-100	079	030	064
08	0025	010	007	00	00	07	12	027	030	017 9	-085	076	052	053
09	0029	009	013	00	00	05	11	028	030	021 4	-114	079	044	049
10	0019	003	006	00	00	05	11	027	028	022 7	-141	072	055	046
11	0023	007	015	00	00	04	10	030	032	026 3	-116	081	044	041
12	0027	005	015	01	00	03	28	030	028	027 6	-142	077	045	037
13	0015	006	007	00	00	03	28	036	027	029 5	-171	079	043	030
14	0017	000	012	03	00	03	11	000	032	032 2			054	033
15	0024	000	018	00	00	03	10	000	030	036 1			059	034
16	0024	000	016	04	00	03	08	000	028	037 0			070	028
17	0022	006	010	00	00	03	00	030	027	041 8	-211	085	075	035
18	0025	003	014	01	00	03	11	181	028	042 4	-127	090	082	031
19	0025	010	011	00	00	04	10	028	025	045 8	-207	080	088	041
20	0021	005	013	01	00	04	11	021	025	047 1	-216	073	098	040
21	0011	002	006	00	01	07	12	023	019	050 6	-263	090	095	063
22	0011	007	003	00	00	07	12	021	019	052 0	-234	086	110	057
23	0001	001		00		08	08	018						
24	0005	000	004	00	01	07	09	000	017	056 9			126	030
25	0004	004	000	00	00	08	11	019	000	060 4	-263	105		
26	0001	001		00		08	08	018						
27	0002	002	000	00	00	09	12	018	000	065 2	-249	126		
28	0006	005	000	00	00	09	12	019	000	066 9	-271	133		
30	0003	003	000	00	00	09	09	018	000	071 7	-280	118		
32	0001	001		00		10	10	018						
34	0001	001		00		12	12	021						
35	0002	000		01		11	14	000						
36	0003	002	000	00	00	11	15	019	000	086 6	-262	158		
39	0001	001		00		15	15	019						
40	0001	001		00		16	16	019						

NOTE: TABULAR DATA PARAMETERS ARE:
FR = ELEVATION SCAN FRAME NO.
DATA PTS = NUMBER OF DATA POINTS IN INDIVIDUAL SCAN FRAMES
COR PT (P&S) = NUMBER OF DATA POINTS IN THE CORRELATION RADIUS FOR THE PORT (P) AND STARBOARD (S) VORTICES
ANGLE (MN MX) = MINIMUM AND MAXIMUM ELEVATION ANGLE FOR WHICH DATA POINTS ASSOCIATED WITH THE VORTICES ARE FOUND FOR A GIVEN ELEVATION SCAN FRAME
PK VEL (P&S) = PEAK VELOCITY ASSOCIATED WITH THE PORT (P) AND STARBOARD (S) VORTICES
TIME = TIME ASSOCIATED WITH THE VORTICES' POSITION FOR AN INDIVIDUAL SCAN FRAME AND MEASURED FROM THE FLYBY TIME GIVEN IN THE HEADER INFORMATION
PORT POS = PORT VORTEX POSITION IN FEET MEASURED RELATIVE TO THE RUNWAY CENTERLINE
STARB POS = STARBOARD VORTEX POSITION IN FEET MEASURED RELATIVE TO THE RUNWAY CENTERLINE

EOF READ

Figure 4-6. Sample tabular data output.

FLY-BY 00000 DAY 296 TIME 02 10 51 A/D WHEEL
R= 77 A= 01 B= 02 NS= 02 I= .25 D= 01

FR	DATA PTS	COR P	COR S	PT P	PT S	NOISE P	NOISE S	ANGLE MN	ANGLE MX	PK P	VEL S	TIME	PORT POS X	PORT POS Y	STARB POS X	STARB POS Y
01	0131	000	130	00	00	00	00	000	014	003	7				169	002
02	0107	000	107	00	00	00	00	000	014	006	1				168	002
03	0116	000	107	00	00	00	00	000	014	007	1				165	002
04	0149	000	148	00	00	00	00	000	014	011	1				177	002
05	0123	000	122	00	00	00	00	000	014	013	6				169	002
06	0153	000	136	00	00	00	00	000	014	013	7				168	002
07	0150	000	145	00	00	00	00	000	014	018	6				170	002
08	0099	000	098	00	00	00	00	000	014	018	7				165	002
09	0088	000	088	00	00	00	00	000	014	023	6				160	002
10	0129	000	126	00	00	00	00	000	005	026	0				168	002
11	0109	000	109	00	00	00	00	000	014	028	6				164	002
12	0119	000	116	00	00	00	00	000	016	028	6				156	002
13	0122	000	122	00	00	00	00	000	014	033	5				169	002
14	0122	000	111	00	00	00	00	000	014	033	6				165	002
15	0130	000	130	00	00	00	00	000	014	038	5				169	002
16	0130	000	120	00	00	00	00	000	014	041	0				164	002
17	0125	000	125	00	00	00	00	000	014	043	5				169	002
18	0117	000	117	00	00	00	00	000	014	045	9				172	002
19	0127	000	127	00	00	00	00	000	014	046	0				170	002
20	0105	000	105	00	00	00	00	000	014	050	9				153	002
21	0106	000	106	00	00	00	00	000	014	053	5				165	002
22	0113	000	113	00	00	00	00	000	014	055	3				165	002
23	0133	000	127	00	00	00	00	000	014	058	5				167	002
24	0131	000	131	00	00	00	00	000	016	058	5				168	002
25	0145	000	118	00	00	00	00	000	014	063	4				160	002
26	0117	000	117	00	00	00	00	000	014	065	9				179	002
27	0099	000	096	00	00	00	00	000	014	068	4				172	002
28	0128	000	126	00	00	00	00	000	014	070	9				156	002
29	0102	000	101	00	00	00	00	000	014	073	4				158	002
30	0126	000	121	00	00	00	00	000	014	075	8				164	002

AVG=(00566.00002) STD=(005.000)

FR	DATA PTS	COR P	COR S	PT P	PT S	NOISE P	NOISE S	ANGLE MN	ANGLE MX	PK P	VEL S	TIME	PORT POS X	PORT POS Y	STARB POS X	STARB POS Y
01	0016	016	000	00	00	00	00	016	000	001	7		-161	000		
02	0031	030	000	00	00	00	00	016	000	004	0		-157	000		
03	0031	029	000	00	00	00	00	018	000	006	6		-153	000		
04	0058	055	000	00	00	00	00	019	000	008	8		-155	000		
05	0030	025	000	00	00	00	00	018	000	011	4		-153	000		
06	0056	054	000	00	00	00	00	016	000	013	7		-153	000		
07	0072	063	000	00	00	00	00	018	000	016	2		-159	000		
08	0030	030	000	00	00	00	00	018	000	018	5		-153	000		
09	0047	047	000	00	00	00	00	016	000	021	0		-162	000		
10	0038	035	000	00	00	00	00	016	000	023	3		-147	000		
11	0036	036	000	00	00	00	00	016	000	025	7		-149	000		
12	0032	032	000	00	00	00	00	018	000	028	1		-152	000		
13	0049	048	000	00	00	00	00	016	000	030	5		-157	000		
14	0046	046	000	00	00	00	00	018	000	032	8		-160	000		
15	0016	016	000	00	00	00	00	018	000	035	2		-145	000		
16	0038	036	000	00	00	00	00	016	000	037	7		-159	000		
17	0037	034	000	00	00	00	00	016	000	040	1		-154	000		
18	0037	037	000	00	00	00	00	016	000	042	5		-161	000		
19	0031	030	000	00	00	00	00	018	000	044	9		-165	000		
20	0019	016	000	00	00	00	00	016	000	047	3		-153	000		
21	0037	036	000	00	00	00	00	018	000	049	4		-159	000		
22	0035	035	000	00	00	00	00	016	000	052	1		-160	000		
23	0030	028	000	00	00	00	00	013	000	054	2		-156	000		
24	0030	030	000	00	00	00	00	016	000	056	7		-160	000		
25	0036	035	000	00	00	00	00	016	000	059	3		-144	000		
26	0027	027	000	00	00	00	00	013	000	061	7		-160	000		
27	0044	044	000	00	00	00	00	018	000	064	1		-153	000		
28	0025	024	000	00	00	00	00	018	000	066	4		-155	000		
29	0030	029	000	00	00	00	00	016	000	068	9		-140	000		
30	0053	045	000	00	00	00	00	016	000	071	2		-162	000		

AVG=(00555.00000) STD=(005.000)

EOF READ

Figure 4-7. Sample calibration data output.

4.2.2.1 V_{pk} Scatter

The V_{pk} scatter algorithm displays the raw data points in the post processing mode, showing their location in the vertical scan plane and their velocities within 10 ft/sec (3 m/s). The characters 0 through 9 correspond to 10 ft/sec (3 m/s) velocity increments which start at 20 ft/sec (6 m/s) for 0 and go to 120 ft/sec (36 m/s) for 9. The 10 highest velocity data points have the actual velocities printed at the bottom of the display in ft/sec. Those 10 velocities are plotted as characters A through J. The V shown in the scatter plots indicates the calculated centers for vortices using the V_{pk} location algorithm parameters given at the top of Figure 4-8.

4.2.2.2 I_{pk} Scatter

The I_{pk} scatter algorithm displays the raw data points in the post processing mode, showing their location in the vertical scan plane and their signal amplitude within 10 units. The characters 0 through 9 correspond to 10 amplitude unit increments which start at 20 for 0 and go to 120 for 9. The 10 highest signal amplitude data points have the actual amplitudes printed at the bottom of the display (scale from 0 to 256). Those 10 signal amplitudes are plotted as characters A through J. The I shown in the scatter plots indicates the calculated centers for vortices using the I_{pk} location algorithm parameters given at the top of Figure 4-9.

4.2.2.3 DBUG

The DBUG algorithm is used to provide a numerical listing of the raw positions, intensity, and velocity data in counts which is accepted and recorded by the PDP-11 data algorithm processor. This enables the operator to determine the correctness/reasonableness of the input parameters to the data-algorithm processor. An example of this display is shown in Figure 4-10.

4.2.2.4 Wind Profile

The wind profile data algorithm requires the simultaneous operation of both SLDV in the elevation and range scanning modes for collection of the data. The data processing is performed in a post processing mode and requires that a common area of space be covered by both systems. For wind profile

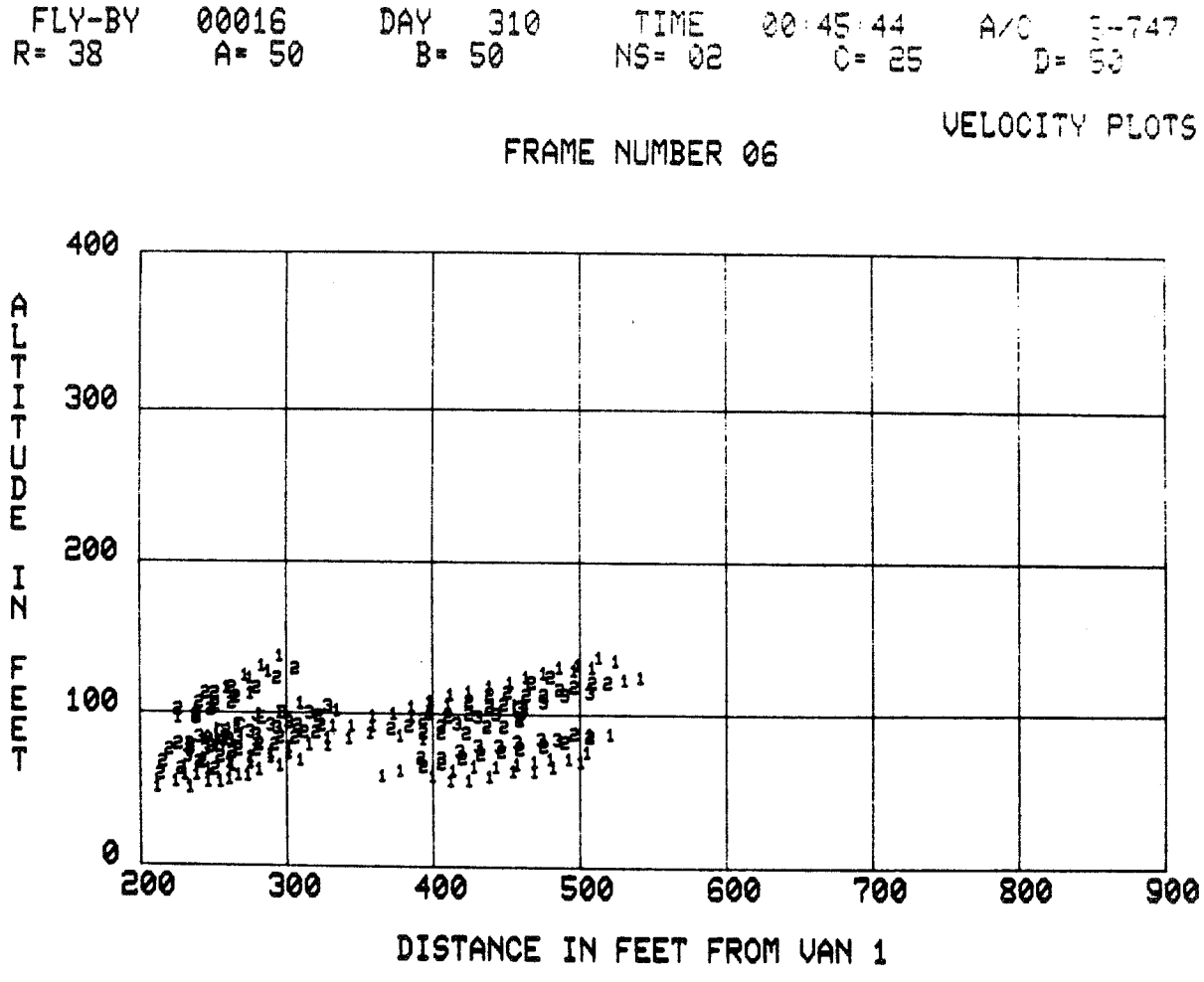

Figure 4-8. Sample V_{pk} scatter plot.

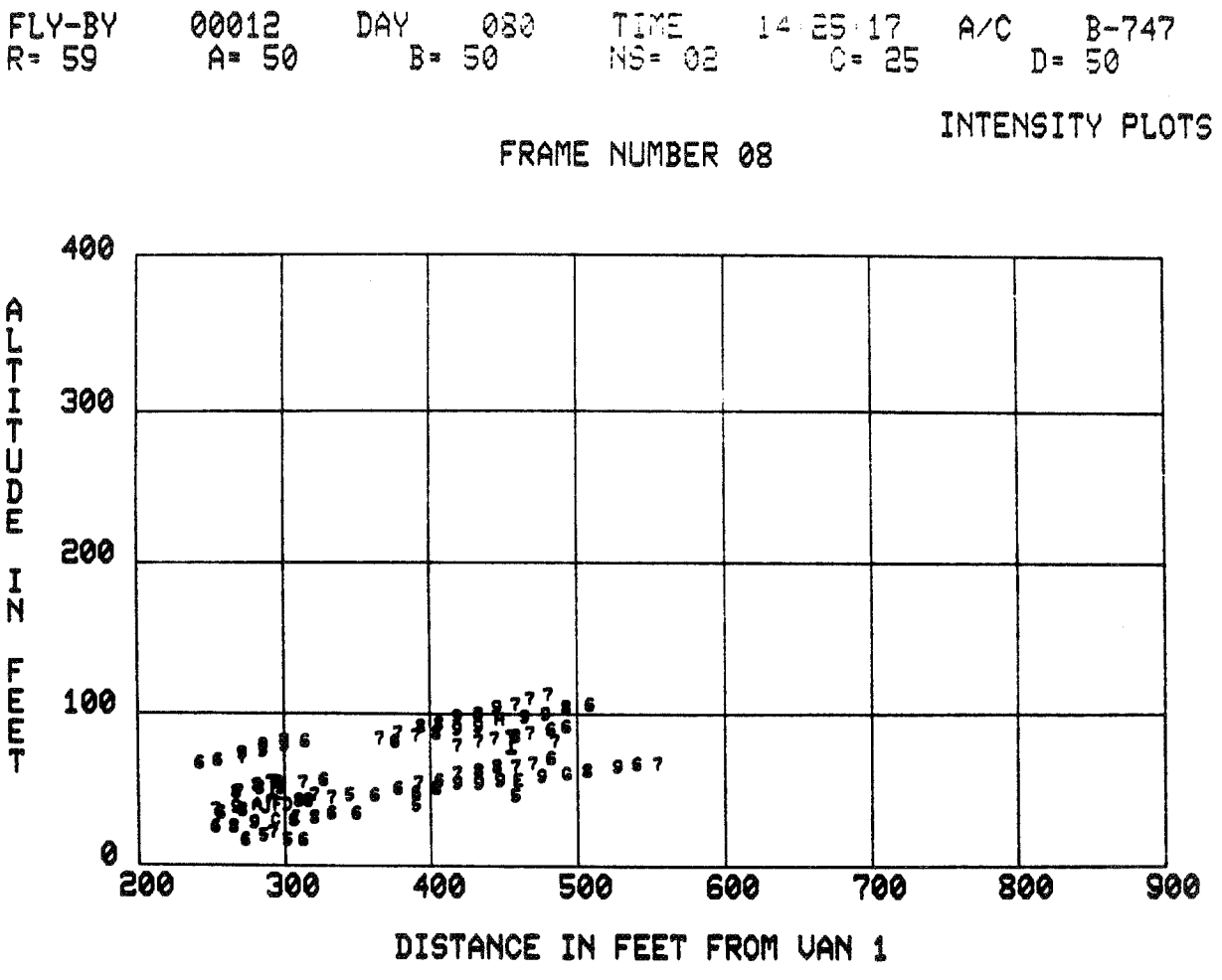

Figure 4-9. Sample I_{pk} scatter plot.

```
IFLY=    12     IFRM=   -15     FIRST TIME =    34  25463     LAST TIME=    34  25511
IDAY=    80 IPLN=    10 NUMPTS=    110

MINIMUM INTENSITY =    73

                  X          Y          I          N         UP         UM
  1             178         11        153          3         19         18
  2             186         11         93          2         18         17
  3             192         12         88          2         18         17
  4             200         13         77          1         18         18
  5             214         14         80          2         18         17
  6             267         17         76          2         18         18
  7             355         24         76          1         17         17
  8             242         16         85          2         19         19
  9             234         15         77          1         17         17
 10             220         15         77          1         18         18
 11             214         14         80          1         18         18
 12             206         14         76          1         19         19
 13             191         13        104          4         21         21
 14             184         13        104          3         19         18
 15             177         12        140          5         21         19
 16             170         11        148          5         21         19
 17             162         11        145          4         20         18
 18             155         10        140          4         20         19
 19             147         10         97          3         20         18
 20             140          9        108          3         19         18
 21             133          9         89          1         18         18
 22             137          9         89          2         20         19
 23             146         10        160          5         21         20
 24             154         11        161          4         20         18
 25             160         12        148          6         22         18
 26             166         12        120          5         21         19
 27             173         12        117          5         21         19
 28             180         13        108          3         19         18
 29             187         13         84          2         20         19
 30             194         14         81          1         19         19
 31             202         15         77          1         19         19
 32             208         15         81          1         19         19
 33             332         26         81          1         17         17
 34             339         27         97          1         17         17
 35             346         27         96          1         17         17
 36             351         28        108          1         17         17
 37             357         29        112          2         18         17
 38             364         29        116          2         18         17
 39             368         30        105          1         17         17
 40             371         30        104          2         18         17
 41             368         30        124          2         18         17
 42             367         30        117          2         18         17
 43             360         30        117          2         18         17
 44             354         29        104          2         18         17
 45             347         28        116          3         19         18
 46             342         28         81          2         18         17
 47             336         28         89          2         18         17
 48             330         27        100          2         18         17
 49             325         27        112          2         18         17
 50             319         26         89          2         18         18
 51             313         27         96          2         18         18
 52             307         26        128          3         19         18
 53             301         26         96          2         18         18
 54             295         25         89          2         18         18
```

Figure 4-10. Sample DBUG output.

NOTE: THE FIRST COLUMN INDICATES THE DATA POINT NUMBER. THE OTHER COLUMNS GIVE THE VALUE OF THE PARAMETER IN COUNTS.

measurements, the systems are employed in the same configuration as in the vortex measurements. Data acquisition is accomplished using the same basic system operating parameters. The amplitude and velocity thresholds of the signal processor are set to insure atmospheric wind detection and to eliminate signal noise. The signal integration time may be increased as desired to reduce the total number of data points in the scan frame. The data from the two independent systems are then processed to insure time correlation between scan frames and data points. After a time correlation is obtained, the data are examined to find the data points from each sensor that are most closely correlatable spatially. These points, together with their velocity information, are stored and compared to an input spatial correlation requirement. The pairs of data points that meet the requirement are analyzed to provide the vertical and horizontal velocity components associated with their common position in the system's scan plane. Figure 4-11 shows the average horizontal and vertical wind velocity in the common scan area of the vertical plane between the two sensors as a function of altitude for a given time. Time correlation, spatial correlation, and altitude increments for the calculations in this figure are 1.25 sec, 7 ft (2 m), and 20 ft (6 m), respectively.

4.2.2.5 Least-Square Curve-Fit Calculation for Vortex Tracks

An onsite application software package which applies curve fitting to two-dimensional displays of data points was developed to provide least-square curve-fitted vortex tracks (Fig. 4-12). A Chebyshev least-square curve-fitting algorithm was used. The curve fitting, in general, applies to spatially distributed location points as well as time-based plots of data. A complete documentation of this least-square curve-fit calculation technique, including software programs, is given in Reference 9.

4.3 Offsite Data Processing and Displays

Offsite processing is accomplished on the data which are recorded directly from the signal processor filter bank. This high speed PCM tape (see Section 3.11) is then processed according to the flow chart shown in Figure 4-13. This tape is used for detailed data/system analysis and system performance evaluation. In the early program development this tape was used to help determine the computing requirements of the real time computer to be used in the system and to develop and check out the algorithms to be used in the on-line data algorithm processor. A processed data tape, created from the high speed PCM tape by PCM decommutation and computer reformatting, serves as input

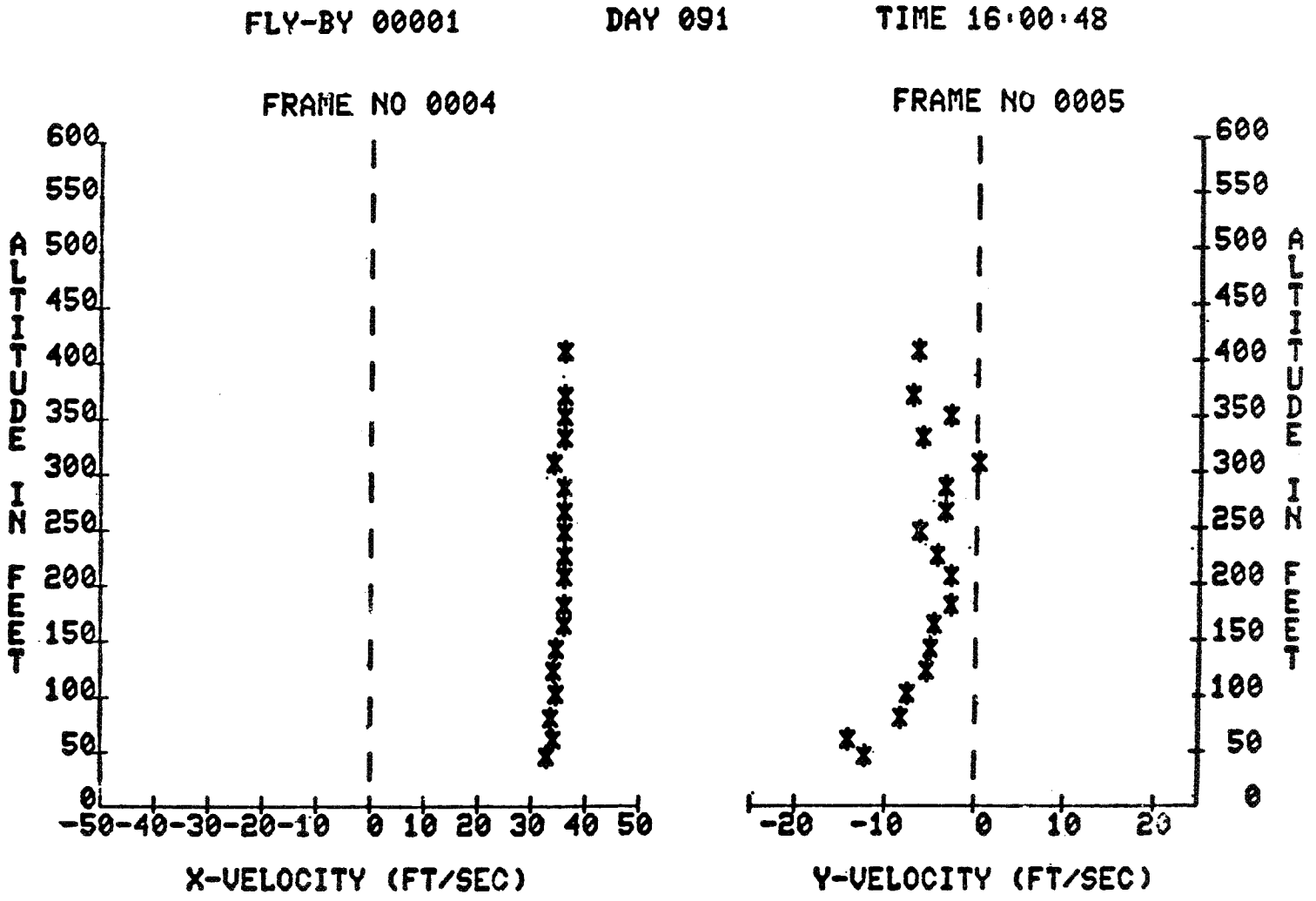

Figure 4-11. Sample wind profile plot.

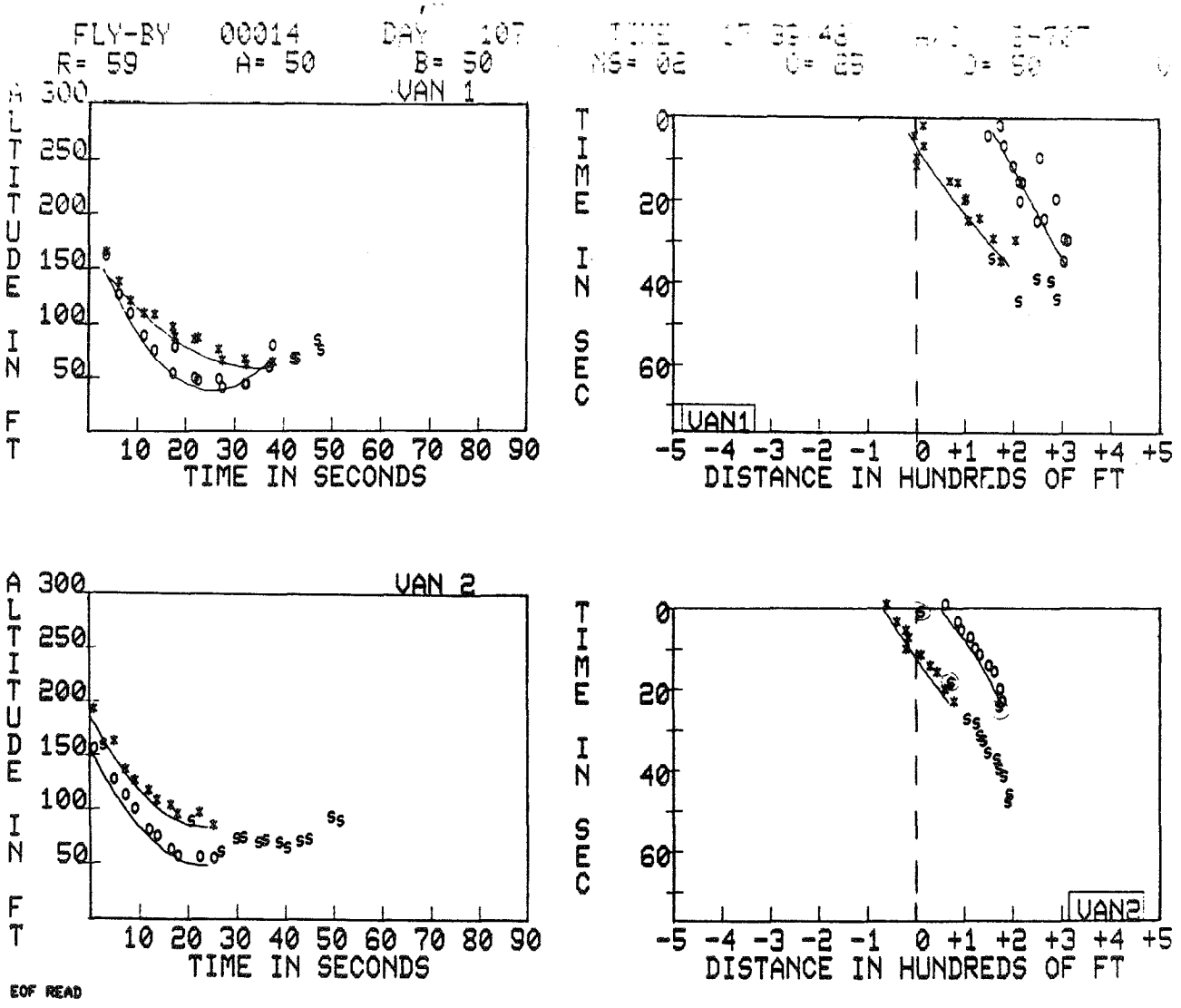

Figure 4-12. Sample least-square-fit vortex transport plot.

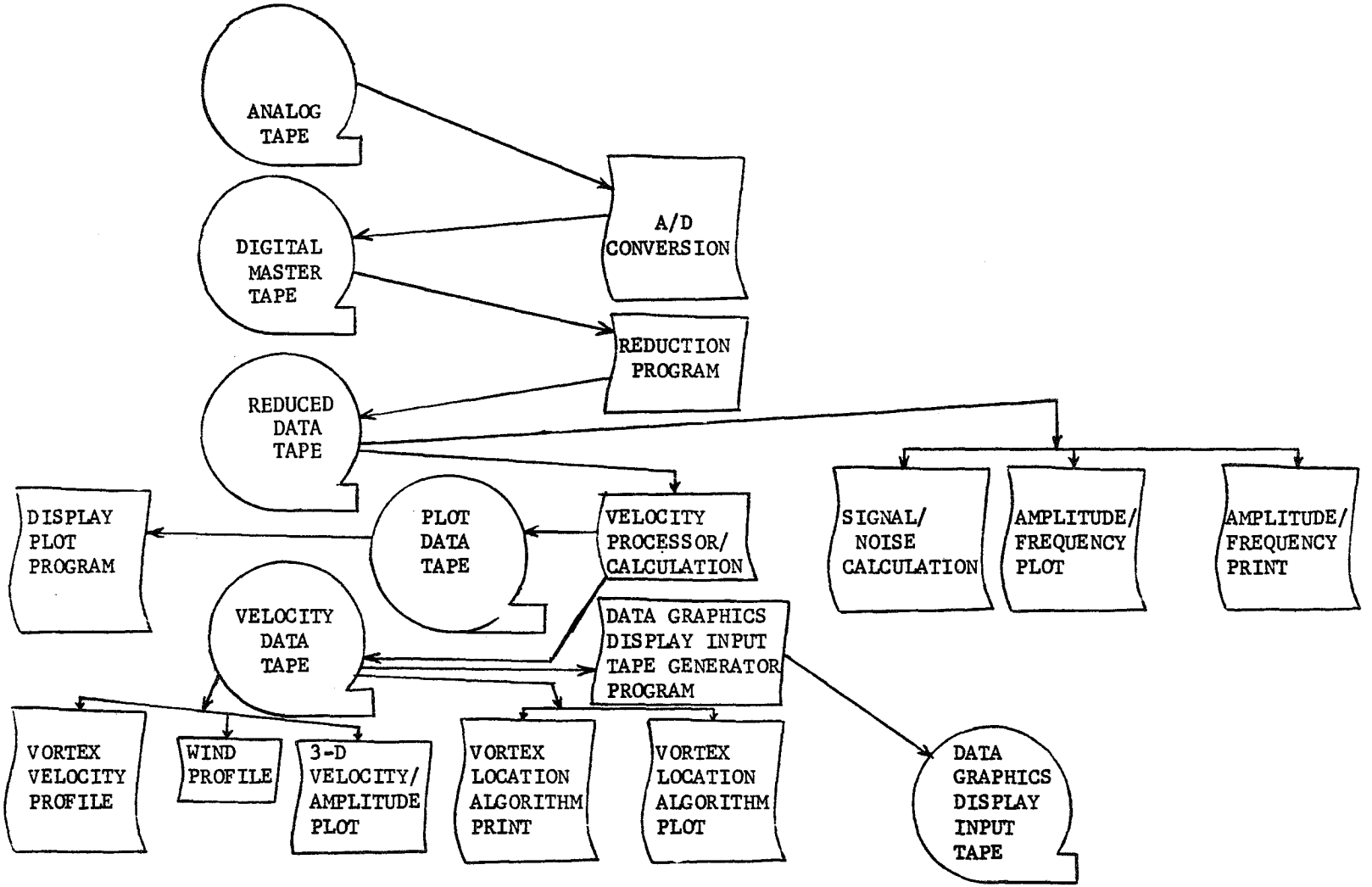

Figure 4-13. High speed data processing flow chart.

to the vortex location program. This program consists of several location algorithms and is used to select the optimum method of real-time processing and display. Comparisons of this processed tape with data from the on-line data algorithms processor provides a very important system data verification mechanism.

4.3.1 High Speed Data Processing

In the operation of the Laser Vortex Detection System, a tape recording is made of pulse-code-modulated data consisting of a data frame number, x and y coordinates, time, and the amplitudes of 104 integrated velocity filters following the surface acoustic wave spectrum analyzer. Also included in these data is identification of the run number and the mode of operation of the system for the particular test. These data represent all the information which the system collects during the selected integration time (0.5 to 64 ms). These data are more than sufficient to determine vortex location and is, in fact, processed in order to reduce the data before any information is sent to the real-time data algorithm processor. However, for system analysis and more detailed study of the flow field of a vortex, it is desirable to have this complete set of data available. Thus, a number of programs were developed to analyze these data for various purposes. The high speed data are converted from PCM format to digital format on the MSFC PCM decommutation system. The MSFC Univac 1108 computer reformats the data to seven track magnetic tapes and these tapes are employed for data and system analysis. These data tapes are used for three specific purposes during the analysis program. First, the data are used to evaluate system performance and to determine specific system problems when they occur. Second, when the system is operating correctly, the data are used in development of the optimum algorithm and in determination of the required thresholds and other processor settings to be used. Third, when the vortex location task is being performed reliably in real time by the on-line data algorithm processor, these data are used primarily for analysis of vortices in greater detail to include flow field analysis and circulation calculations. During the entire analysis program, continual assessment of system performance and analysis of specific problems were performed. These requirements were met with programs described in the following sections. In Section 4.3.1.1, the cell output program is described. This program merely presents all data of interest in a format in which it can be clearly understood and easily evaluated. In Section 4.3.1.2, a program is described which analyzes the data from calibration runs yielding results which are useful in determining the signal-to-noise ratio and range resolution from hard target tests.

Section 4.3.1.3 describes a vortex location algorithm which is used on the data to produce vortex locations in each scan of data. This algorithm represents the end result of a number of different attempts at vortex location which were made to determine the optimum location algorithm. Various modifications tested on this program led to numerous suggestions and several modifications regarding the format of the optimum real time algorithm. At the point when vortex location could be successfully done in real time with the data algorithm processor, the primary use of the vortex location program became reduction of the data for further processing and evaluation of system performance. In connection with this algorithm, a number of graphing and curve-fitting routines were developed. These are described in the last two sections. In the analysis of flow fields, the first step is the development of velocity versus angle data, which are initially obtained from the vortex location algorithm. Using the velocity versus angle data, calculations of a quantity proportional to the vortex rolling moment are possible and lead directly to a quantity defined as the effective circulation. In addition to these programs, printouts of the noise from noise runs and data recorded in the log books were used to complete the analysis.

The results of this analysis includes hard-target signal-to-noise ratio, range resolution and calibration accuracy, wind and vortex signal-to-noise ratios and average atmospheric backscatter coefficients, and vortex transport and circulation analyses. Thus, the developed programs provide an efficient means of performing system evaluation and vortex analysis from the PCM data obtained from the Laser Vortex System.

4.3.1.1 Cell Output

To analyze the raw data, for example in the development of algorithms, a cell output program was developed which displays the data in a conveniently usable form. Inputs to this program consist of the initial and final data frame numbers of a region of time for which the data are desired, a number indicating how many regions of data frame numbers are desired, and a number indicating the first cell number for which amplitudes are desired. The output consists of a header and the data frame number, x and y coordinates, and the amplitude in each filter starting with the first filter requested and continuing for 27 filters. This number of filters was chosen because the data will completely fill a line on a 130 character line printer. The header may be repeated each time a page is filled and printing continues until the maximum frame number requested is reached. An option is provided whereby either one or two sets of data frame numbers may be used in one run. If two sets are desired, the

initial and final data frame numbers of each must be specified and the section having larger data frame numbers must be specified as the second section. It is also possible with another option to start at the beginning of the data and print a specified number of data frames. This is especially useful before any of the data is analyzed and data frame numbers in regions of interest are not known, but it is desirable to be able to look at a random portion of the data. For example, this procedure could be useful by requesting a thousand data frames to determine the required threshold settings for a vortex location algorithm run. An example of the output of this program is shown in Figure 4-14.

FRAME= 8277 TIME= 462770/2754 X= 85.000 Y= 34.375 RADIUS= 91.680 THETA= 22.019

CELL	AMP	CELL	AMP	CELL	AMP	CELL	AMP	CELL	AMP	CELL	AMP	CELL	AMP	CELL	AMP
1	0	14	0	27	4	40	23	53	17	66	12	79	8	92	0
2	0	15	0	28	7	41	19	54	17	67	13	80	6	93	0
3	0	16	0	29	11	42	19	55	18	68	12	81	3	94	0
4	0	17	0	30	15	43	11	56	14	69	15	82	0	95	0
5	0	18	0	31	16	44	17	57	15	70	14	83	0	96	0
6	0	19	0	32	17	45	13	58	16	71	12	84	0	97	0
7	0	20	0	33	16	46	15	59	18	72	9	85	0	98	0
8	0	21	0	34	22	47	17	60	17	73	8	86	0	99	0
9	0	22	0	35	19	48	21	61	13	74	9	87	0	100	0
10	0	23	1	36	13	49	16	62	14	75	10	88	0	101	0
11	0	24	43	37	17	50	17	63	12	76	14	89	0	102	0
12	0	25	57	38	15	51	16	64	14	77	14	90	0	103	0
13	0	26	11	39	15	52	17	65	12	78	9	91	0	104	0

Figure 4-14. Sample cell output data tabulation.

4.3.1.2 Calibration Run Analysis Program

In the initial setup of the system for a day of testing, one of the procedures consists of scanning in range against a hard target at a known distance from the van. For most of the tests, the target was located at 560 ft (171 m) from the van being used. At this range, the system range resolution is predicted theoretically to be approximately 19 m. A program has been developed which goes through the data and prints the integrated signal for each range within a specified range interval. When one range scan has been completed, the program determines the range at which the maximum signal occurred. This procedure is repeated for each half-range scan until the end of the tape. At this time, the range is divided into range bins of 10 m in length and the average signal and standard deviation of the signal in each range bin is computed. To properly integrate the signal, it is necessary to remove the logarithmic conversion introduced by the processor. This is accomplished by the following equation,

$$A' = 2^{A/16} \quad ,$$

where A is the amplitude output by the processor and A' is the new amplitude. When hard target measurements are being made, sufficient attenuation is introduced in the system so that the noise always indicates zero least significant bits. Thus, the total signal may easily be obtained as the sum of the quantities A' for all filters in which A is not equal to zero.

4.3.1.3 Vortex Location Algorithm

The vortex location algorithm accomplishes a number of different functions. First, it determines the starting and ending frames of each scan of the elevation scanner. Next, it provides for thresholding and width (frequency) integration of the data. Points having high amplitudes are selected by a triplet algorithm and printed out for each scan. An iterated centroid calculation is performed on the data to obtain the locations of the vortices. At the end of a run, a summary output is presented, which includes the x and y coordinates and time for each vortex in each scan along with diagnostic data. Finally, output files are generated for further data analysis.

The end of a scan frame is, in principal, determined by noting when the angle scan reverses direction. However, since there is quantization noise and possibly other noise associated with the angle scan, this process is not straightforward. Accurate location of the end of a scan frame is important whenever a vortex is near the edge of the scan. Failure to locate the end of the scan correctly may lead to missed detections or errors in vortex locations on frames which end early or start too late. The most successful means of locating the end of a scan frame is the "split gate" method. This method averages out the fluctuations in angle and provides the ability to terminate a scan with angle turnarounds at any value, even if the angle limits are changed during a scan. The method may be explained with the aid of Figure 4-15. Initially, the program looks at the first 400 frames of data and multiplies each value of θ by the gate value. The gate value is -1 for frames 1 to 200 and +1 for frames 201 to 400. The results are added together and the sign of the sum is determined. The gate is maintained at a width of 400 frames and advanced in time by one frame. If the sign of the sum does not change, the process is repeated. If the sign of the sum changes, the scan ends with the last frame number before the middle of the gate.

In the low-speed tape data, amplitude and velocity thresholds and width integration have been set by the system hardware. The values of I_{pk}, V_{pk}, V_{max}, N, x, and y are obtained whenever the threshold conditions are

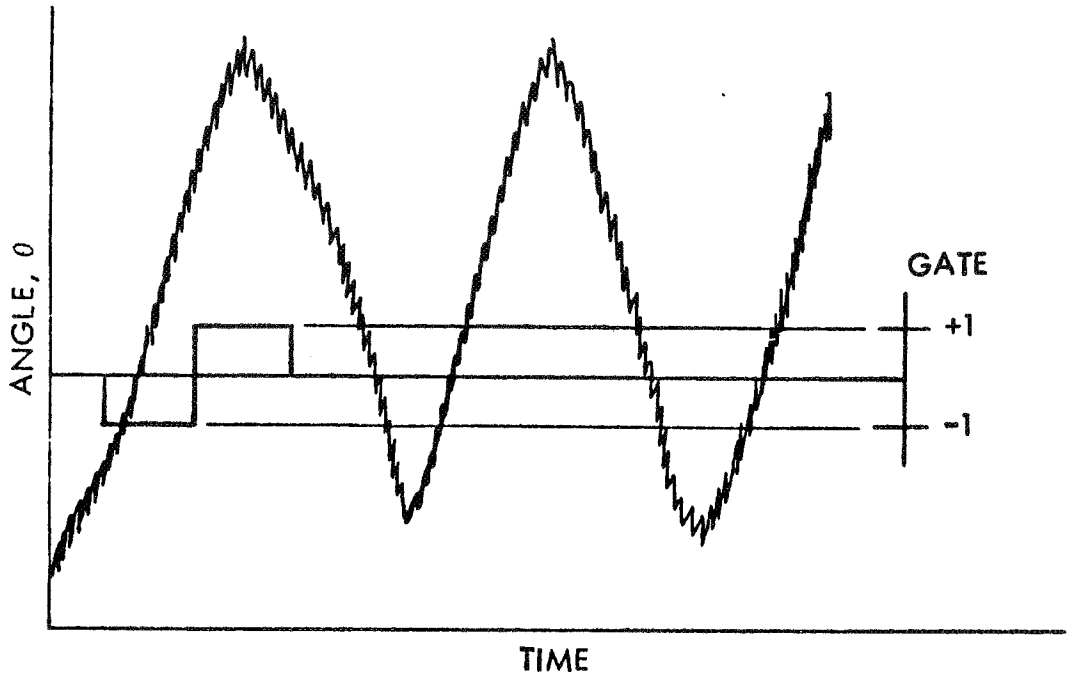

Figure 4-15. Split gate method of determining angle turn-around.

satisfied. With the high speed tapes, amplitudes of all filters are given, allowing the algorithm to employ any combination of thresholds and width integrations (longer than the hardware fixed integration time). For additional width integration I_{pk} is located first by finding the highest amplitude above the velocity threshold. This highest amplitude is then averaged with the desired number of adjacent amplitudes and if the resulting averaged I_{pk} is above the selected amplitude threshold, it is used in locating the vortex position. The width integration process is not identical to that performed by the processor, but should almost always give the same result and may be performed in considerably less time. The values of V_{max} and V_{pk} are determined at this point in the high speed data tape processing together with the sum of the signal amplitudes for cells that satisfy the amplitude and velocity thresholds.

A triplet algorithm is used to reduce the number of data points required for location of vortex centers. This triplet algorithm searches the SLDV system data points in range and in elevation to find those data points that have relative maxima in I_{pk} and use only those data points in determining

vortex position. The relative maxima data points are found using the following technique. As the data are read in the computer, the algorithm looks at the three points, one immediately before and after the one under consideration. If neither satisfies the threshold conditions, the point is discarded. If one of these points satisfies the threshold conditions, the point under consideration is accepted if its I_{pk} is greater than or equal to I_{pk} of the adjacent point. If both adjacent points satisfy the thresholds, then the given point is accepted only if its I_{pk} is greater than or equal to that of both adjacent points.

If R_{min} is the range position of the lowest data point and R_{max} the highest, R_l and R_u are defined as $R_l = R_{min}$ and $R_u = R_l + 10$. A flag is set to 1 for all points with $R_l \leq R \leq R_u$. Taking these points, the triplet algorithm is performed. Any time it succeeds, the given point is accepted. If $R_u < R_{max}$, R_l and R_u are increased by 10 and the process is repeated. After this has been done until $R_u \geq R_{max}$, all relative maxima of I_{pk} versus range and angle have been obtained. All points having I_{pk} less than γ times the highest I_{pk} are eliminated with γ being an input variable between zero and one.

A number of modifications to the program have been incorporated and may be used by selecting the appropriate inputs. An important one of these is the end of scan exclusion which eliminates all data points which fall in a range bin near the end or beginning of the range scan. This bin has been chosen to be 16 ft (5 m) in width. Also an edge of scan exclusion exists for angles where all points within a certain distance presently specified as 1° from the edge of the angle scan are excluded. In addition, a point which has been selected by the triplet algorithm in range may be accepted if it is more than 2° from all other points in the same range bin even though it is not a relative maximum in angle. Also, a comparison may be performed with the previous scan and the algorithm made to reject all the data in the scan if the highest I_{pk} is less than a specified fraction of the I_{pk} in the previous scan. Upon completion of this process, a data printout is made of all of the data points which were selected by the above criteria. Included in this tabulation are the x and y coordinates of the focus, the values of I_{pk}, V_{max}, V_{pk}, and a flag identifying which vortex the point is associated with, and the data frame number of the point. In the latest version of the program, the integrated signal over the whole spectrum is also included. This signal is obtained in the same way as the signal in the calibration run

program described in Section 4.3.1.2. Before this printout, some significant information describing the details of the particular scan are given; specifically, the scan number, the starting and stopping data frame number, the starting and stopping scan angle, starting and stopping time, the change in time, the change in angle, and the ratio of these two quantities, the highest and lowest total signal, the number of points in the scan, the minimum and maximum range in the range scan, and the number of points which were deleted because they had I_{pk} less than two times the highest I_{pk}.

When this process is completed, the vortex location is determined using an iterated centroid method. The location of the first vortex is determined by locating the highest I_{pk}, considering all of the selected points falling within a correlation circle of specified radius about this point, and calculating the centroid weighted with the amplitude above the threshold. A similar procedure is used to locate the second vortex using the highest I_{pk} outside of the correlation circle defined for the first vortex. Points occurring in both circles are considered to be associated with both vortices for purposes of the centroid. The locations thus determined are used as centers for new centroids. If a majority of the points in either vortex is in the overlap region, the point which initiated the location of vortex two is deleted and the iteration procedure is begun again. The x and y locations of each vortex center are shown after each stage of the iteration and an informative message is printed if it is determined that a majority of the points in one vortex lie in the overlap region. Three iterations are used on each vortex and a maximum of three points may be deleted in the location of the second vortex.

The above procedure occurs for every scan frame in the data tape, and after the last scan frame a summary output is produced. This output shows the x and y coordinates and time for each vortex in each scan frame and the number of points used to locate each vortex, the number of points not used, and the number of points in the overlap region. In addition, at this time, two output files are generated for further processing. The first of these is identical in content to the summary output and is to be used for plotting and curve fitting in the study of vortex transport. The second is a plot of V_{pk} as a function of angle for each vortex in each scan.

4.3.1.4 Graphing Routines

One of the output files of the vortex location algorithm is a table of vortex transport data. It is desirable to be able to graph these data in different ways to study vortex transport and evaluate algorithm operation. The plotting is accomplished with the aid of a set of subroutines collectively identified as GRAPHX. GRAPHX is a device independent plotting package which consists of a set of Fortran-callable subroutines which allow the user to produce identical plots using a line printer, teletype, pen plotter, CRT plotter, or Zeta time sharing plotter simply by changing a single subroutine call. GRAPHX is designed to provide considerable flexibility, while at the same time being simple to use. GRAPHX has the capability of superplots with axis labels, annotations, and legends as well as the capability to determine the appropriate limits and scale factors to produce a plot of the desired size.

Plots of horizontal and vertical position as a function of time are produced with identifiers showing the run number and identification of port and starboard vortices. Finally, a plot of vertical position as a function of horizontal position is produced.

4.3.1.5 Least-Square-Fit

Least-square-fit is often useful to obtain average vortex transport velocities from the data produced by the vortex location algorithm. This is accomplished by a Fortran program which performs least-square-fits to the data. The program operates as follows: if more than six scans contain two vortices each, the program eliminates three scans and determines a least-square-fit to a straight line for each vortex using the remaining data. This process is repeated until all possible combinations of three scans each have been eliminated from the data. The fit producing the smallest standard deviation is selected as the best fit. Finally, of the three scans which were not previously used, the vortex in each scan which is nearest to one of the fitted curves is associated with that curve and a new fit is computed. At the present time, the fit is performed only on the horizontal position versus time data. At the end of the program, fits are calculated for the vertical transport versus time and the vertical versus horizontal position using the data points selected in the previous portion of the program. If insufficient data for this procedure are available, the program simply calculates the least-square-fit using the data directly as it is obtained from the vortex location algorithm.

4.3.1.6 Vortex Flow Field Analysis

The analysis of the vortex flow field makes use of a number of programs which use the velocity versus angle data from the vortex location algorithm. The first step in vortex flow field analysis is simply to plot these data. Typical plots are shown in Figure 4-16. This figure shows that the core of the vortex may be identified with the peaks in velocity and the center of the vortex may be defined at the minimum between these peaks. It is then possible to determine a quantity proportional to the rolling moment by integrating the product of distance from the center and velocity associated with that distance over limits determined by the wingspan of the simulated following aircraft [10]. The slope of the moment versus wingspan graph should be proportional to the circulation. The circulation is therefore determined by finding the slope of this graph over a central region which is unaffected by peculiarities in the vortex core or the lack of data at large wingspans. The normal procedure for calculating circulation involves performing the integral from minus one-half wingspan to plus one-half wingspan from the center. However, when the vortex is near the edge of a scan, there may be insufficient data to perform this calculation. Therefore, a procedure has been developed to make an estimate of the circulation by performing the integration from zero to one-half wingspan and multiplying by two to obtain approximately the same results as would be obtained over the whole wing.

4.3.2 Low Speed Data Processing

The low-speed data processing refers to the processing of the PDP-11 generated tapes which include the V_{pk}, V_{max}, I_{pk}, and N parameters as well as x, y, and time. These tapes may be processed either on the PDP-11 in real time, in post analysis, or on the IBM-370 computer.

4.3.2.1 IBM-370 Processing

A program was developed using the IMB-370 computer to read and process the nine-track tapes generated by the PDP-11. The program performs, as closely as possible, the same functions as the vortex location algorithm described in Section 4.3.1.3. The main difference is that data on the PDP-11 tape have already been thresholded and the parameters of the spectrum determined, thus resulting in a reduced data rate and simplified processing. These data are analyzed on the IBM-370 because it is the most compatible computer (8-bits byte, nine-track tape transport) for PDP-11 generated slow speed data tapes.

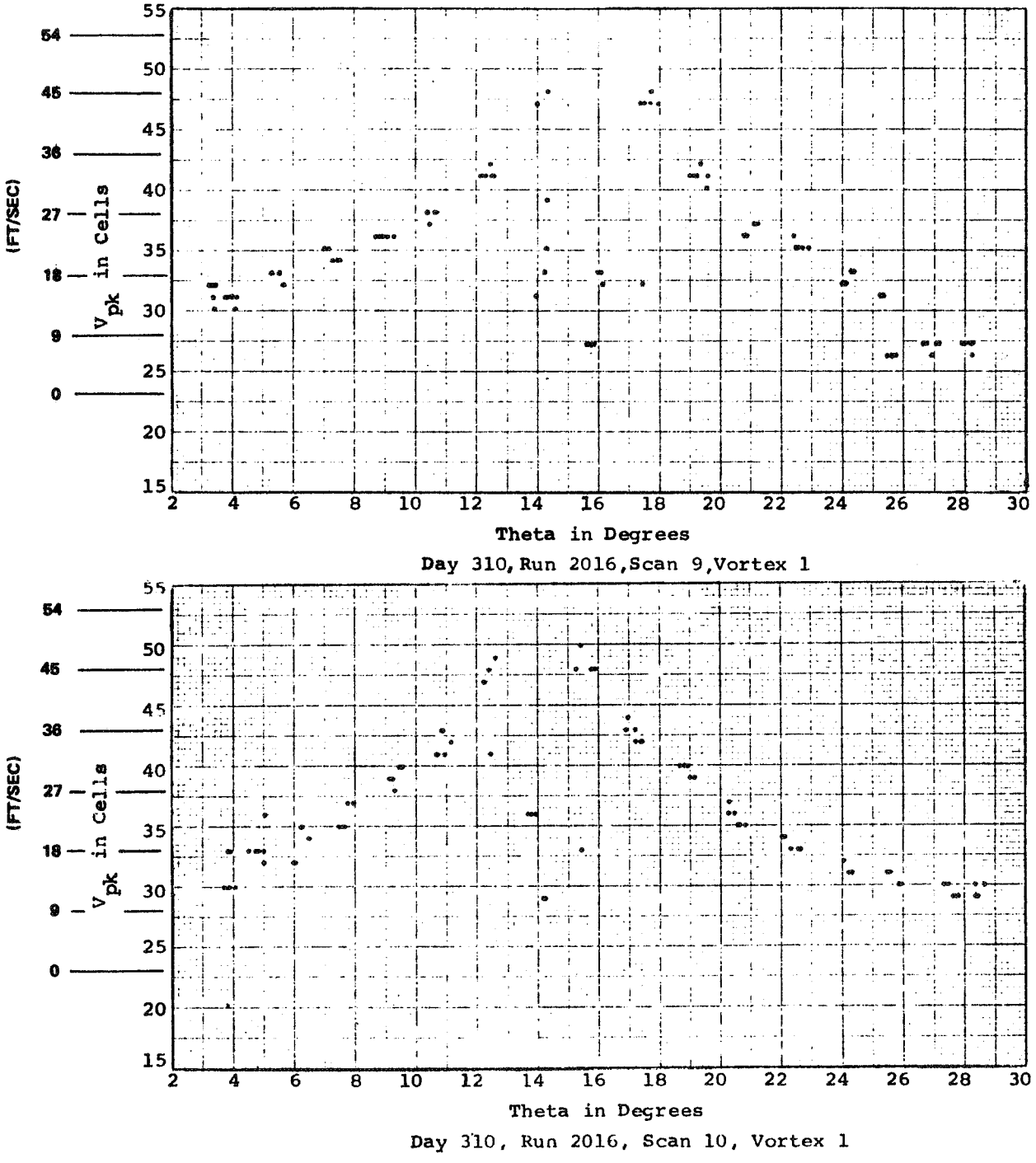

Figure 4-16. Sample vortex flow-field plot.

The processing algorithm performs the triplet selection of data points except that in processing these data, it is not known if an adjacent point failed to satisfy the threshold. The data points selected are used in an iterative centroid calculation similar to that used in the location algorithm described in Section 4.3.1.3, and the results are placed on punched cards to be read into the CDC-6700 for further processing of the data. This program is extremely useful in reducing the cost of data analysis because a large portion of the data rate has been dramatically reduced on these tapes. However, these data are not as useful as the high speed data because the process of thresholding has greatly reduced the potential for the detailed analysis possible with the high speed PCM data.

5.0 TEST OPERATION

5.1 Introduction

Testing, with the SLDV systems, was performed at JFK Airport in two separate test periods. The first series of tests were carried out during the time between September 7, 1974, when the equipment was installed, and December 13, 1974, when the system was placed in a standby condition. During this time, the Data Algorithm Processor was installed in the system and on-line data reduction was begun. The second series of tests was performed from March 3, 1975, when the systems were returned to an operational status, through June 2, 1975, when the systems were returned to MSFC. This second test period saw changes in the software control programs and updates in the algorithms used in resolving the vortex tracks. A special series of long range flyby tests were also performed to test the ability of the system to resolve vortex tracks at long ranges and to obtain information about the action of vortices well out of ground interaction.

During the two test periods, information was recorded on more than 1600 aircraft landings. This section will describe the installation and operation of the SLDV systems at JFK Airport and will provide a summary description of the tests on a day-to-day basis.

5.2 Installation

5.2.1 Test Site Description

The test site chosen for the wake vortex tests is shown in Figure 5-1. It is located near the middle marker of runway 31R, JFK Airport. The site was operated by the National Aviation Facilities Experiment Center (NAFEC) for the Transportation Systems Center (TSC), and FAA. In addition to the SLDV systems, five other systems were installed by TSC at the site. These systems included a Pulsed Acoustic System, Acoustic Doppler System, Monostatic Acoustic System, Ground Wind System, and Meteorological Tower System.

5.2.2 Site Preparations

Certain site preparations were performed by NAFEC prior to the installation of the SLDV systems. The preparations included the provision of 100 A, 220 V, single ϕ service to the van locations and the installation of pads to support the SLDV vans. A view of one of the pads and transformers prior to installation of the SLDV is shown in Figure 5-2.

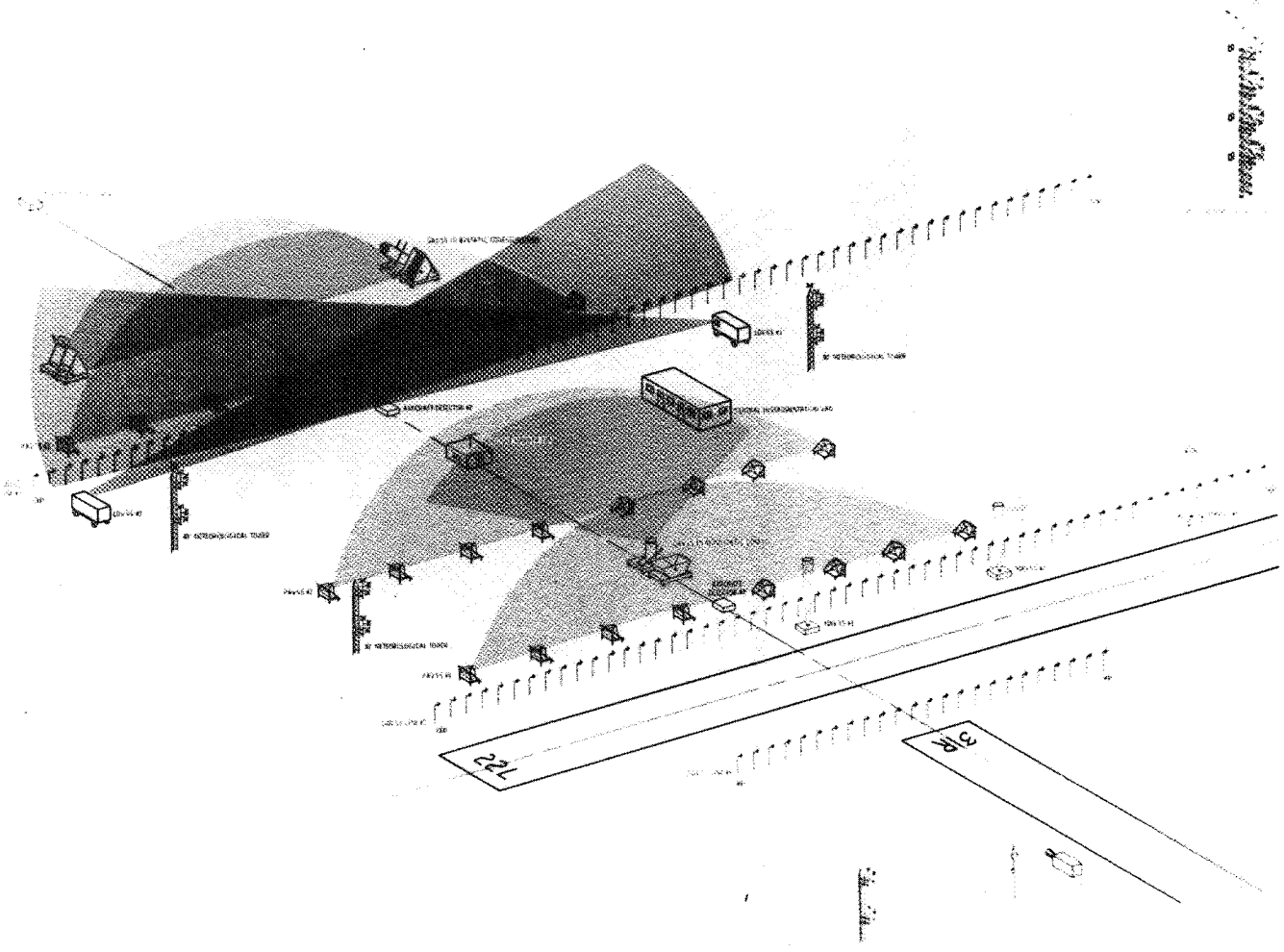

Figure 5-1. Test site layout.

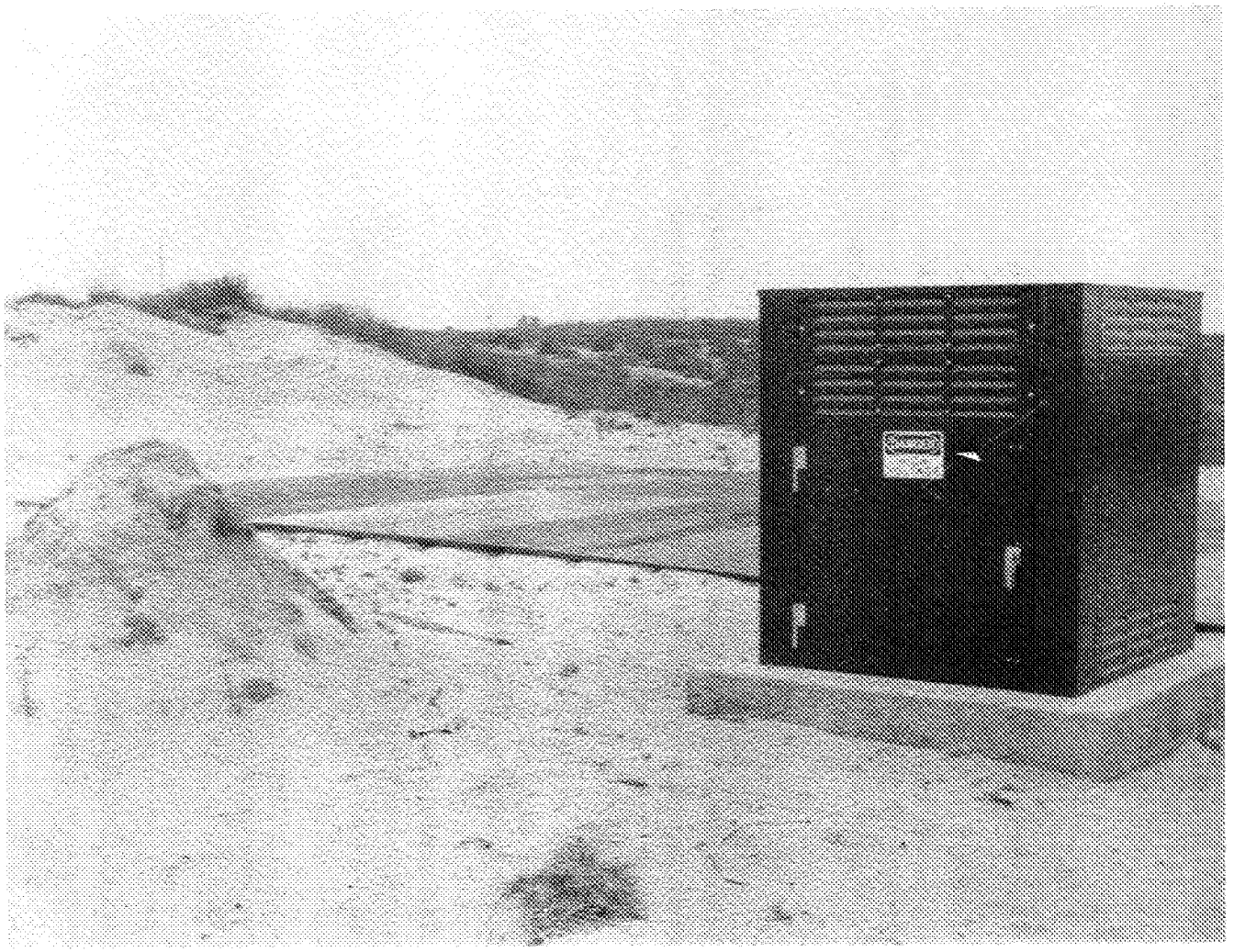

Figure 5-2. Instrument van pad and transformer.

5.2.3 Instrument Van Transportation

The two 28 ft semitrailer vans which housed the SLDV systems and a four-wheel drive support truck were hauled to Lockheed Aircraft Service at JFK Airport by tractor from MSFC, arriving on August 26, 1975. A subcontractor was hired by Lockheed Missiles and Space to haul the vans across the airport to the test site location. No difficulties were experienced in this move; however, due to the terrain, heavy equipment had to be used to place Van 2 on its pad (Fig. 5-3).

5.2.4 Optics/Electronics Transportation

The optical and electronic equipment was transported to JFK Airport by a NASA plane in three flights. This equipment was offloaded at Lockheed Aircraft Service and hauled by truck to the test site where it was installed in the vans. Figure 5-4 shows the internal layout of the two vans.

5.2.5 System Layout

The SLDV was located as shown in Figure 5-5, 200 ft (61 m) in front of the middle marker and 400 ft (122 m) on either side of the extended runway center line. The vans were installed on a pad constructed of aircraft landing mats and tied down using steel cable, screw anchors, and dead weights. Calibration wheels are located on towers spaced 560 ft (170 m) from each van. The vans are aligned so as to be parallel to the runway with their windows directly across from each other. Electrical service is provided by transformers located at each pad. The vans are interconnected by cables for telephone service, data transmission, intercom service, and time code transmission. All cables are below ground. The trailers are grounded by 40 ft (12 m) ground rods. Equipment storage and office facilities are located in two trailers adjacent to the middle marker. A view of the completed installation is shown in Figure 5-6.

5.2.6 Safety

The laser system has been registered with the state of New York and has received registration number LSR0528. The entire system has been inspected and approved by the New York Department of Labor, Division of Industrial Hygiene. A 30 ft (9 m) corridor running between the two vans has been roped off and marked with "DANGER — LASER RADIATION" signs at intervals of 50 ft (15 m). Flashing red lights have been placed on the calibration towers as a

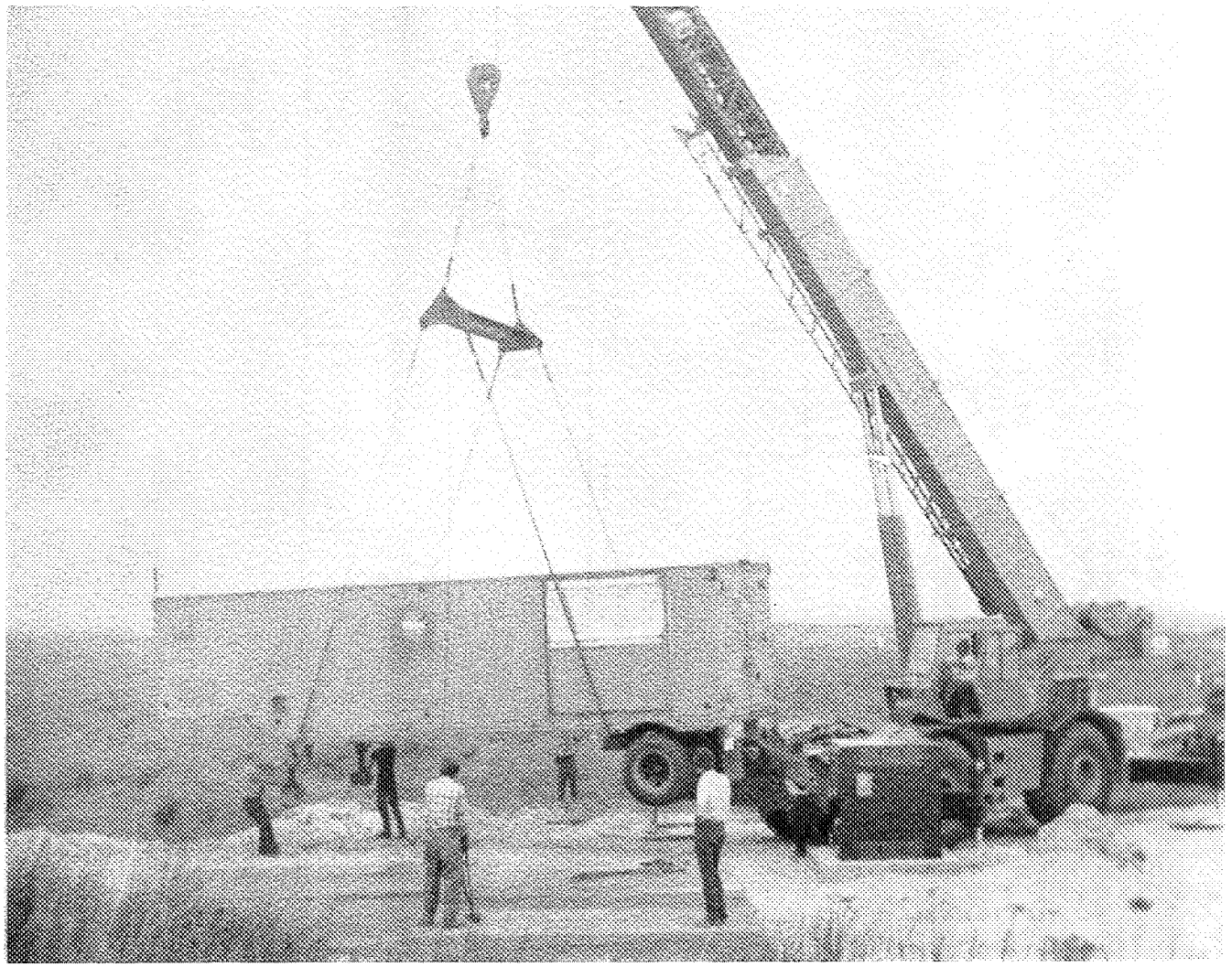

Figure 5-3. Van installation.

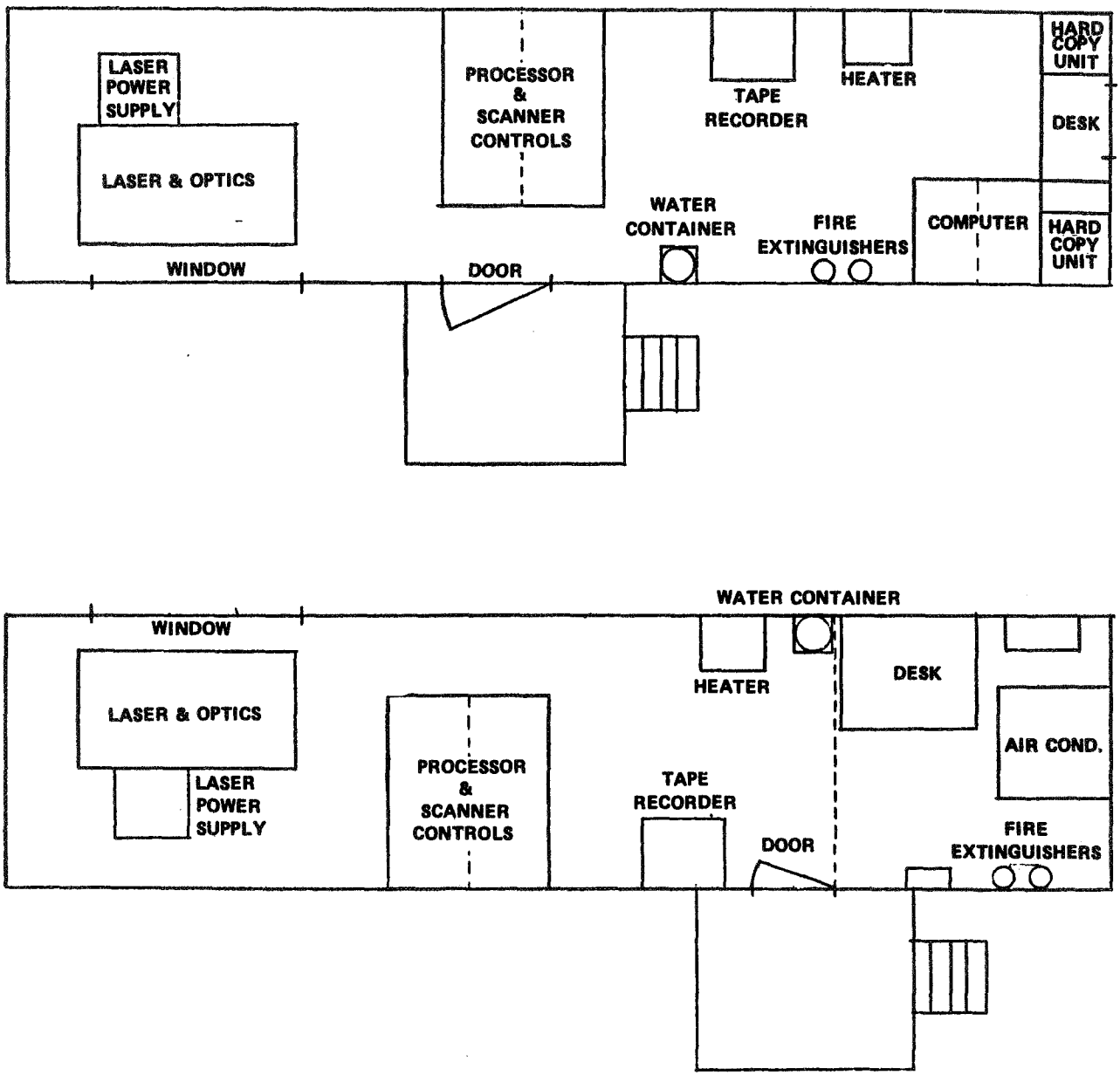

VAN 2

Figure 5-4. Van layout.

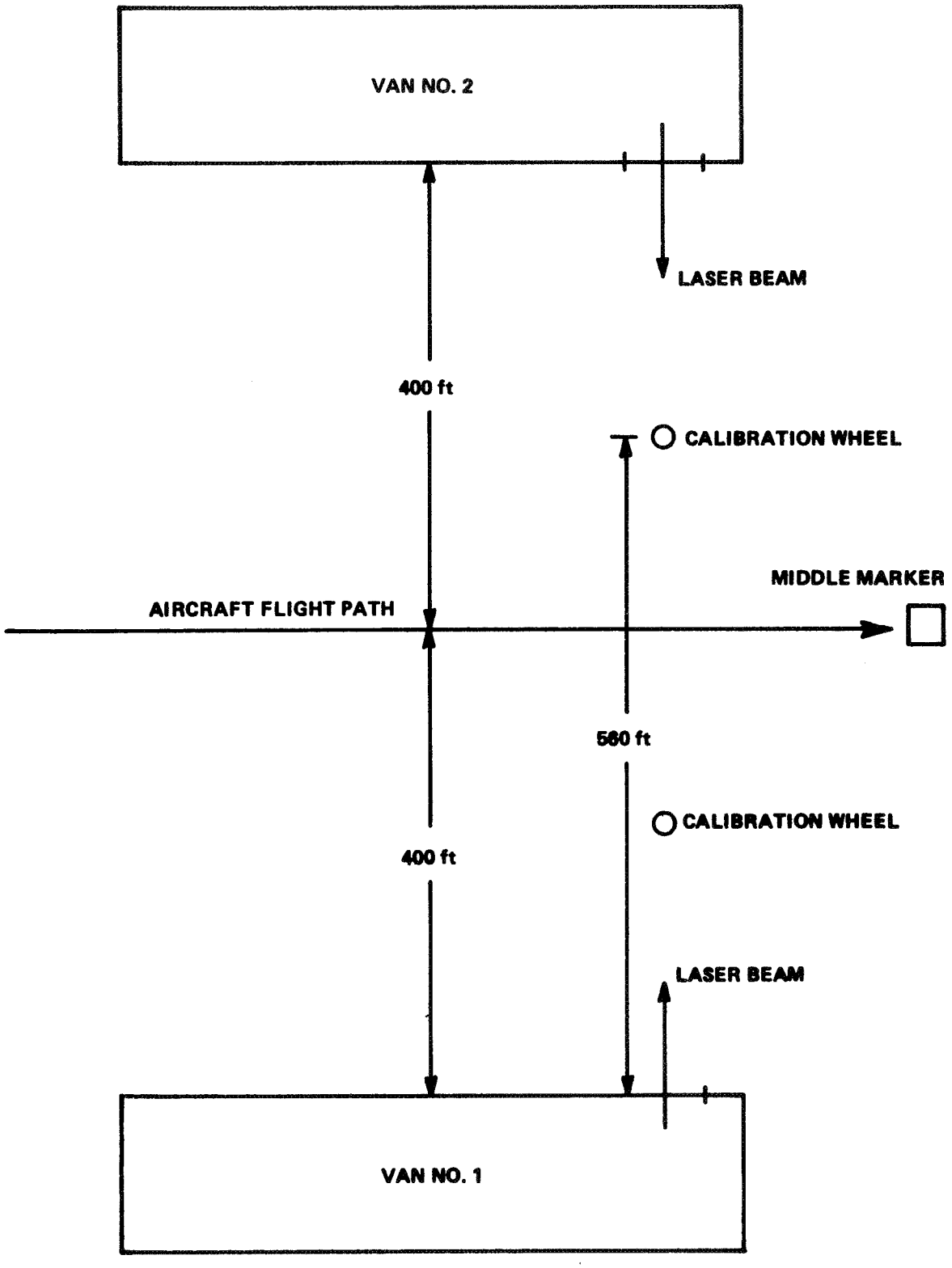

Figure 5-5. System layout.

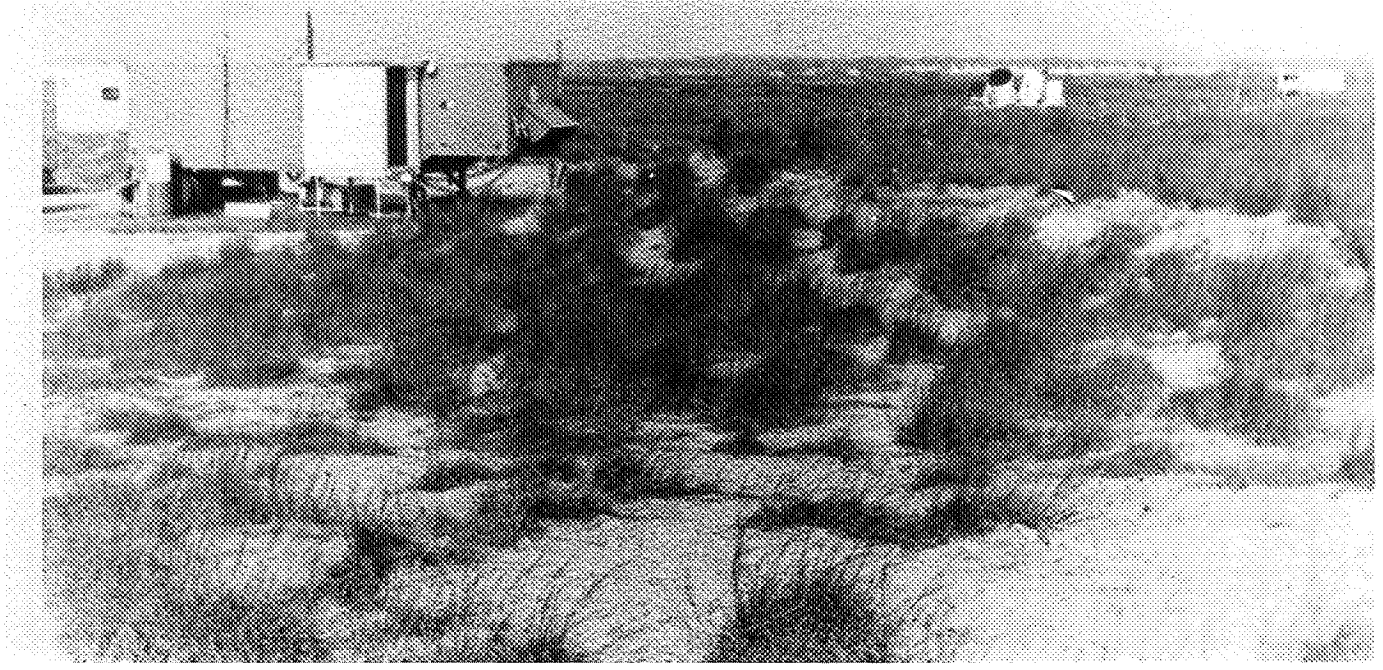

Figure 5-6. JFK test site.

warning during operation of the system. Mechanical stops have been installed to prevent the mirrors from scanning below 3°. Additional safety considerations are covered in "Safety Procedure Breadboard Scanning Laser Doppler System for Detection and Tracking of Aircraft Wake Vortices" dated 16 July 1974.

5.2.7 System Support

Shortly after arrival at JFK Airport, it became apparent that an office area would be required for preparing data, equipment repair, and equipment and data storage. A spare trailer was made available by TSC for the duration of the test and was moved to an area adjacent to the middle marker. Communication with the two SLDV vans was accomplished by the installation of an intercom and telephone system in the office trailer. Because of the vast amount of data obtained daily, together with the distribution requirements, it was necessary to lease a xerox copier which was installed in the office trailer.

Local vendor sources were established for electrical and mechanical hardware, liquid nitrogen service, and propane (required for heating of office trailer). Contacts were also established for equipment repair, primarily through Lockheed Electronics Company in nearby Plainfield, New Jersey.

Airport security badges for the SLDV contractors were provided through Lockheed Aircraft Service. Security badges for the NASA personnel were arranged for by NAFEC.

In addition to site preparation, NAFEC and TSC personnel provided aid in establishing local contacts, and provided support to the operation of the SLDV systems throughout the test program.

5.3 Calibration

Calibration can be separated into two categories: component calibration and system performance calibration. Component calibration was carried out at selected intervals, while system performance calibration was performed daily.

5.3.1 Component Calibration

Upon arrival and installation of the equipment at JFK Airport, all equipment was given a detailed checkout and calibration. The calibration of the equipment is covered in detail in the individual component manuals. This

calibration was repeated throughout the test period as deemed necessary by the results of the system performance calibration.

5.3.2 System Performance Calibration

The calibration of the system consisted primarily of calibration of the range scanning mechanisms. Due to the inherent physics involved, the range is not directly measurable. A fixed hard target was located at an accurately known distance from the system to dynamically check the calibration. To statically set the range, a micrometer was adjusted to peak the signal after the scanner had been set at the desired range. While the system was peaked for range, signal to noise calculations, and other measurements were made with the SLDV. To dynamically calibrate the range, the range scanner which scanned the beam focus through the target was activated. The signal processor was then set at a high amplitude threshold where only the peak of the signal was visible. The computer would at this time calculate the range at which the peak velocity occurred and print it out in graphical and tabular form. The computer would also calculate standard deviation and mean range. From this information, the secondary mirror could be positioned to provide the correct range to the target.

The signal-to-noise measurements taken during this time provided a measure of the overall system performance from which any problem areas could be isolated. This was particularly effective in determining the optical alignment of the system.

5.4 Operation

The daily operation of the system was as follows:

a. The laser is turned on and allowed to warm up for a period of 30 min or until the laser has stabilized.

b. After stabilization of the laser, beam alignment is checked in the telescope, and general alignment of the interferometer and detector is checked using temperature sensitive paper.

c. Following alignment of the telescope and interferometer, the system is focused on a wheel located 560 ft (171 m) from the van, and a signal-to-noise ratio measurement is made. Minor adjustments are then made to obtain the highest possible signal-to-noise ratio.

d. Following the signal-to-noise ratio measurement, the system is scanned on the wheel and the data fed to the computer where the range calibration is checked. Adjustments are then made in the position of the secondary mirror to provide the proper range calibration.

e. Following the range calibration, the processor is set up for the desired integration time, input level, etc.

f. At the same time, the scanner is set up to provide the desired scan angles, ranges, and rates.

g. The analog tape recorder is then checked to determine if the signals are being recorded properly.

h. The computer system is also checked to determine if data are being received from both systems.

i. When these checks have been completed and the range calibration recorded, the processor thresholds are set to discriminate against the wind velocity and the noise floor amplitude.

j. The noise and wind data are then recorded on tape.

k. The system is now ready to monitor and track vortices.

l. When a test has been completed, the wind, noise, and wheel tests are repeated and the system is shut down.

5.5 Data Handling

At the end of each test day, the analog tapes recorded by each system were logged and stored for shipment to MSFC for detailed analysis. The digital tape of the data input to the algorithm processor was also logged and stored for onsite post processing and later shipment to MSFC. Copies of the "hard copy" vortex data were also made for transmittal to TSC and MSFC; originals were logged and stored on site. A report which included the hard-copied data and a summary of the week's events was provided each week.

During the second series of tests, changes were incorporated in the data algorithm processor which allowed the vortex data to be stored on disk and later transferred to magnetic tape. Following this change each day's data were transferred to tape and at the end of the week this tape together with the associated hard copy data was provided to the NAFEC site manager for forwarding to TSC.

All analog and digital tapes from these tests are presently stored at MSFC. All available vortex data tapes have been sent to TSC.

5.6 Test Summary

A cross reference and index to the data collected are located in Appendix A. Test log sheets for each day are located in Appendix B and the actual data sheets are contained in Appendices C through K. A summary of the collected data is shown in Table 5-1.

During the two test periods at JFK Airport, a total of 1633 landings were monitored on 41 days with a total recorded data time of 118 hr 09 min.

5.7 Hardware Evaluation

In general, the SLDV system performed with relatively few malfunctions, most of which could be directly attributed to large temperature fluctuations in the vans. The following section describes the problems encountered during the test operations at JFK Airport on a component basis.

5.7.1 Laser

Although the lasers rarely failed to operate, considerable difficulties were encountered involving beam wander, output power stability, and output power degradation. These problems were overcome by allowing lengthy warm-up periods to stabilize the output, periodic pump-down and refilling of the laser to maintain power levels, and adjustment of the telescope and interferometer to compensate for beam wander. These procedures are time consuming and require a highly qualified operator to be in continuous attendance.

TABLE 5-1. DATA SUMMARY

Day No.	Date	No. of Runs	Vans Operating	Day No.	Date	No. of Runs	Vans Operating
266	9-23-74	53	1&2	079	3-20-75	91	1&2
270	9-27-74	27	1&2	080	3-21-75	44	1&2
273	9-30-74	8	1&2	085	3-26-75	24	1&2
275-1	10-2-74	14	1	086	3-27-75	23	1&2
275-2	10-2-74	30	1	090	3-31-75	62	1
276	10-3-74	37	1	094	4-4-75	32	1
279	10-4-74	24	1	098	4-8-75	72	1
282	10-9-74	18	1&2	099	4-9-75	10	1
283	10-10-74	24	1&2	107	4-17-75	14	1&2
288	10-15-74	116	1&2	111	4-21-75	11	1&2
290	10-17-74	33	1&2	115	4-25-74	34	1&2
294	10-21-74	78	1&2	118	4-28-75	26	1&2
296	10-23-74	51	1&2	126	5-6-75	9	1&2
310	11-6-74	41	1&2	127	5-7-75	56	1
319	11-15-74	81	1	136	5-16-75	77	1
322	11-18-74	14	1	140	5-20-75	20	1
323	11-19-74	3	1	141	5-21-75	16	1
325	11-21-74	41	1&2	147	5-27-75	37	1
326	11-22-74	60	1&2	148	5-28-75	57	1
329	11-25-74	55	1&2				
337	12-3-74	54	1&2				
339	12-5-74	4	1&2				
343	12-9-74	52	1&2				

5.7.2 Interferometer

Although daily adjustment of the interferometer was required for optimum operation, it is felt that this is due primarily to the laser beam wander. The size of the interferometer could be reduced considerably reducing any possible thermal problems and allowing a much more compact system. The amount of reduction in size is dependent upon whether or not a translator is required.

5.7.3 Telescope

Minor adjustments in mirror positions were required daily, again due to laser beam wander. The primary difficulty encountered was due to the apparent expansion and contraction of the telescope table due to thermal problems. This problem resulted in a change in distance from the primary to secondary mirrors, thereby causing a change in the range calibration of the system. Better temperature control of the van is required together with the possible use of less temperature sensitive materials in the telescope table.

5.7.4 Detector

The only problem encountered with the detector involved the hold-time of the LN_2 dewar. The average time between refills was on the order of 20 min.

5.7.5 Receiver

Basically no problems were encountered with the receiver during test operations. It is possible, however, to obtain a better impedance match to the detector by using transimpedance amplifiers. This will provide some improvement in the efficiency of the system.

5.7.6 Scanner

Several problems were encountered with the scan control system. These included cable slippage on the secondary mirror drive, vibration of the secondary mirror mount, drive transients, and electronic component failure. Component failure and drive transients were attributed to thermal problems in the vans. Midway through the test period, improved air circulation through the scanner helped reduce these problems. The secondary mirror mount was also reinforced; however, the method of driving the secondary mirror should be modified for optimum operation.

5.7.7 Signal Processor

The major problem encountered in the signal processor involved the loss of a power supply in both systems. This was caused by a faulty design in the supply and has since been corrected. The signal processor appeared to be the most temperature sensitive of the SLDV system components and, therefore, a number of electronic components in the processor failed. Improved cooling of the processor needs to be implemented.

5.7.8 Recorders

Although the data recorders were the only items which did not survive the transportation from MSFC to JFK Airport, once they were returned to an operational status, they performed satisfactorily throughout the tests.

5.7.9 Data Algorithm Processor

Once this system was installed and checked out, the only problems encountered were due to apparent line voltage transients and thermal problems. The graphics tablet and display terminal could not be operated above 95° without resulting in intermittent problems. The cooling for this system must be improved.

5.7.10 Vans

As can be determined from the preceding subsections, temperature control of the van interior is a major problem. The use of Teflon to cover the beam exit window during operation has considerably improved the situation; however, this results in a signal/noise loss of approximately 3 dB. The air conditioning system should be reworked to provide direct cooling to the system components. In addition, the moving and installations of the vans provide major problems which could be eliminated through the use of a more mobile self contained unit.

6.0 DATA/SYSTEM ANALYSIS

As described in Section 4.0, data processing takes place onsite using the PDP-11 and offsite using the high speed PCM tape generated by the SLDV System. This section will describe the results of the analysis of selected test data involving system performance and calibration and vortex transport and flow fields. It will also cover verification of the data as well as a statistical analysis of the overall test data. Additional information will be found in Reference 8.

6.1 Phase I Airport Tests

During this phase of testing, over 900 aircraft landings were monitored, including a wide variety of aircraft types and atmospheric conditions. Vortices were detected from aircraft as small as a single engine propeller aircraft. Vortices from larger aircraft were monitored for as long as 80 sec and reliably located at ranges as great as 800 ft (244 m). The system was shown to operate reliably with the thresholds set by the operators. The parameters used in the real time data analysis were not optimized for the aircraft being considered. Therefore, many of the results do not reflect the actual transport of a pair of wake vortices, but the data available as recorded on the PDP-11 tape are sufficient to perform this location. In post analysis of data from days 310 and 343, it was shown that good tracks may be obtained from most runs by proper analysis. Also, the optimum processing parameters for each type of aircraft commonly encountered were determined during this test. Preliminary studies of vortex flow fields were begun, and the data received by the PDP-11 are verified by comparison to the PCM data.

6.1.1 Hard Target Analysis

In daily operation of the system, data were obtained from a hard target which consisted of a sandpaper disk mounted at an angle to the beam and rotating to produce a Doppler signal. These data were used to evaluate system performance in terms of signal-to-noise ratio, range resolution, and calibration.

The signal-to-noise ratio is linearly related to the system efficiency which may be determined from experimental measurements. Laboratory measurements conducted by the manufacturer before delivery of the interferometers and detectors produced the efficiency measurements shown in Table 6-1.

TABLE 6-1. SYSTEM EFFICIENCY FROM LAB MEASUREMENTS

Van 1	Efficiency
Detector 1031	0.475
Interferometer 1	0.38
Telescope	0.6
Net Efficiency	0.11
Van 2	
Detector 972	0.30
Interferometer 3	0.53
Telescope	0.6
Net Efficiency	0.10

Experimental data on hard target measurements were used to determine the experimental efficiency shown in Table 6-2. Table 6-2 shows an unexplained loss of approximately 10 dB for Van 1 and a loss of 17 dB for Van 2. The data for this measurement were obtained from the spectrum analyzer so that the effect of integration by the processor is not required in the analysis.

An investigation of the system range resolution using the program described in Section 4.3.1.2 was performed from data taken on day 310. The results of several scans are summarized in Figure 6-1. The data in these figures were separated to include only that data obtained while the range scanner was scanning in a particular direction. Thus, in both cases of Figure 6-1, the range scanner was scanning in such a way that range was increasing with time. Similar results were obtained when the range was decreasing with time. The purpose of this separation of the data was to determine whether there were hysteresis effects in the scanner. Analysis indicated that if there were any hysteresis effects, they were negligible. The numbers on each graph identify scan numbers and show the amplitude associated with a particular range for the scan number indicated. The letter T denotes a point on a theoretical signal

TABLE 6-2. SIGNAL TO NOISE CALCULATIONS

Van 1, Day 310	
Spinning Wheel	
SNR = 57 dB (Spectrum Analyzer)	$\eta_{TOTAL} = 0.0097$
SNR (Processor) = 68 dB	$(\eta_{LAB} = 0.11)$
Van 2, Day 310	
Spinning Wheel	
SNR = 50 dB (Spectrum Analyzer)	$\eta_{TOTAL} = 0.0022$
SNR (Processor) = 61 dB	$(\eta_{LAB} = 0.10)$

versus range curve having a peak at the same range with the same integrated signal as the experimental curve. It may be seen that the range resolution of Van 1, as indicated by the top figure, was considerably worse than theoretical while the range resolution of Van 2, as indicated by the bottom figure, was actually slightly better than theoretical. In the theoretical calculations for range resolution, it is assumed that the output beam shape is Gaussian in energy distribution. It is also assumed that the local oscillator beam shape is Gaussian. At the time of these field measurements of range resolution, it was observed that the output beam shape of the laser from system 1 was irregular whereas the beam shape of the laser from system 2 was Gaussian with a very clear shape. It has been confirmed that bad output beam shape (non-Gaussian) causes a degradation in system range resolution and it is believed that this accounts for the system performance of Van 1.

6.1.2 Wind Measurements

During each day of testing, a run was recorded on PCM tape using only the ambient wind as a target. The results of the analysis of one set of data are shown in Figure 6-2. Theoretically, it is anticipated that the wind

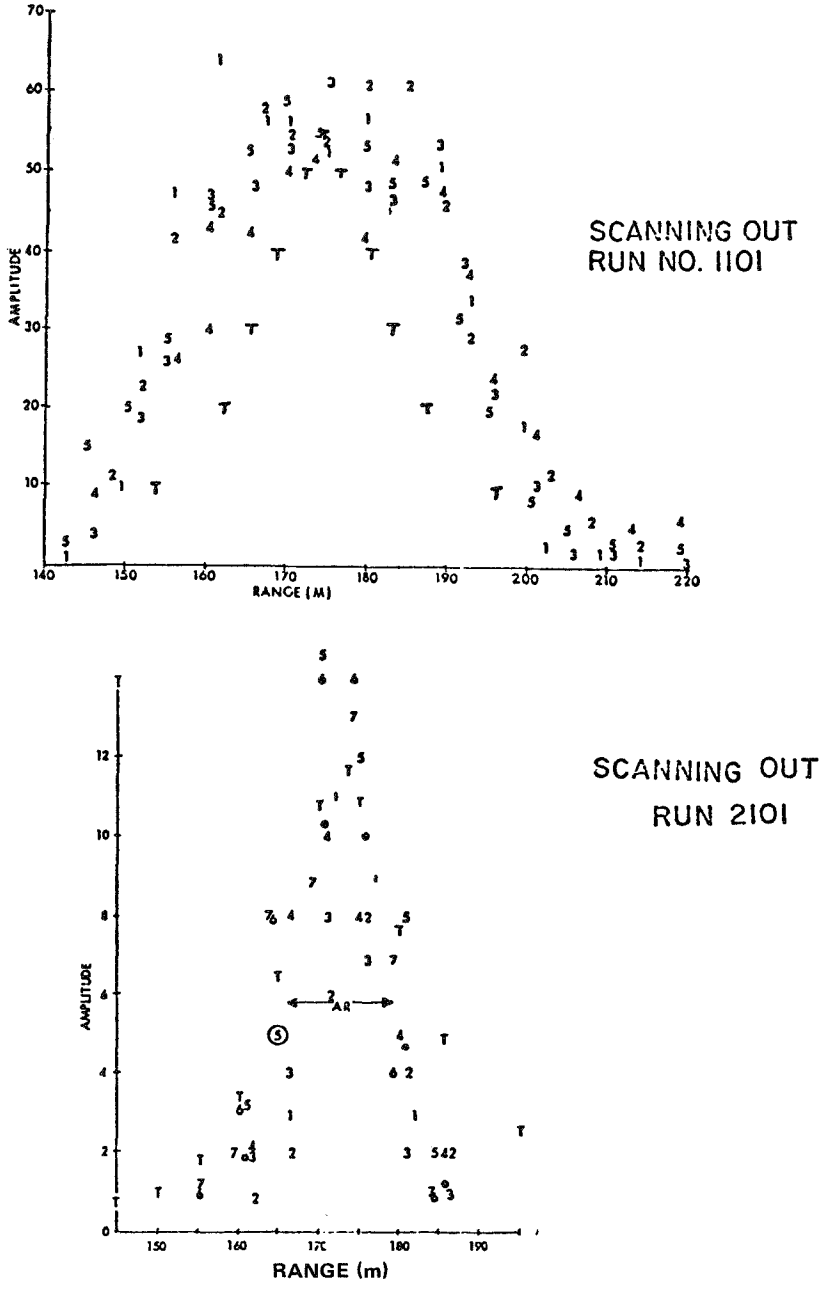

Figure 6-1. Integrated intensities from a hard target as a function of range.

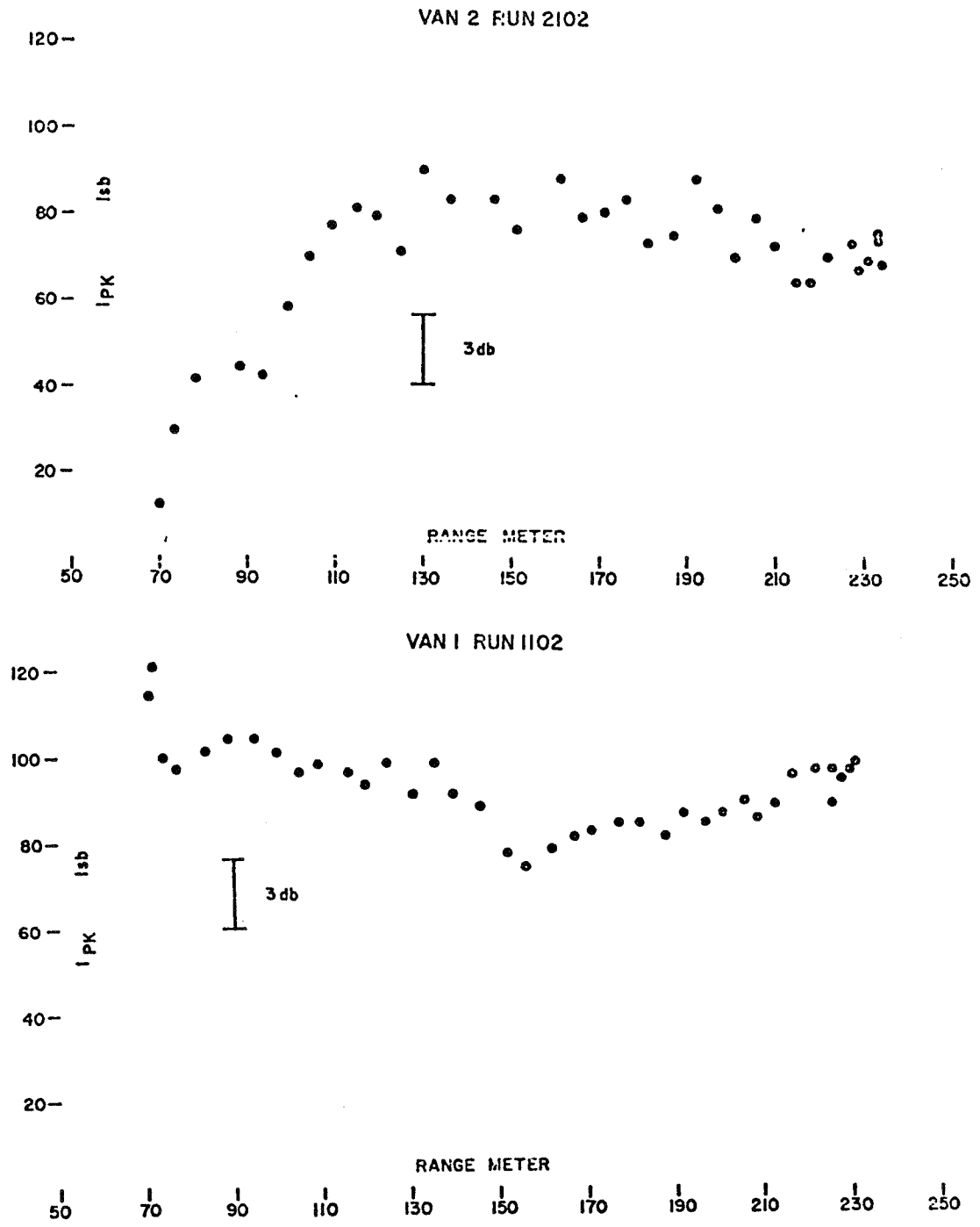

Figure 6-2. I_{pk} from the wind as a function of range.

signal-to-noise ratio should be independent of range. It may be seen that for Van 1, as indicated by the bottom portion of the figure, the signal-to-noise ratio was essentially constant from 230 to 755 ft (70 to 230 m) in range. The slight peak below 230 ft (70 m) is believed to be caused by vibration of the telescope secondary during range turnaround. A dramatically different picture is seen in the case of Van 2 in the top figure. The signal-to-noise ratio was approximately constant from 426 to 787 ft (130 to 240 m), but dropped rapidly inside 426 ft (130 m), being down approximately 12 dB at 230 ft (70 m) which corresponds to the minimum range of the scan. This phenomenon may be due to a misalignment of the telescope or to some other unknown cause, and further investigation is warranted.

In addition to these measurements, absolute wind signal-to-noise ratio measurements were made. Results of these are shown in Tables 6-3 and 6-4 for Vans 1 and 2, respectively. Since the wind signal-to-noise ratio is obtained from the PCM data, which is an output of the processor, it is necessary to modify the system efficiency by considering the gain caused by integration in the processor. This gain typically amounts to 11 dB since approximately 125 samples are considered during an integration time. Using this information, it is possible to obtain a value for the atmospheric backscatter coefficient used in the atmospheric signal-to-noise ratio equation. A value of 2×10^{-7} m^{-1} was obtained using data from Van 1 and a higher value was obtained from Van 2. In addition, a number of vortex signal-to-noise ratio measurements were made with Van 1 and effective backscatter coefficients were obtained as shown in Table 6-3. These values are approximately 1 order of magnitude higher than the backscatter from the ambient wind and represent an average over a space larger than the vortex core itself. Thus, it may be concluded that the aircraft engine exhaust introduces at least a factor of 10 increase in atmospheric backscatter coefficient at 10.6 μ.

6.1.3 Vortex Transport Analysis

Excellent results were obtained on a number of runs by analysis of the PCM data. Furthermore, using the post analysis capability of the PDP-11, a number of runs from days 310 and 343 were processed with excellent results. A number of real time results did not produce useful data because the parameters used in the vortex location algorithm in real time were not optimized for the aircraft being considered. The most frequent result of this problem was that two vortices would be located in a region where, in fact, only one existed. This problem, when it occurred, was immediately obvious by analysis of the scatter plots generated in post analysis. A typical vortex time history as obtained from

TABLE 6-3. SIGNAL TO NOISE CALCULATIONS

Van 1, Day 310	
Spinning Wheel	
SNR = 57 dB (Spectrum Analyzer)	$\eta_{TOTAL} = 0.0097$
SNR (Processor) = 68 dB	$(\eta_{LAB} = 0.11)$
Wind	
SNR = 32 dB	$\beta = 2 \times 10^{-7}\ m^{-1}$
Vortex	
B-747 SNR = 42 dB	$\beta = 2 \times 10^{-6}\ m^{-1}$
B-707 SNR = 39 dB	$\beta = 1 \times 10^{-6}\ m^{-1}$
B-727 SNR = 39 dB	$\beta = 1 \times 10^{-6}\ m^{-1}$

TABLE 6-4. SIGNAL TO NOISE CALCULATIONS

Van 2, Day 310	
Spinning Wheel	
SNR = 50 dB (Spectrum Analyzer)	$\eta_{TOTAL} = 0.0022$
SNR (Processor) = 61 dB	$(\eta_{LAB} = 0.10)$
Wind	
SNR = 34 dB	$\beta = 3 \times 10^{-7}\ m^{-1}$

analysis of the PCM data is shown in Figure 6-3. This shows the vortex time history obtained from run 1034 on day 310. The aircraft in this run was a DC-8. A number of correlations were performed to assess the reliability of the system in vortex location. Table 6-5 shows the correlation of tracks generated by the 2 vans using the same algorithm on the same data. The columns in this table identify ΔX, the average difference in position horizontally between the locations of the vortex by the two vans over the length of the run, X_{VAR} the variance in this difference, and ΔY and Y_{VAR}, the same quantities for the vertical displacements. These are each shown for the port and starboard vortices separately. It may be seen that although the average differences are small, in some cases there are very large variances. This indicates that a number of location errors have been made due to the poor choice of parameters in the algorithm. These variances are reduced somewhat by processing the high speed (PCM) data with the vortex location algorithm as may be seen from Table 6-6. The overall result of the vortex transport studies was that good vortex transport information could be obtained, but that new processing parameters were required for optimum real time performance.

6.1.4 Vortex Flow Fields

During this phase of the tests some preliminary analyses of vortex flow fields were performed. By analyzing the function V_{pk} versus angle, it is possible to obtain a plot of the tangential velocity profile of the vortex using the assumption of circular symmetry. V_{pk} is especially useful for this purpose because it does not require that the system be focused at the correct range for the given vortex. Considering ranges which fall within the range bin of the vortex range ±33 ft (±10 m), the value of V_{pk} for any point in this range should be a measure of the tangential velocity of the given vortex at the angle associated with that point. A typical plot of V_{pk} as a function of angle is shown in Figure 6-4. It may be seen that the vortex consists of two high velocity regions which may be associated with opposite sides of the vortex core, and a null between them which may be associated with the vortex center. It will be noted that one of the velocity peaks is higher than the other, indicating that this side of the vortex had a velocity which added to the ambient wind velocity. It will also be noted that the high velocities expected at the vortex core are absent in this picture. This is believed to be a result of the fact that the regions of high velocity are too small to be seen by the system. Referring to Figure 6-5, it

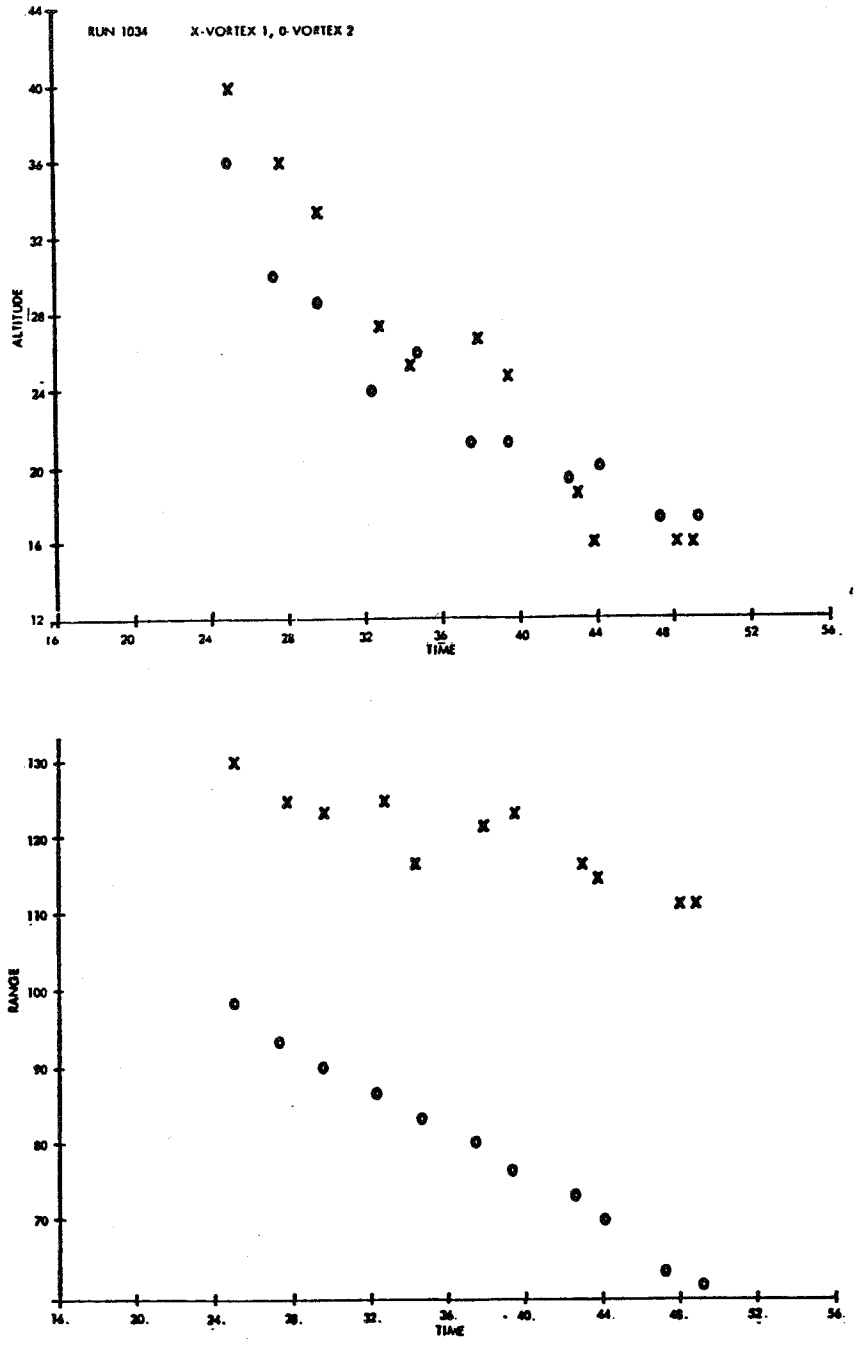

Figure 6-3. Vortex time history.

NOTE: RANGE IS IN METERS, TIME IS IN SECONDS

TABLE 6-5. SENSOR CORRELATION

Real Time V_{scat}									
Day 310									
		Port				Starboard			
Run	Aircraft	ΔX	X_{VAR}	ΔY	Y_{VAR}	ΔX	X_{VAR}	ΔY	Y_{VAR}
29	B-707	- 2.5	33.8	- 3.6	8.3	-17.3	62.8	- 0.8	12.3
34	DC-8	-12.9	35.2	-10.7	10.9	11.9	38.1	13.3	19.7
41	B-727	- 3.1	49.1	- 5.1	9.6	-19.9	28.2	- 7.7	19.9

TABLE 6-6. SENSOR CORRELATION

Day 310, Run 36, B-707								
	ΔX	X_{VAR}	ΔY	Y_{VAR}	ΔX	X_{VAR}	ΔY	Y_{VAR}
PDP-11 V_{SCAT}	14.0	51.2	7.9	11.7	17.9	32.7	6.5	15.7
High Speed	-2.5	20.1	0.8	8.3	2.2	14.7	2.5	8.3

Note: x, y units in meters.

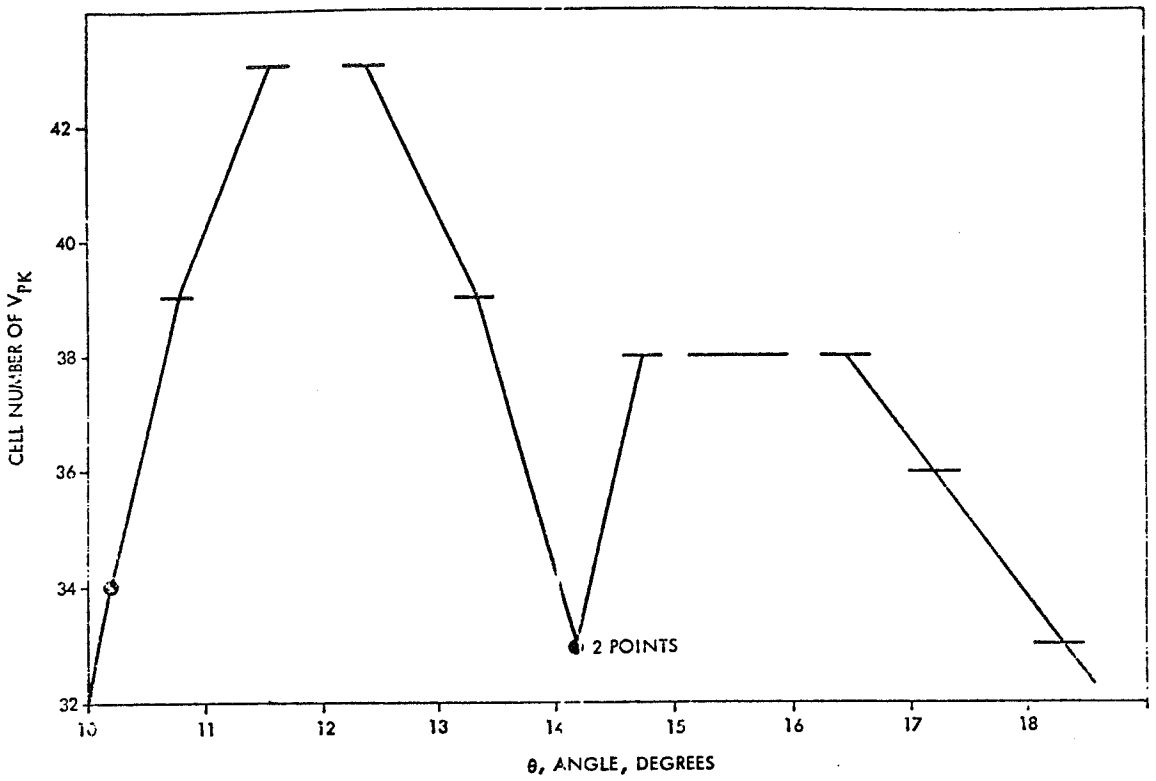

Figure 6-4. V_{pk} versus θ for a B-707 vortex Day 310, Run 1029, scan 1 vortex 1 range = 100 ± 20 m.

may be seen that with a given signal-to-noise ratio from the wind signal, there is a minimum detectable target length below which the system will not receive a signal above threshold. In Figure 6-5 the signal-to-noise ratio is represented by the horizontal axis which shows the wind amplitude above threshold in least significant bits with 16 least significant bits corresponding to 3 dB. The minimum detectable target length is proportional to the range resolution with the proportionality factor shown on the vertical axis. For a typical case on day 310 with the wind signal averaging 52 least significant bits above threshold, the minimum detectable target is slightly greater in size than two tenths of a range resolution element. This corresponds to a length of approximately 10 ft (3 m) at a range of 492 ft (150 m). Typical vortex velocity profiles are illustrated in Figure 6-6 where lines of constant parallel component of velocity are shown. The figures show the vortex velocity profiles for conditions of no wind, a moderate cross-wind, and a reasonably strong cross-wind. The maximum tangential velocity

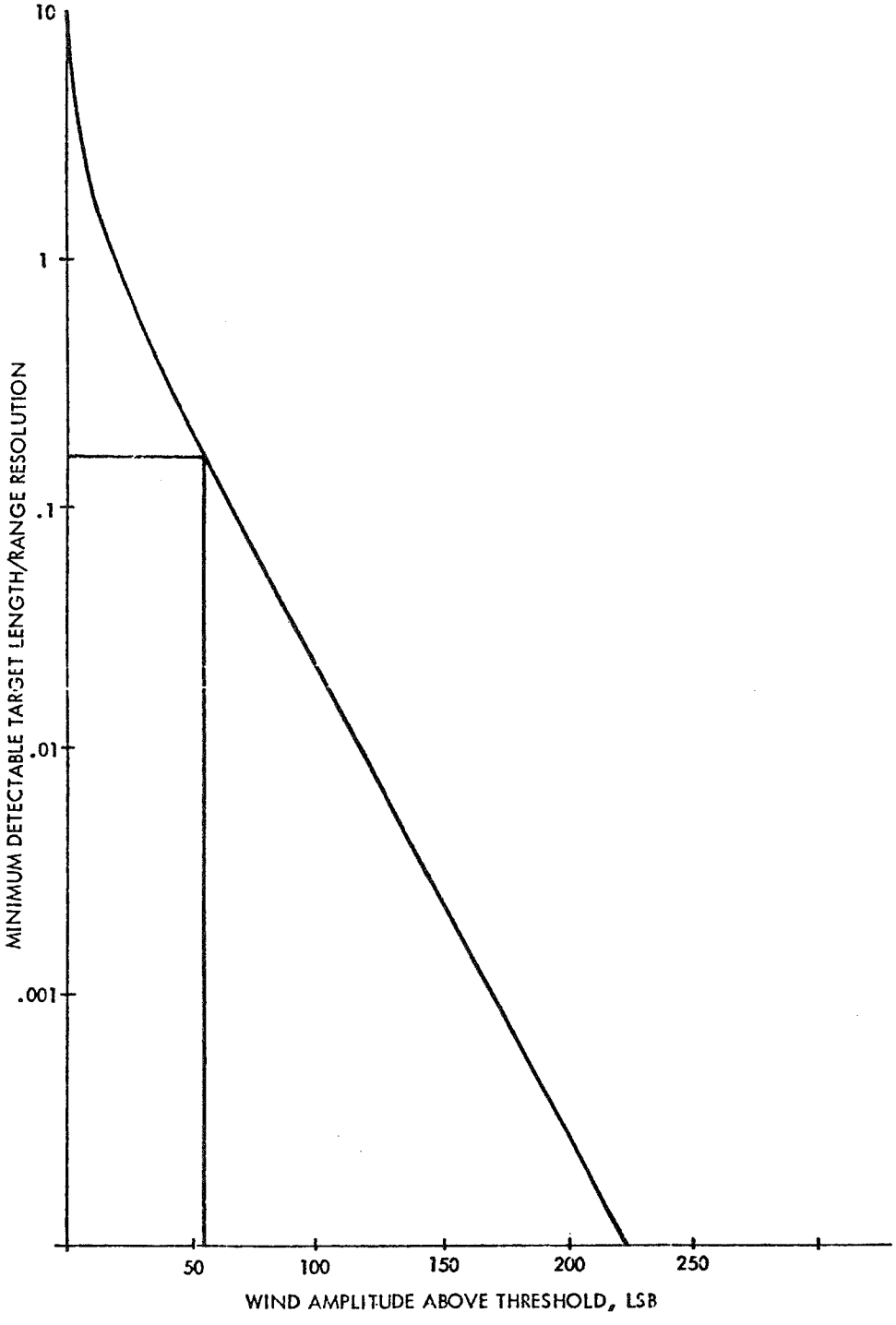

Figure 6-5. Smallest detectable target size as a function of wind amplitude above threshold.

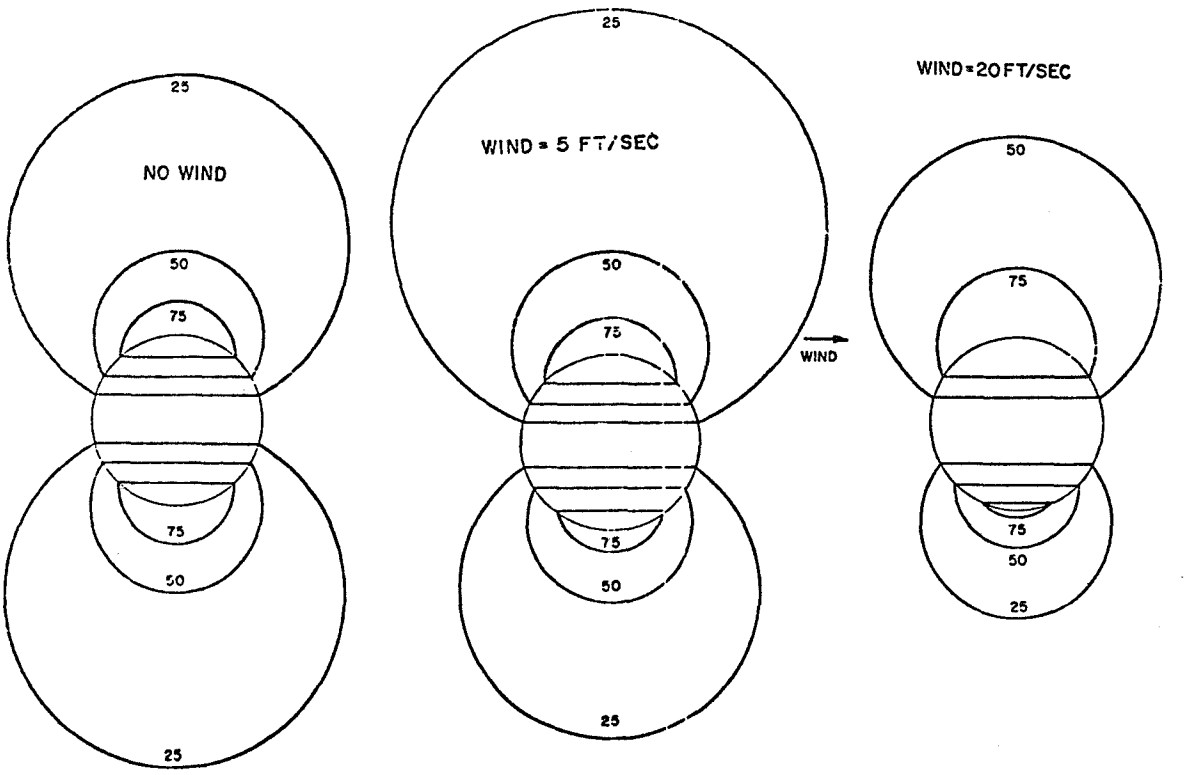

Figure 6-6. Interaction of vortex and wind vortex V_{max} = 100 ft/s.

of the vortex is assumed to be 100 ft/sec (30 m/s). It may be seen that the regions containing velocities greater than 75 ft/sec (23 m/s) are extremely small. Furthermore, as the cross-wind velocity increases, the regions on the side of the vortex which oppose the wind become even smaller and those on the other side become larger. Since these regions are extremely small, it is anticipated that they will not be seen with the Laser Doppler System.

In addition, the cross-wind increases the size of the regions on the side of the vortex which add to the wind and makes the detection of these regions more probable than the detection of the same velocity on the opposite side of the vortex. The result of this is a high probability that the top of one vortex and the bottom of the other vortex of the pair will be located by the system. This leads to an altitude difference between the vortices, immediately after their formation, with the down-wind vortex being lower in altitude. This has been observed in most of the data which has been analyzed where a significant cross-wind was present.

Several calculations of vortex circulation were made using the programs described in Section 4.3.1.6. A sample result of this analysis is shown in Figure 6-7. These data were obtained from run 1029 on day 310 with a B-707 aircraft. The circulation initially was somewhat in excess of 4000 ft^2/sec (372 m^2/s) and dropped rapidly with time. The circulation program was very successful in analysis of data from day 310, partly because the cross-wind velocities for these runs were very low.

6.1.5 Data Verification

The data received by the PDP-11 were verified by comparison to the PCM data. This was accomplished by introducing known signals to the system and examining the output of the PCM data tapes as well as the values of various parameters indicated by the PDP-11. It was determined that a scale factor was used on the I_{pk} for the PDP-11 so that the resulting I_{pk} was approximately three-fourths of that on the PCM data. The exact number may be calculated as follows: take the original number 58 (binary 111010) and divide by 2 to get 29 (binary 11101); then divide 58 by 4 to get 14 (binary 1110). Add 29 and 14 to get the exact number 43 (binary 101011).

The data verification consisted of real time and post analysis testing. Results of the real time tests indicated that the system was always performing correctly. When known signals were input, the correct parameters were always obtained at the computer. Threshold controls were changed during a run and sometimes were held between numbers for a long period of time. Portions of the test were performed at an integration time of 8 ms to reduce the data rates. A few tests were also performed at 2 ms because that was the most commonly used integration time. Furthermore, width integration was tested by inputting a signal which would exceed an amplitude threshold of 83 but not 84 with a width integration of 1, and then increasing the width integration and decreasing the amplitude threshold (A_T) until the signal exceeded it. The results are shown in Table 6-7. This indicates that the width integration is operating correctly.

After the real time results had been analyzed, the PCM data were reduced and compared to the real time data which had been recorded. No errors were located in the I_{pk}, V_{pk}, V_{max}, or N results.

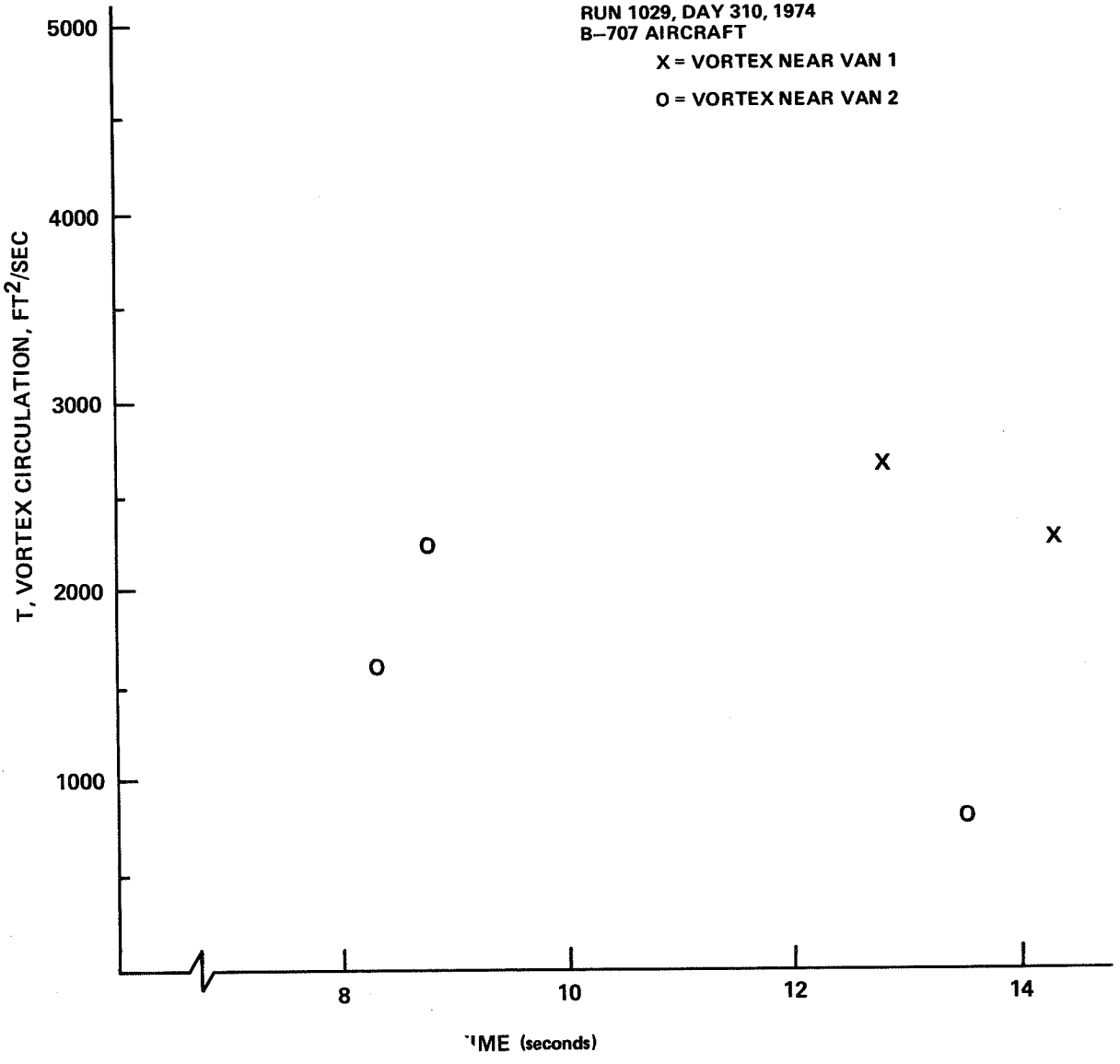

Figure 6-7. Vortex circulation versus time.

TABLE 6-7. WIDTH INTEGRATION TEST

Width	Required A_T to Obtain Signal
1	83
2	40
4	19
8	9
12	6

6.1.6 Thresholds and Algorithm Parameters

A critical part of the operation of the system was the selection of velocity and amplitude thresholds on the processor. The following procedure was established for threshold setting. First, the amplitude threshold was set 10 least significant bits above the noise floor. Then the velocity threshold was adjusted so that no signals were obtained from the ambient wind. These thresholds were varied slightly to meet aircraft and atmospheric conditions as appeared to be necessary during the test. The choices of the thresholds turned out to be adequate for good vortex location in almost all cases.

A number of parameters were available to be used in optimizing the vortex location algorithm in real time as described in Section 4.2. The selection of the otpimum default parameters was performed by post analysis of the data, especially that from days 310 and 343. The results of this analysis produced the default parameters shown in Table 6-8. The primary difference between these parameters and those used during most of the data collection is the increased radius and the use of NR = 2 for larger aircraft. Effectively, the result of these changes was to increase the distance away from the first vortex within which a second vortex could not be located. It was also concluded from this analysis that the use of I_{pk} as opposed to V_{pk} was desirable for vortex location, as indicated by the theoretical analysis in Section 4.

TABLE 6-8. DEFAULT PARAMETERS

Condition Radius	R = 60
Minimum Data Requirements	A = 50 B = 50
Second Vortex Requirement	C = 25
Next Scan Requirement	D = 50
Second Vortex Exclusion Region	NR = 1 for small aircraft 2 for large aircraft

Note: The small aircraft category includes the B-727 and all smaller aircraft such as the DC-9 and B-737. Large aircraft include the DC-8, B-707, C-880, DC-10, B-747, and L-1011

6.2 Phase II Airport Tests

During the second phase of airport tests performed at JFK Airport, over 700 aircraft landings were monitored in a variety of different atmospheric conditions. These were analyzed for studies of vortex transport and flow fields. In addition to the regular tests, two groups of high altitude flybys were made using a Convair 880 aircraft. These provided vortex transport information at high altitudes and, in addition, permitted a system evaluation at long ranges and high angles above the horizontal. A number of the normal landings were selected for further analysis of the vortex transport data generated by the PDP-11. An analysis was performed to determine the number of runs with various types of aircraft and various wind conditions as well as correlations of these parameters with vortex transport phenomena.

6.2.1 High Speed Tape Analysis

Several high speed tapes from day 136 were analyzed to evaluate system performance and to measure vortex flow fields. Noise data for this day were not available at the time the analysis was performed. However, an estimate of the noise was made by calculating the average and standard deviation

of the amplitude in a high velocity filter when no vortex was present along the line of sight. The average noise level was determined to be 45 least significant bits with a standard deviation of 6.8. Using these values, the highest signal-to-noise ratio in a scan for a B-747 vortex varied between 34 and 45 dB and that for a B-727 varied from 26 to 32 dB.

The B-747 vortices were determined to be initially separated by approximately 148 ft (45 m) which compares favorably with theory. In the case for day 136, where a very low cross-wind existed, both vortices were transported almost directly downward with no horizontal component of velocity. Transport plots are shown in Figure 6-8. The effective circulations were intially approximately 6000 ft^2/sec (558 m^2/s) for both vortices compared to a theoretical value of approximately 6500 ft^2/s (604 m^2/s) which was calculated using the assumption of elliptical wing loading and the parameters of a typical B-747 at a landing weight of 500 000 lb and landing at a speed of 152 knots (78 m/s). The circulation strength as a function of time is shown in Figure 6-9.

The B-727 vortices were determined to be initially separated by approximately 92 ft (28 m) which is in good agreement with theory. The vortices for the B-727 case under consideration, moved horizontally at approximately 3 ft/sec (1 m/s) away from Van 1, as shown in Figure 6-10. The vertical transport of the vortices for this B-727 case is shown in Figure 6-11. The effective circulation calculated from SLDV System data at 0.10 sec behind the aircraft indicates a value of approximately 3800 ft^2/sec (353 m^2/s) for one vortex and 2600 ft^2/sec (242 m^2/s) for the other. A plot of effective circulation versus time is shown in Figure 6-12. The theoretical value of 3300 ft^2/sec (307 m^2/s) was computed using a weight of 169 000 lb and landing speed of 152 knots (78 m/s). Calculation of effective circulation for vortices from SLDV data taken less than 10 sec behind the aircraft is not meaningful with existing processing software due to the presence of multiple vortices.

6.2.2 Statistical Analysis of Data

A statistical analysis was performed on a number of the runs analyzed during this test to determine the overall system performance in an airport environment and to study vortex transport as a function of atmospheric parameters. For each run, the aircraft type, atmospheric parameters, vortex transport parameters, and parameters related to system performance were tabulated. It will be shown that more than 95 percent of the available data produced useful results for all larger commercial aircraft and that vortex descent rates comparable with theoretical calculations were obtained. Usable data were obtained at all wind speeds and directions occurring during the test.

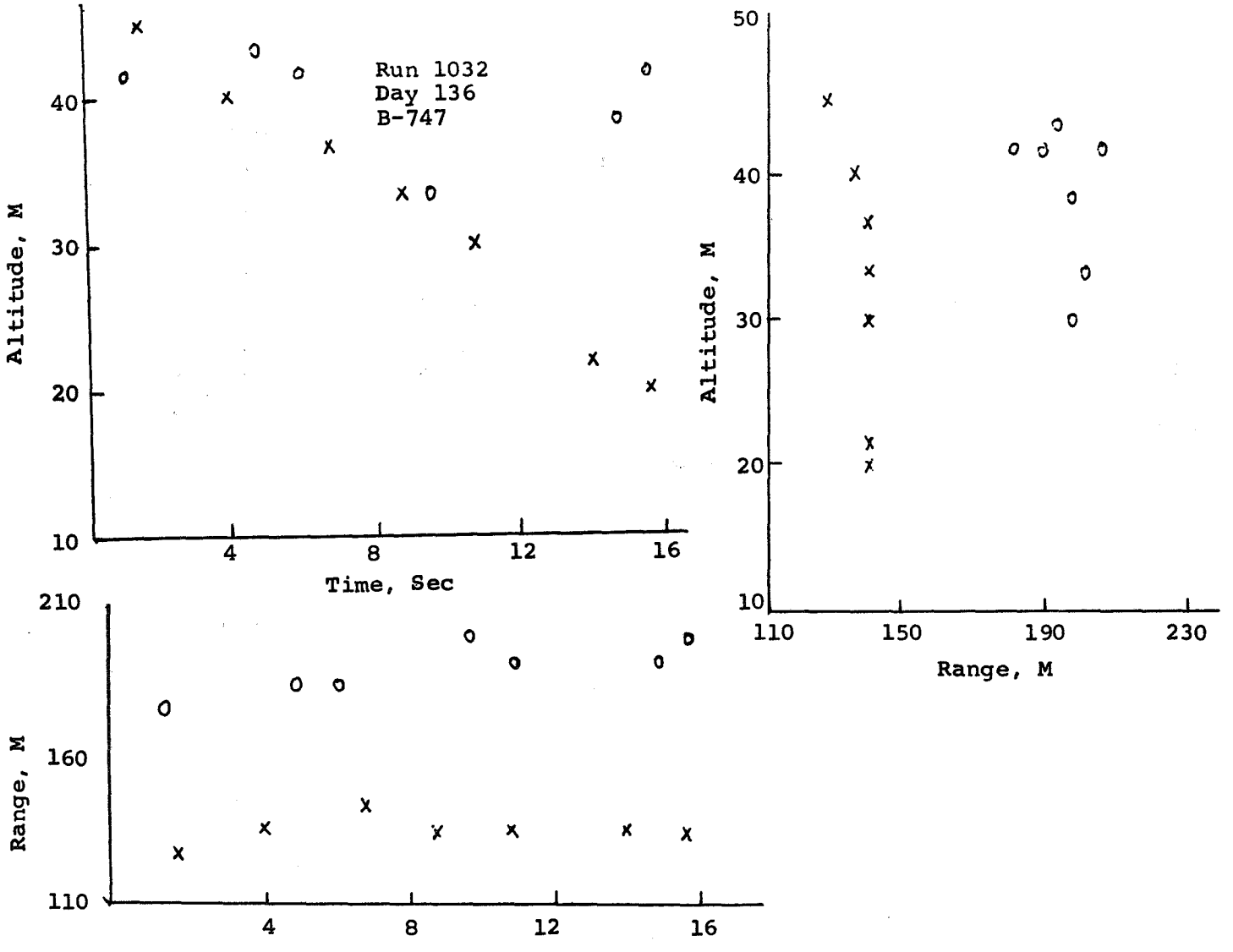

Figure 6-8. Transport of near (x) and far (0) vortices.

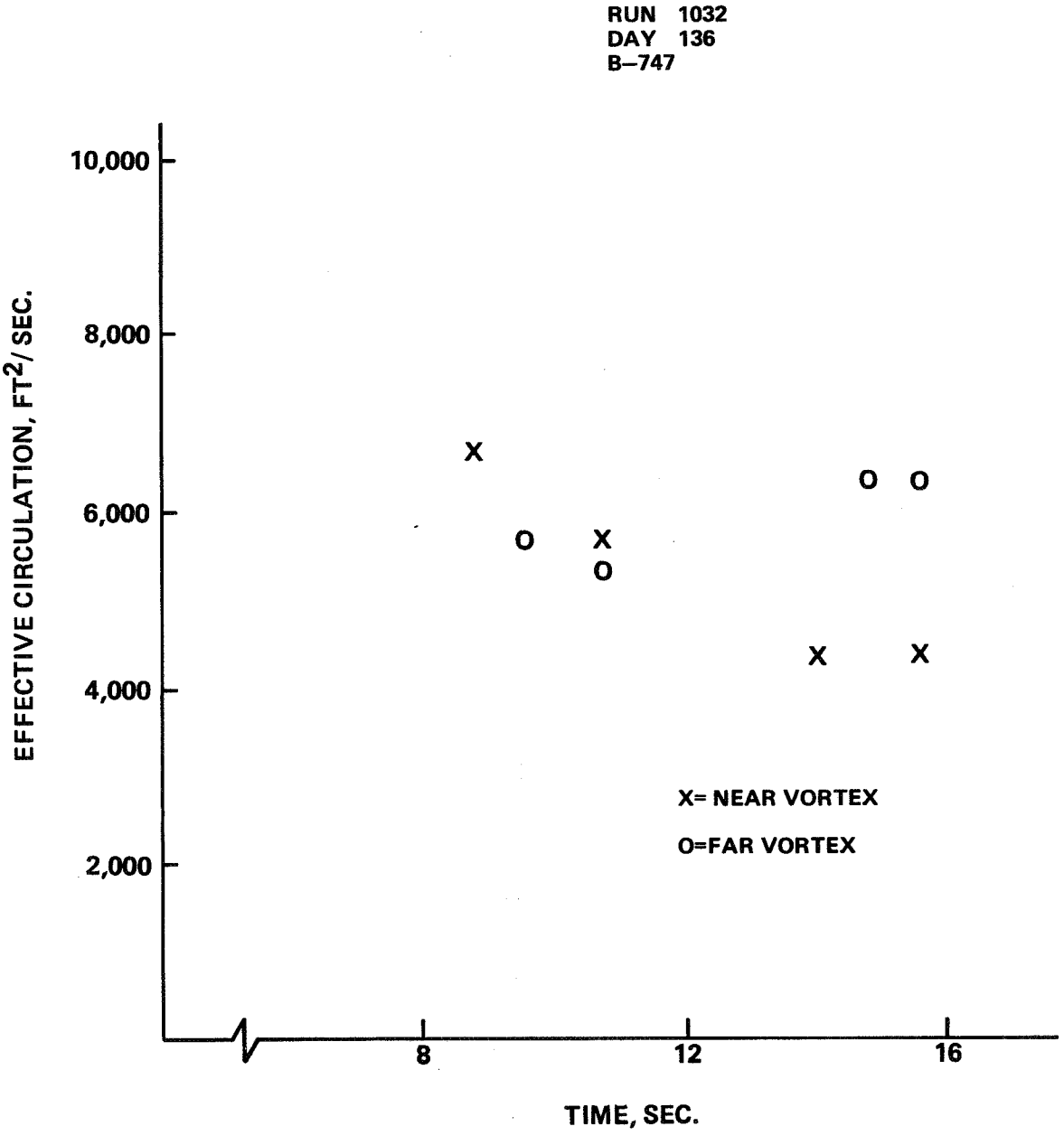

Figure 6-9. Vortex circulation versus time.

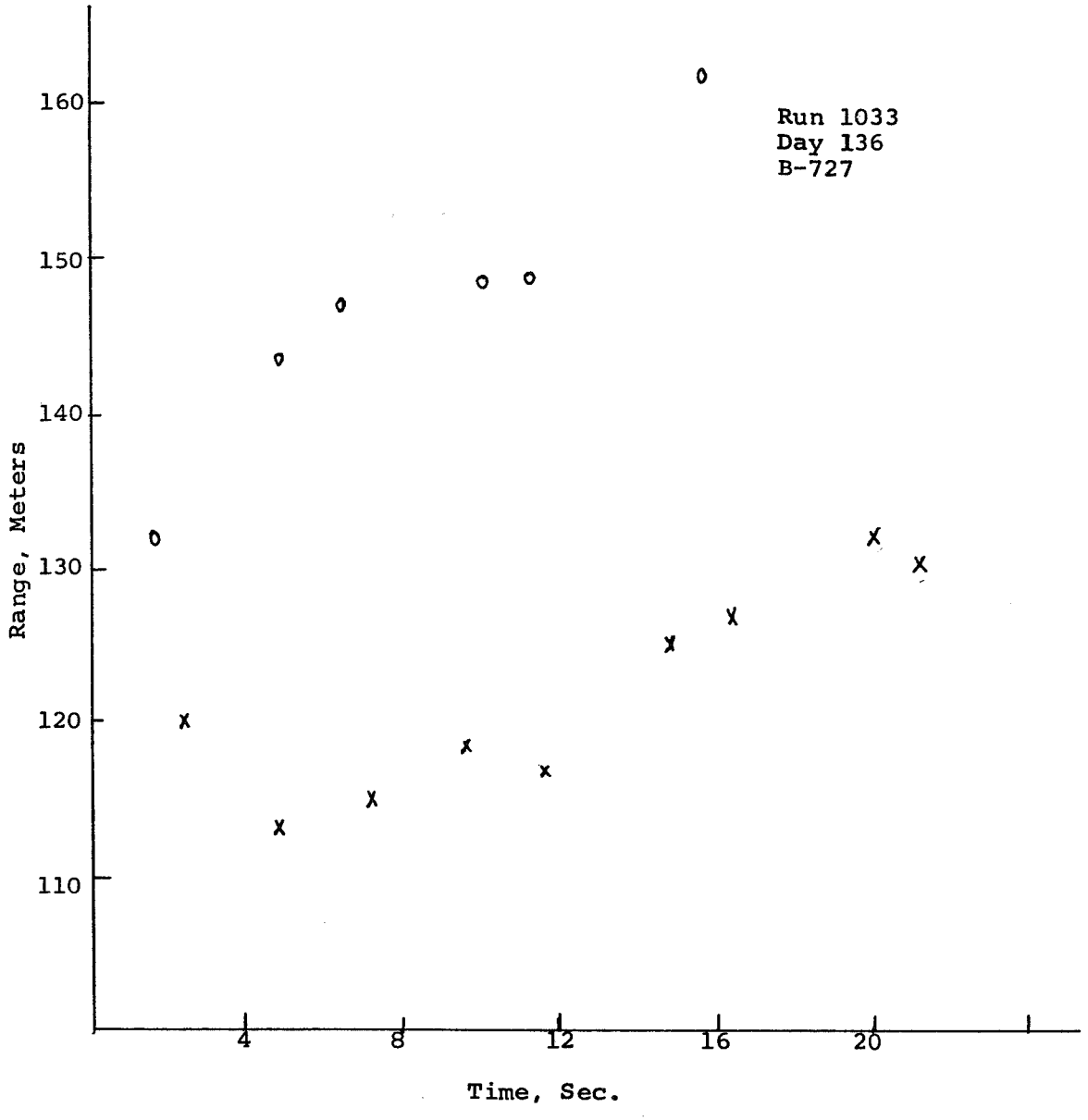

Figure 6-10. Vortex time history; horizontal transport.

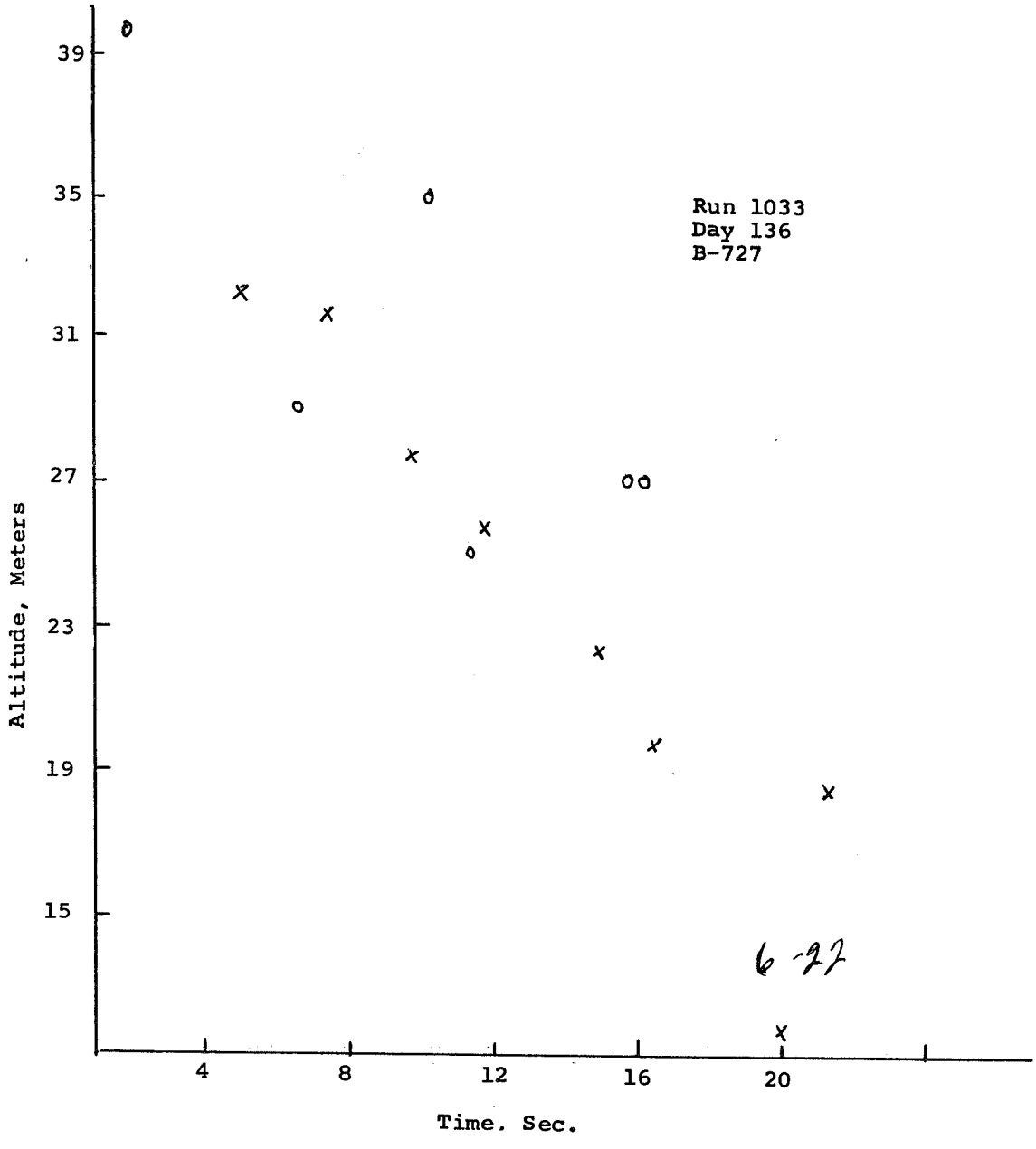

Figure 6-11. Vortex time history; vertical transport.

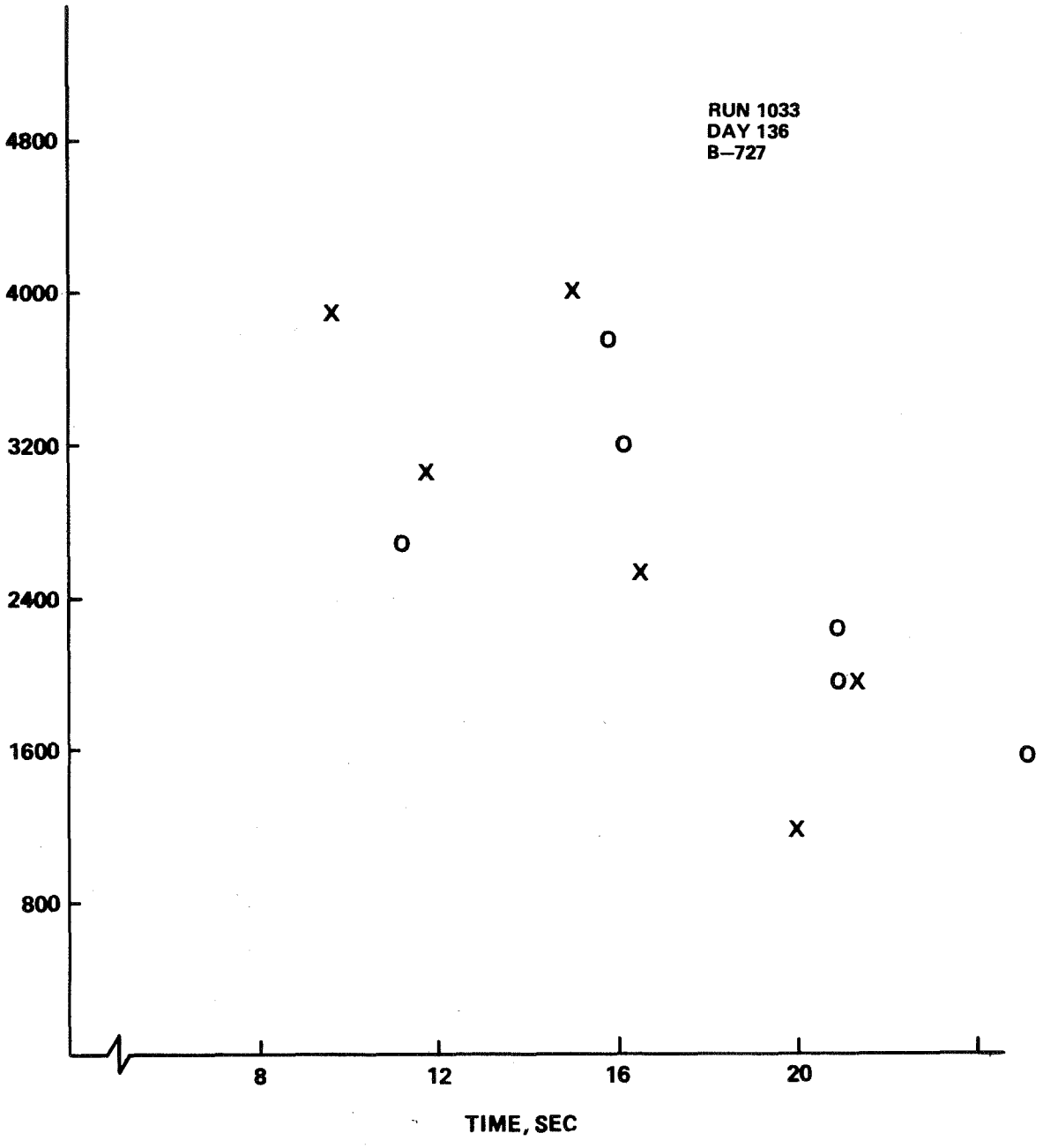

Figure 6-12. Vortex time history; circulation versus time.

A secondary objective of the test was to determine the statistics on aircraft landings at a typical large airport. Figure 6-13 shows a wind rose for runway 31 right at JFK Airport. The number in each sector on this graph indicates the percentage of total landings which occurred during the wind conditions indicated by that sector on the graph. The angular scale shows degrees magnetic heading with the runway heading being approximately 312° and the radial scale shows the wind speed in knots. It may be seen that the majority of the landings occur within 45° of the runway heading, but that a wide variety of directions are represented including a few runs with a slight tail wind. No runs were obtained with a cross-wind component exceeding 15 knots from the southwest (220°) or 10 knots from the north-east (40°). Also, no runs were recorded

Numbers are percent of total landings at each wind velocity.
Shaded areas show regions of more than 10, 20, and 30 landings.
Total: 631 Landings

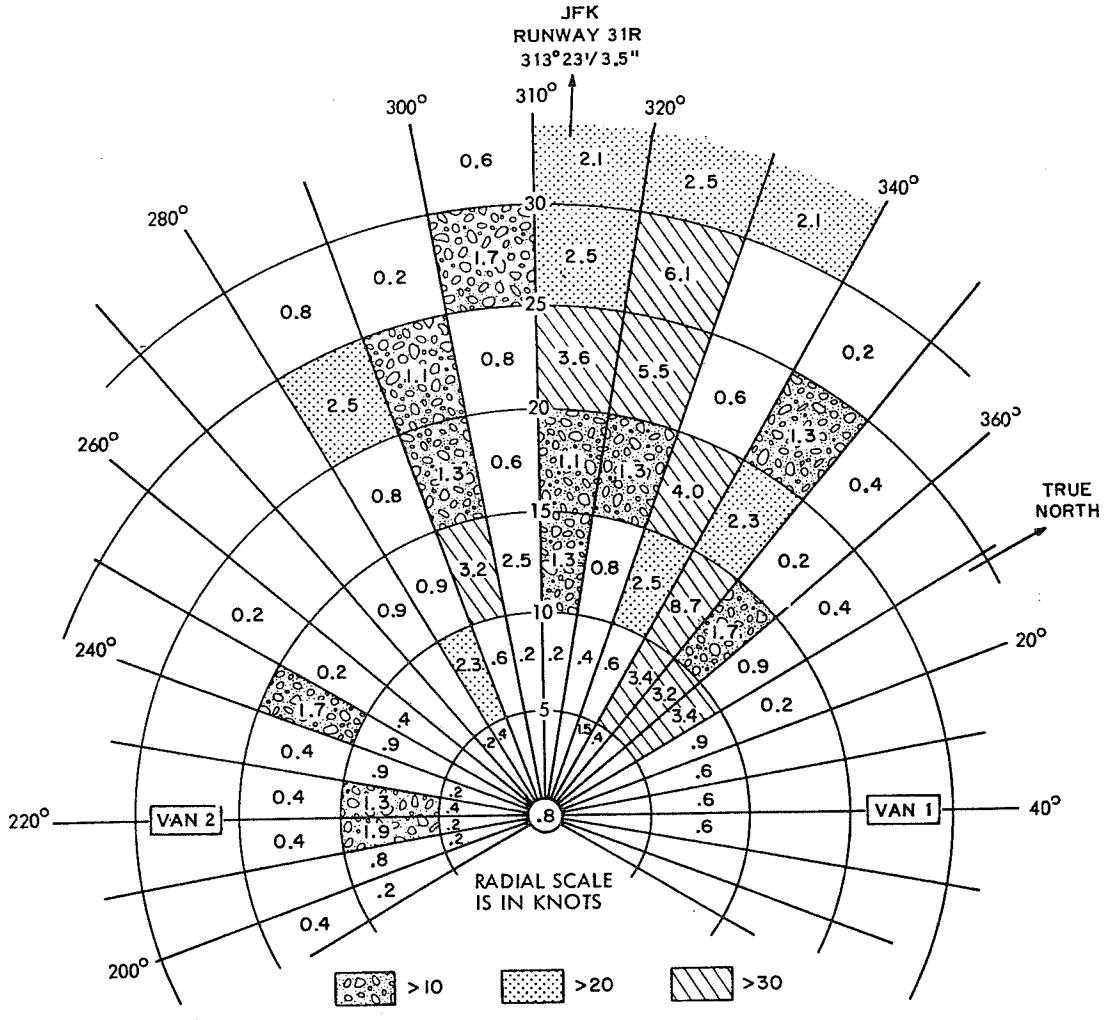

Figure 6-13. Wind rose for runway 31R JFK Airport.

with a tail wind component exceeding 5 knots (wind information taken from JFK Airport control tower). Runway usage is determined by noise abatement requirements as well as wind direction, and it is evident that on a number of occasions the runway usage is not determined by wind conditions alone. Another study of interest in evaluation of airport usage is the number of each type of aircraft using the airport. Table 6-9 shows a sample of each type of aircraft landing on runway 31 right at JFK Airport during the test periods on each day of the tests. Figure 6-14 summarizes the overall results showing the aircraft mix which may be expected on the average on any given day during similar time periods. This represents an average over 631 samples obtained during the test. Aircraft having similar size, weight, and engine configuration are grouped together. The B-737 and DC-9 are also grouped together because, although they are different in configuration, they are similar in size and they represent such a small percentage of the total sample that better statistics may be obtained by grouping them together. The predominant aircraft type is the combination of the B-707 and DC-8 aircraft. These landings account for over 37 percent of the total landings. The next most common type is the B-727 which accounts for over 23 percent of the total landings. This category includes two very different size aircraft, the model 100 and the model 200, which were not identified separately in the data. The B-747 accounts for approximately 18 percent of the total landings and the other large jets DC-10 and L1011 account for only 6 percent. The DC-9 and B-737 make up approximately 11 percent of the total sample and the remaining 3 percent consist of all other types of aircraft, including mainly BAC1-11. Since these include such a small total number, the percentages shown should not be considered representative of the airport.

For evaluation of system performance and vortex transport, a random sample comprising 63 percent of the total runs was used. For this purpose, a "run" is considered to be one landing as observed from one van. This definition provides the best analysis of system performance because it allows each van to be considered independently. The data available for analysis which had all the necessary parameters recorded in the log books consisted of 845 runs from 16 days with the majority of the runs from Van 1, since Van 2 was used for a sizable portion of the time to test the translator operation and was not available for data collection. As shown in Table 6-10, 359 runs were selected from Van 1 and 177 from Van 2 for detailed analysis. These represent the earlier runs from each day's data collection and no effort has been made to select either especially good or bad runs for this analysis. The number of runs evaluated in each wind speed and direction and the aircraft mix for data used in this analysis are shown

TABLE 6-9. SAMPLE NUMBER OF LANDINGS WITH VARIOUS AIRCRAFT TYPES ON EACH DAY OF TEST

Aircraft	Day 79	Day 80	Day 85	Day 86	Day 90	Day 94	Day 98	Day 99	Day 107	Day 111	Day 115	Day 118	Day 126	Day 127	Day 136	Day 140	Day 141	Total
B-707	23	13	9	10	14	5	20	3	4	3	3	6	3	13	15	5	2	151
B-727	18	8	5	5	14	11	20		3	5	13	6	2	10	18	6	5	149
B-737		1						1				1		1	1			5
B-747	16	8	1		15	6	12	2	2	1	2	5		12	15	1	12	110
DC-8	14	7	4	4	4	6	4	2	1	2	4	1	4	6	12	5	5	85
DC-9	8	4	4	3	7	3	6	1			8	3		6	5	3	2	63
DC-10	1	2	1	1	4	1	2		2		1	1		4	5			25
L-1011	1	1			3				2					1	3		1	12
VC-10	1				1		2	1				1		1	2			9
BAC1-11	5						5				2	3			1	3		19
YAC-40									1									1
4 EPR							1											1
2E Jet											1							1
Total	87	44	24	23	62	32	72	10	15	11	34	27	9	54	77	23	27	631

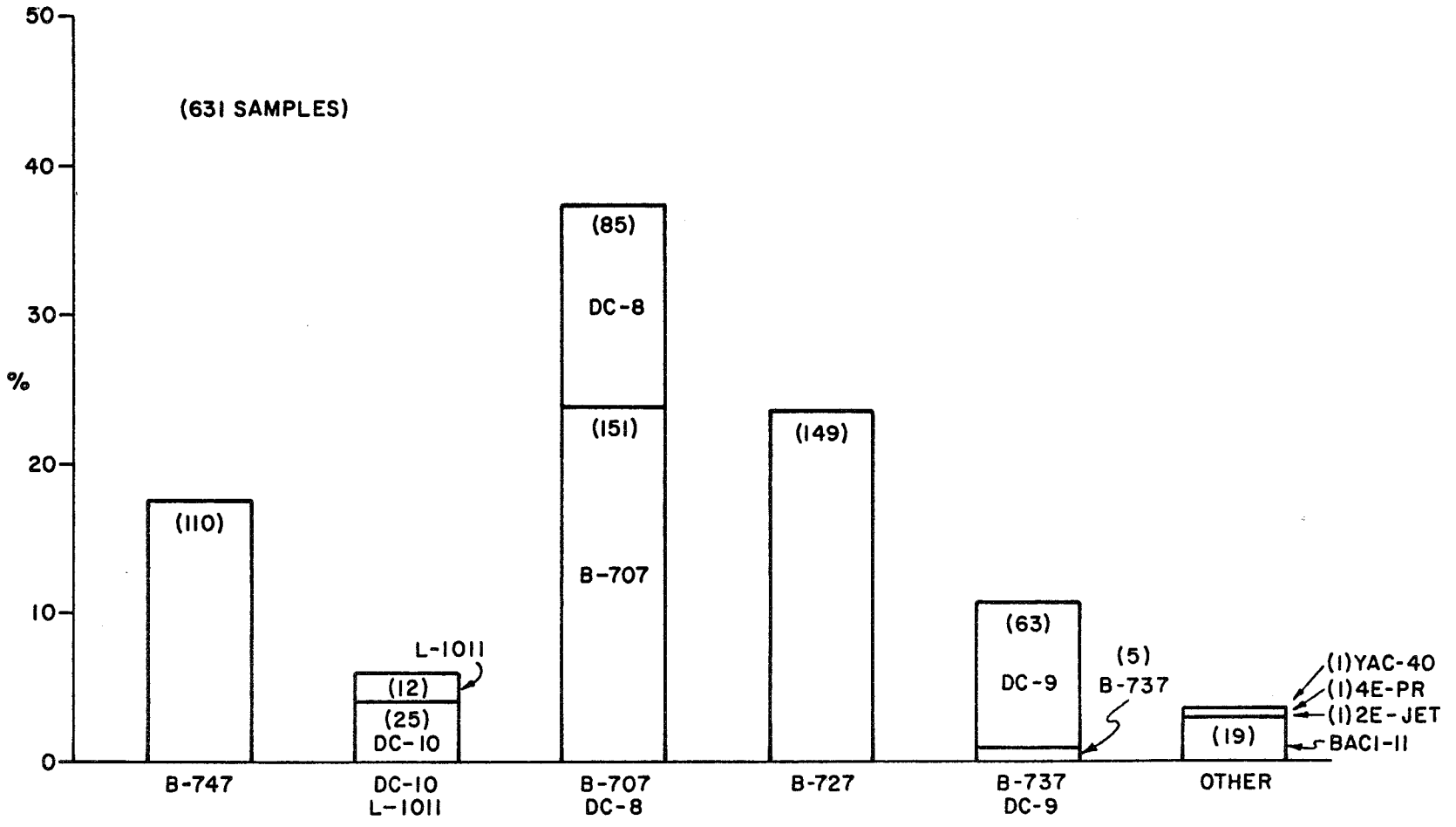

Figure 6-14. Aircraft mix on runway 31R — numbers in parentheses indicate total landings of each aircraft type.

TABLE 6-10. DATA STATISTICS (RUNWAY 31R, JFK AIRPORT, PHASE II)

Data Evaluated for 16 Days	
Data Available	
573 Runs Collected with Van 1	
272 Runs Collected with Van 2	
845 Total Runs	
Data Used in Detailed Analysis	
359 Runs from Van 1	
177 Runs from Van 2	
536 Total Runs Used	
63 Percent of Ttotal	

in Figures 6-15 and 6-16, respectively. These differ from Figures 6-13 and 6-14 in that they consider the total number of runs collected rather than the total number of landings; therefore, in cases where both vans are operational, a given landing is counted twice.

The length of time for which the vortex tracks were observed was also recorded. Figures 6-17, 6-18, and 6-19 show the average length of time for which vortex tracks were obtained at different wind velocities for different aircraft types. Generally, the longer tracks occur at low head winds. The time duration reduces with a large cross-wind due to the vortex being moved out of the scan plane and with a head wind due to the vortex becoming too weak to be detected.

The subjective evaluation of system performance is an important part of the data analysis. System performance may be evaluated according to three criteria: detection of velocities significantly above ground wind velocities in the scan plane region, location of the vortex velocity regions, and separation of the region into two distinct vortices. A further breakdown may be made by judging the ease with which separation is obtained. From these considerations, a subjective scale of numbers from 0 to 5 has been established and the data have been analyzed using this scale. A rating of one was associated with a run in which higher velocities were detected but location could not be obtained. The

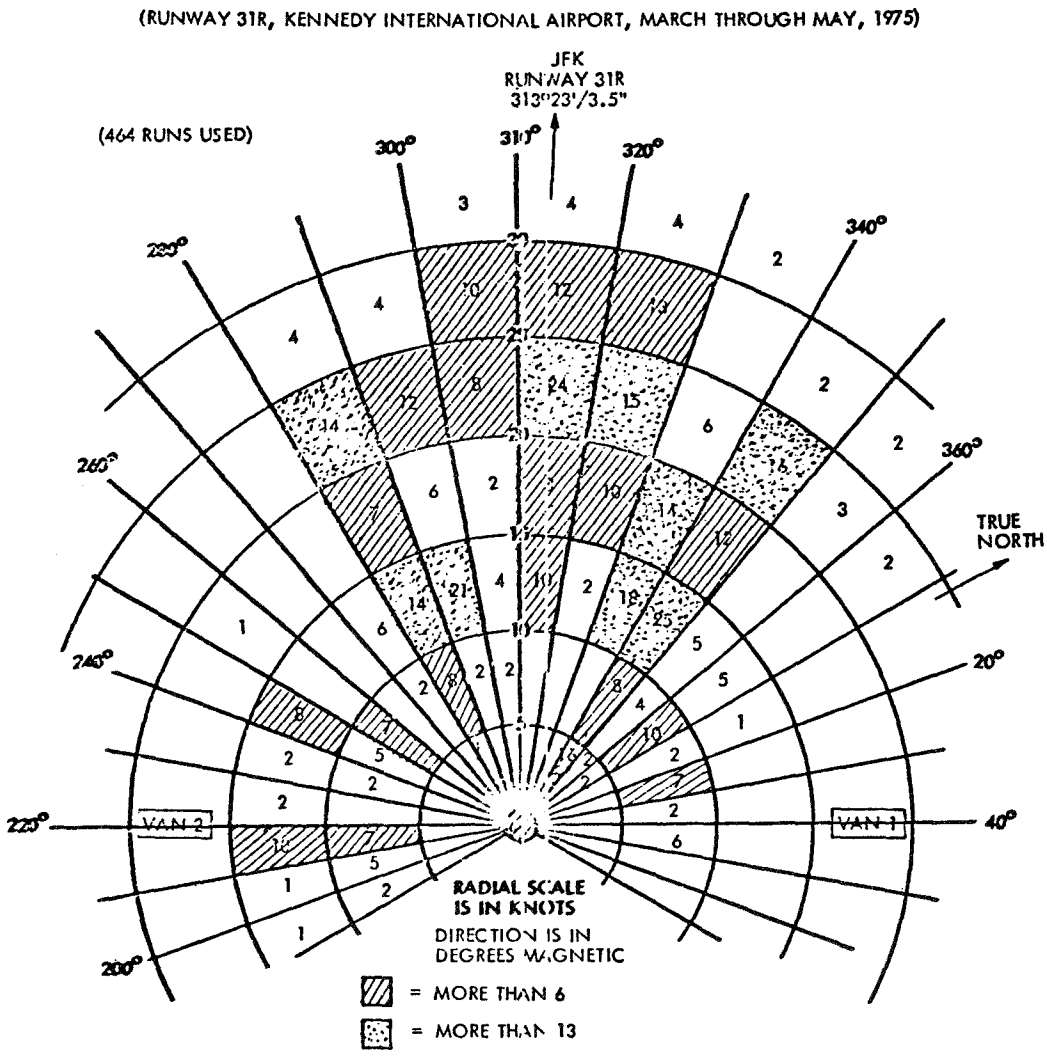

Figure 6-15. Number of runs versus wind speed and direction all aircraft, both vans.

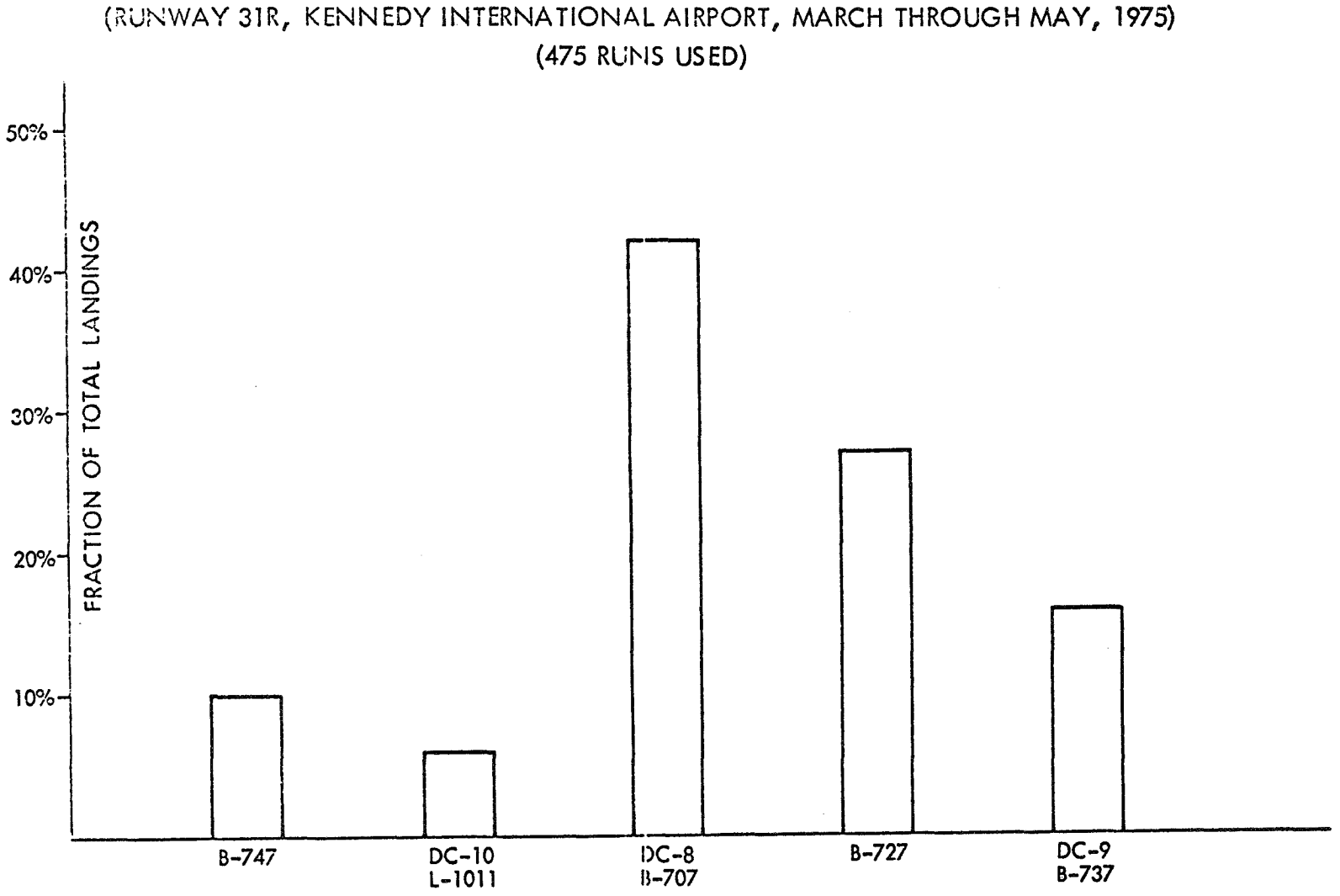

Figure 6-16. Aircraft mix.

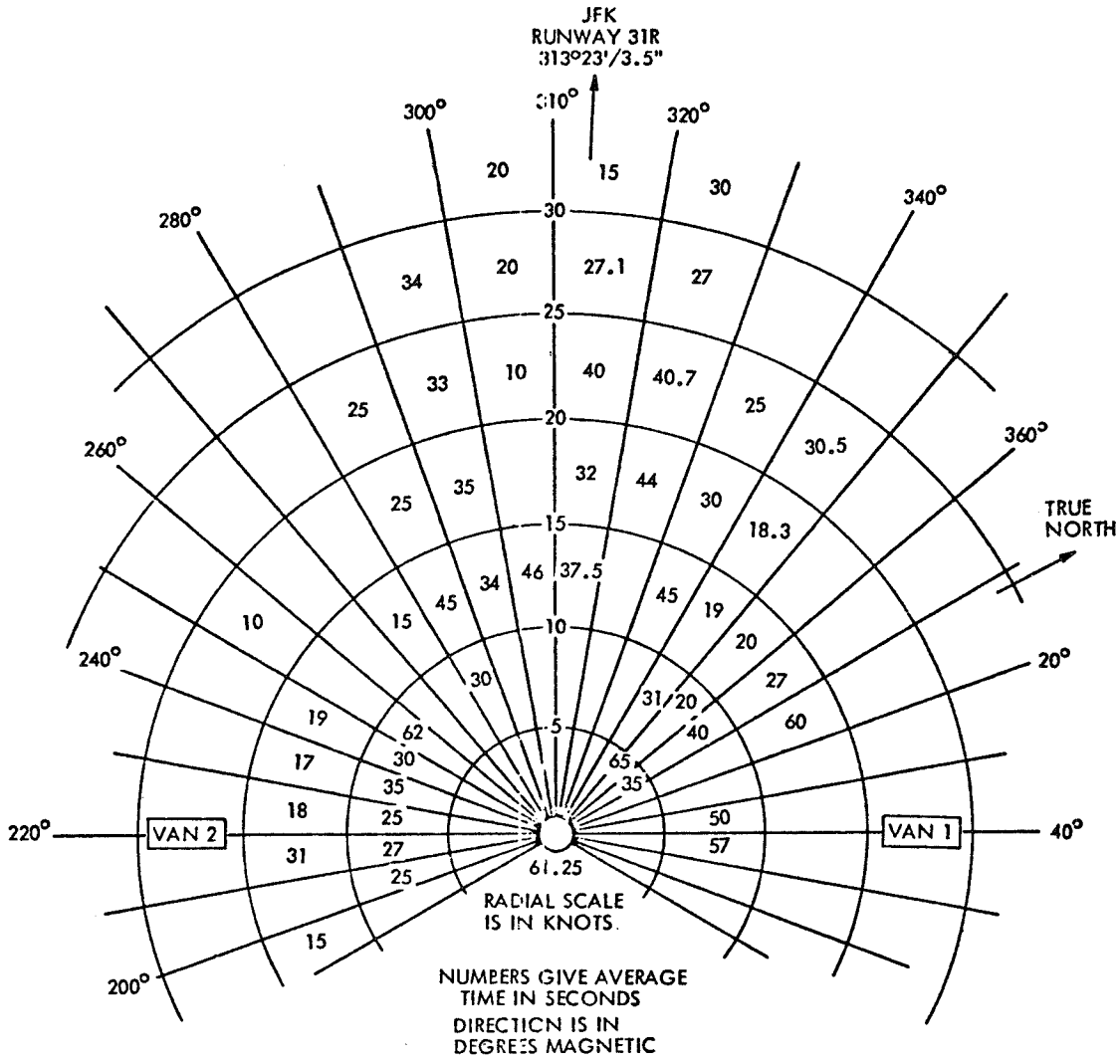

Figure 6-17. Average time of vortex tracks, B-707 and DC-8.

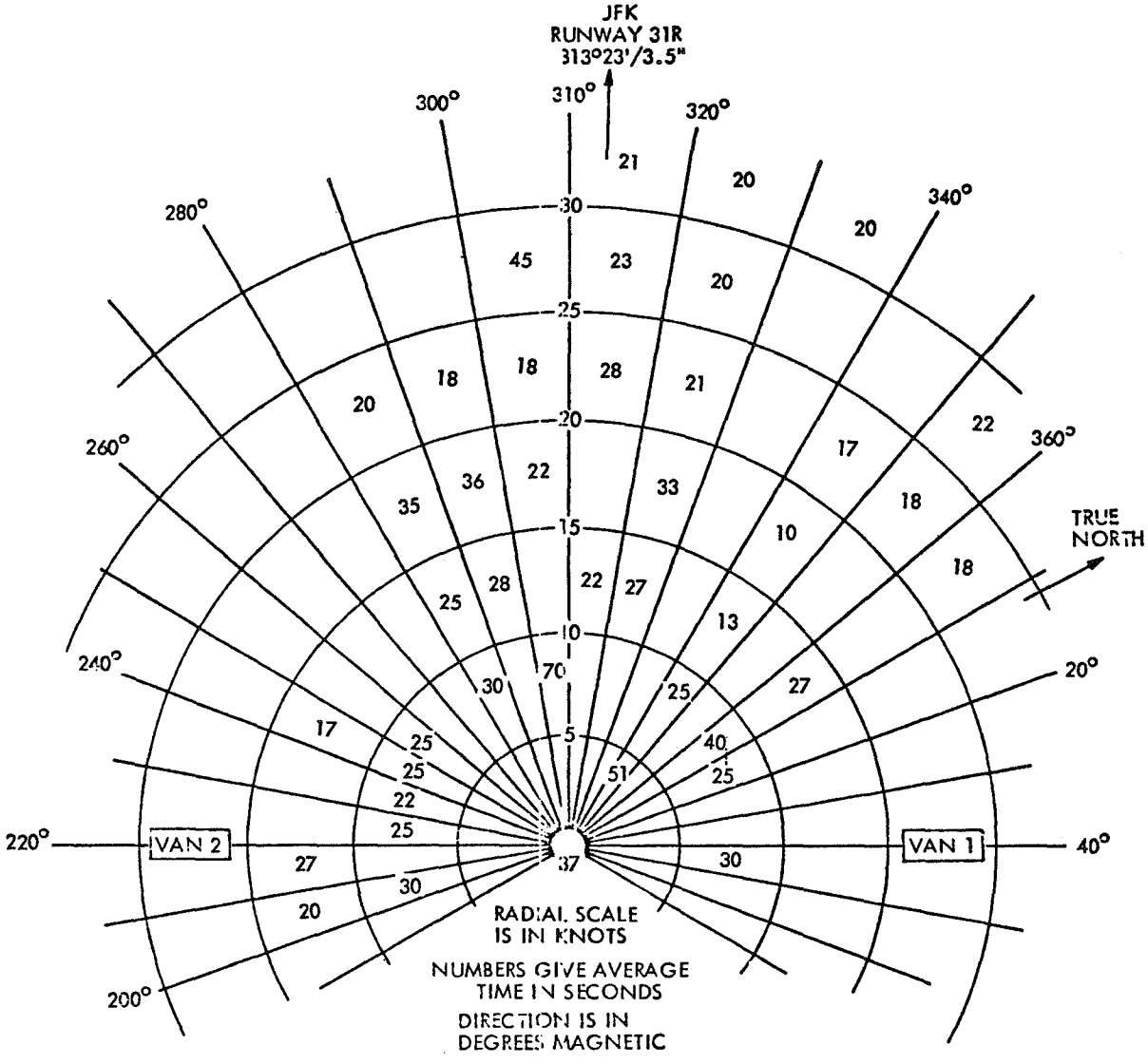

Figure 6-18. Average time of vortex tracks, B-727.

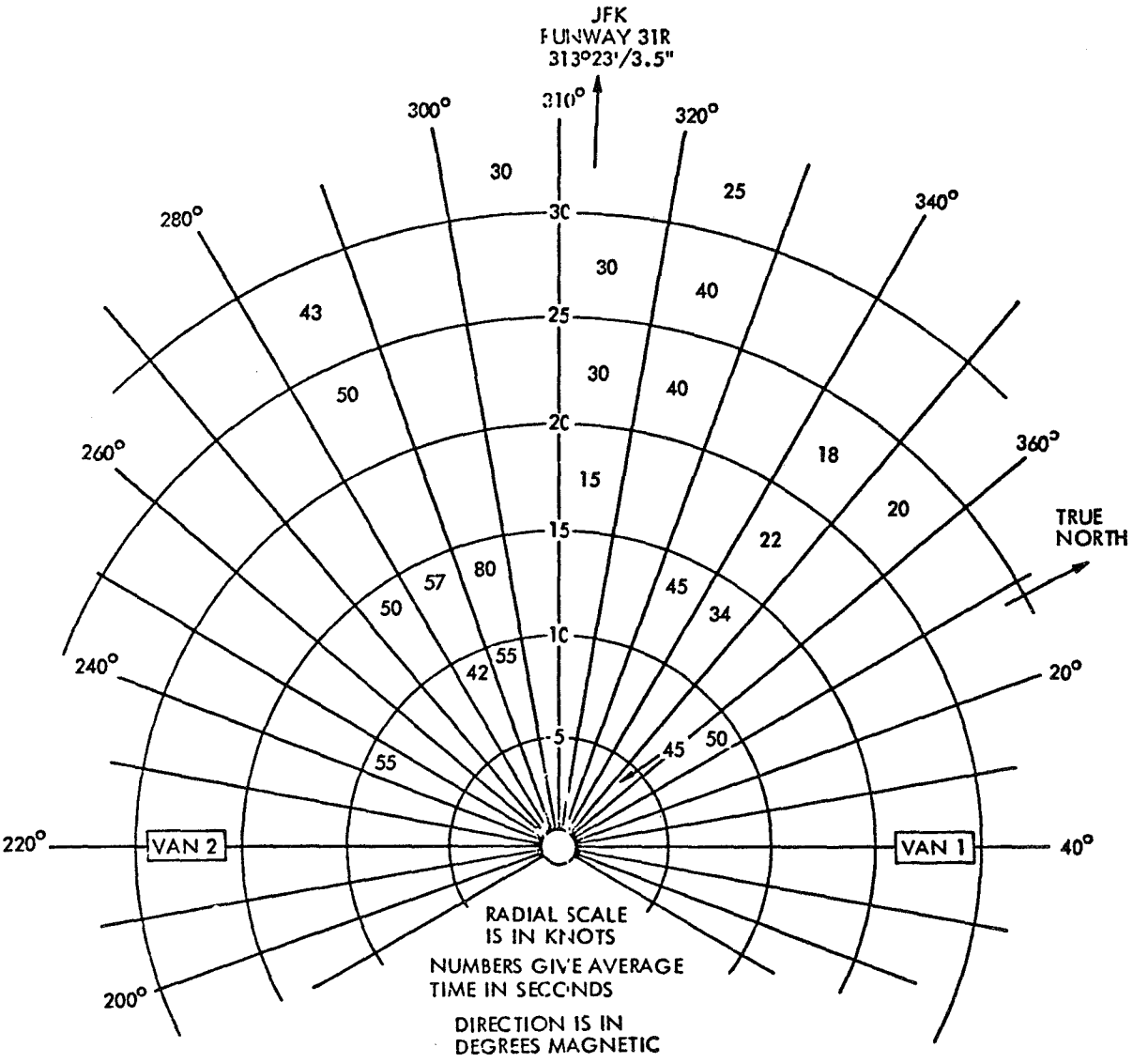

Figure 6-19. Average time of vortex tracks for B-747.

rating was increased to two if it was possible to establish the location of the higher velocity region. If separation of the vortex tracks was possible by examining the entire run, a rating of three was given. If separation was possible on a single scan basis for most scans during the run, a rating of four was given. Finally, a rating of five was given for a run consisting of nearly perfect tracks with almost every scan giving distinct vortex locations. Descriptive adjectives were associated with each of these evaluations as shown in Table 6-11. Assuming that vortex separation is a requirement, the lowest rating producing usable results is three. Figure 6-20 presents sample runs to illustrate data quality evaluation. Evaluating the data from all aircraft types and all wind conditions, it was determined that 88 percent of the data from Van 1 fell into the useable category as did 78 percent of the data from Van 2.

TABLE 6-11. SUBJECTIVE EVALUATIONS

5.	Excellent:	Nearly perfect tracks with almost every scan giving correct vortex locations.
4.	Good:	Separation of vortices possible for most scans.
3.	Fair:	Separation of vortices possible by examining entire run as a whole.
2.	Poor:	Location of region of high velocity only.
1.	Bad:	Detection of high velocities only.
0.	No Data:	Missed detection for the entire run.

The average data quality is shown as a function of wind speed and direction in Figure 6-21. It may be seen that the best runs were obtained when the wind was blowing from Van 2 with a speed less than 10 knots. However, good data were obtained in all directions with a few exceptions which appear to be due to the small size of the data sample. Thus, it may be concluded that the data quality is sufficient for vortex location and separation in all directions. The slight preference for wind velocities from 220° is because of more data being recorded from Van 1 than from Van 2. The average data quality is

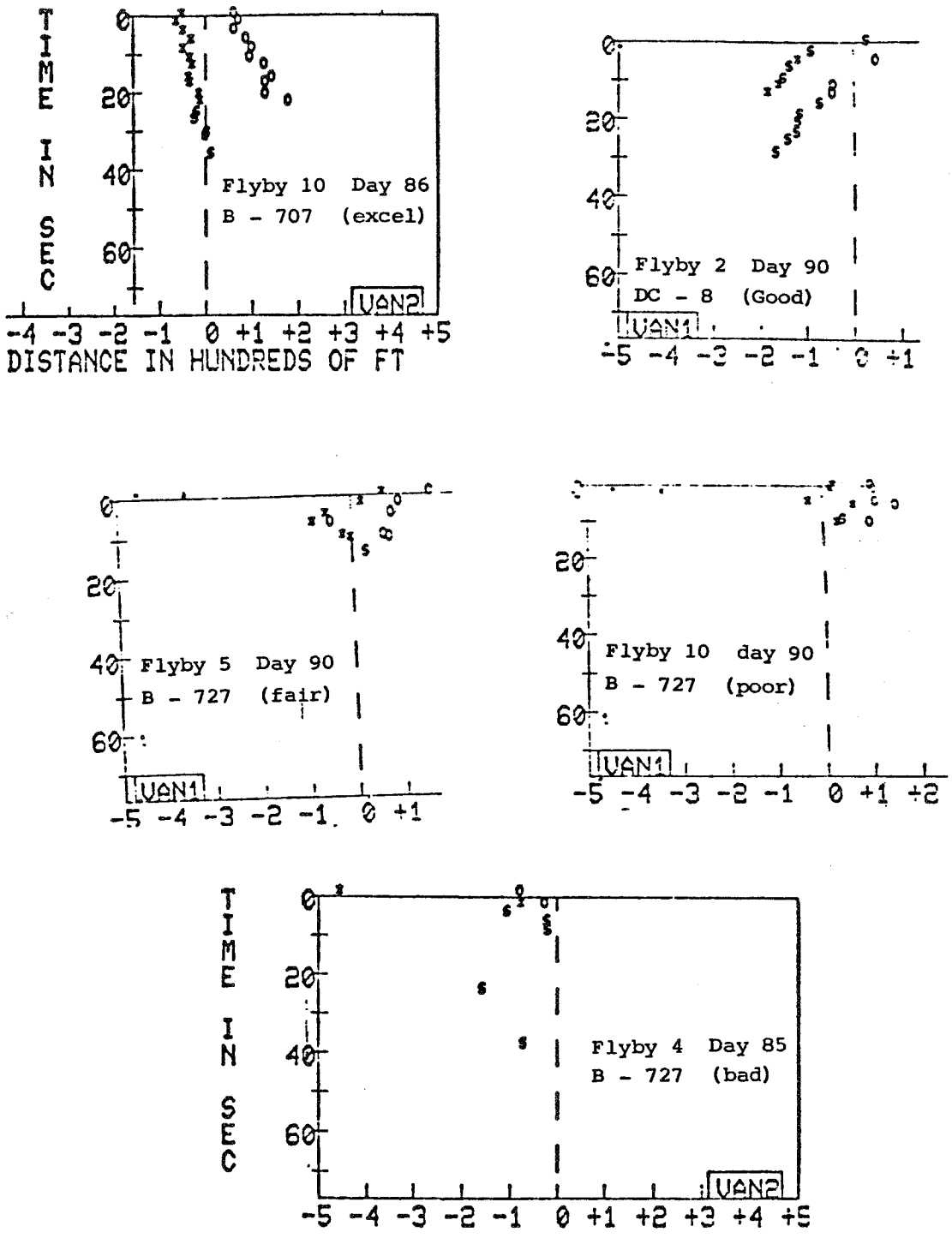

Figure 6-20. Sample data runs indicating data quality.

(RUNWAY 31R, KENNEDY INTERNATIONAL AIRPORT, MARCH THROUGH MAY, 1975)

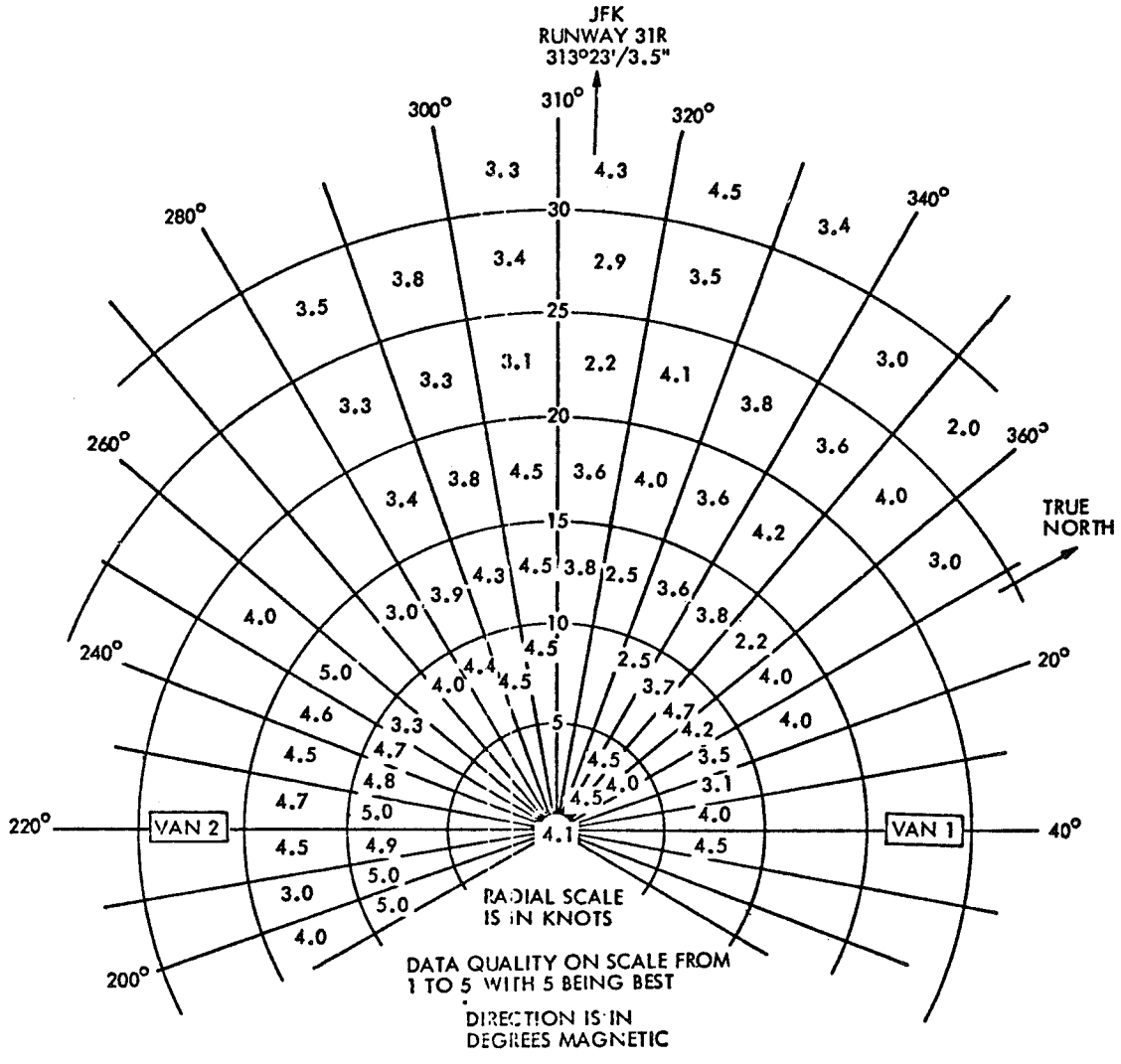

Figure 6-21. Average data quality versus wind speed and direction.

shown as a function of aircraft type in Figure 6-22, where it may be seen that all the aircraft types produced an average data quality of at least three. A more significant display of these data is shown in Figure 6-23 where the percentage of runs producing usable data, i.e., data being evaluated as three or better, are shown. It may be seen that for aircraft as large as or larger than the B-707, greater than 95 percent of all the runs produced usable data and that for all aircraft types an average of 85 percent of the runs produced usable data. Unusable data result primarily from bad operator system setting, high winds and small aircraft.

The average descent rate of vortices as a function of wind speed and direction is shown in Figure 6-24. It may be noted that the descent rate appears to increase with increasing head wind. When the descent rate is plotted as a function of head wind speed, the results in Figure 6-25 are obtained. This shows that the vortices are being blown from the runway toward the system causing the descent rate as a function of head wind speed to be approximately a straight line with a slope corresponding to the 3° glide slope on which the aircraft are descending. For high values of head wind speed, it appears that there is a slight increase in this slope. The descent rate used in these figures is an average overall aircraft types. Table 6-12 shows a breakdown of descent rates by aircraft types and shows an extremely wide variety of descent rates within a given aircraft type. This is probably accounted for by varying aircraft weights, landing speeds, flap settings, and atmospheric wind and stability conditions. When these numbers are averaged, the results shown in Figure 6-26 are obtained.

6.2.3 High Altitude Flyby

High altitude flybys were conducted with a CV-880 aircraft on March 28 and April 10, 1975, at JFK Airport. These flybys produced results showing good vortices may be reliably detected at slant ranges of at least 1500 ft (457 m) and altitudes as high as 900 ft (274 m) and that at higher altitudes two vortices are clearly separable in the scatter plot data. Figure 6-27 gives an intensity scatter plot of a typical high altitude CV-880 flyby for March 28, 1975. The intensity scatter plot format is defined in Section 4.2.2.2. As can be seen from the figure, the system's angular resolution of vortex positions is well defined; whereas, the range position indication is less well defined. The real time vortex location algorithm used in the system was not designed to resolve vortex positions from long range [greater than approximately 1000 ft (300 m)] SLDV operations. The scan frame-by-scan frame analysis of the vortex location algorithm calculations confirms the inadequacy of the algorithm to resolve two vortices consistently with reasonable position coordinates and transport. The system did, however, successfully locate the region in which the vortex pair was located and thus

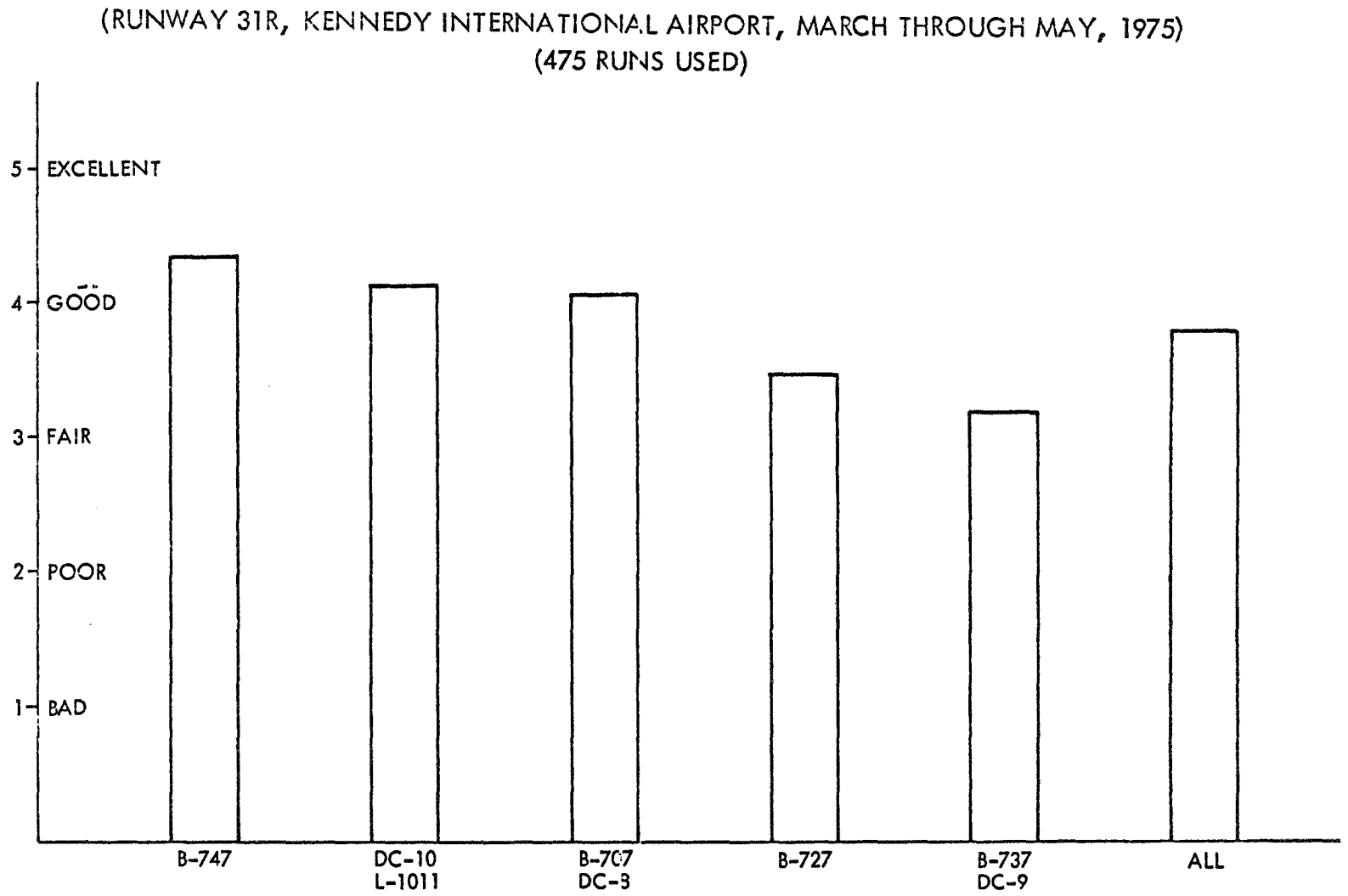

Figure 6-22. Average data quality versus aircraft type.

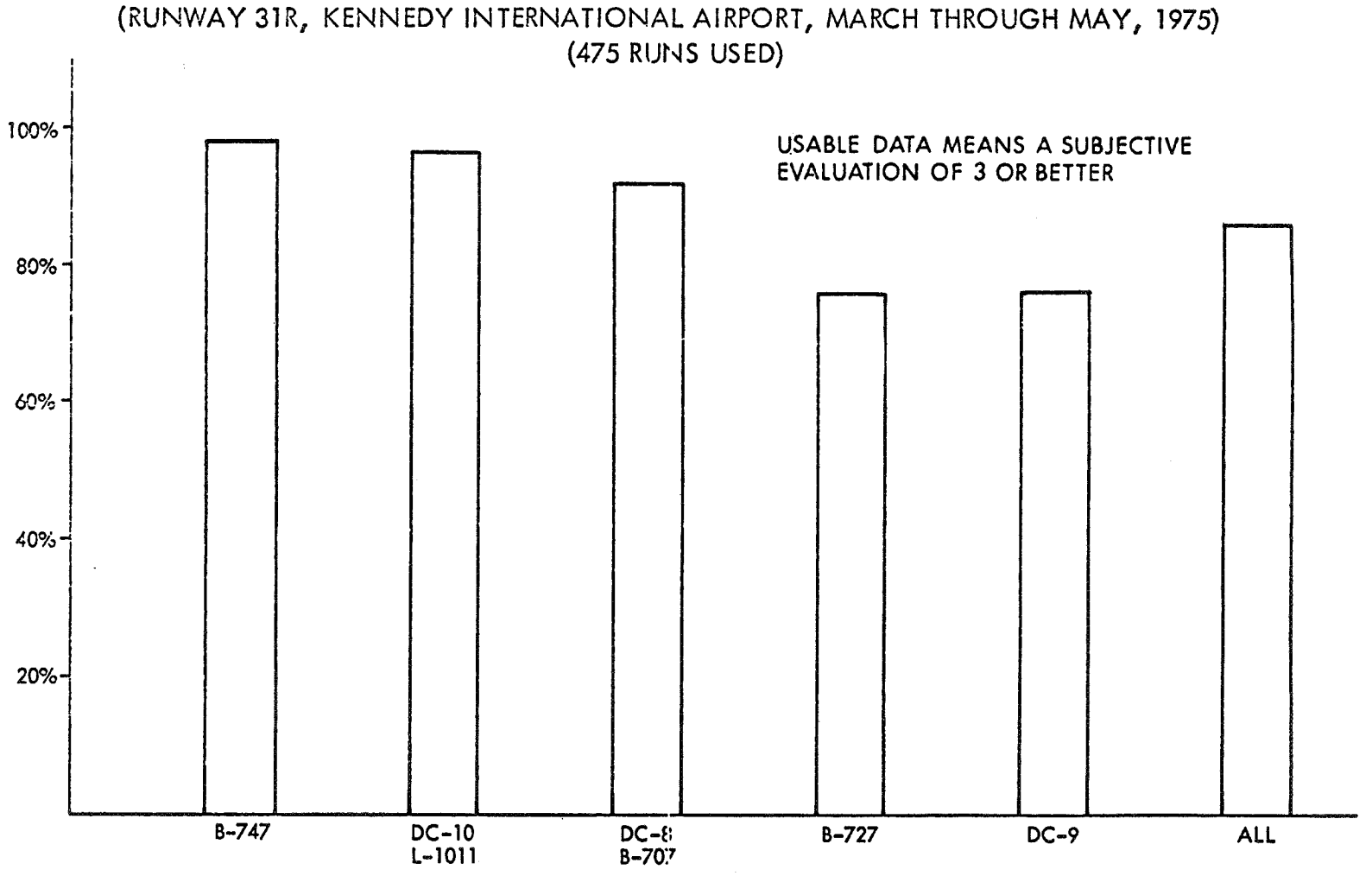

Figure 6-23. Percentage of runs producing usable data versus aircraft.

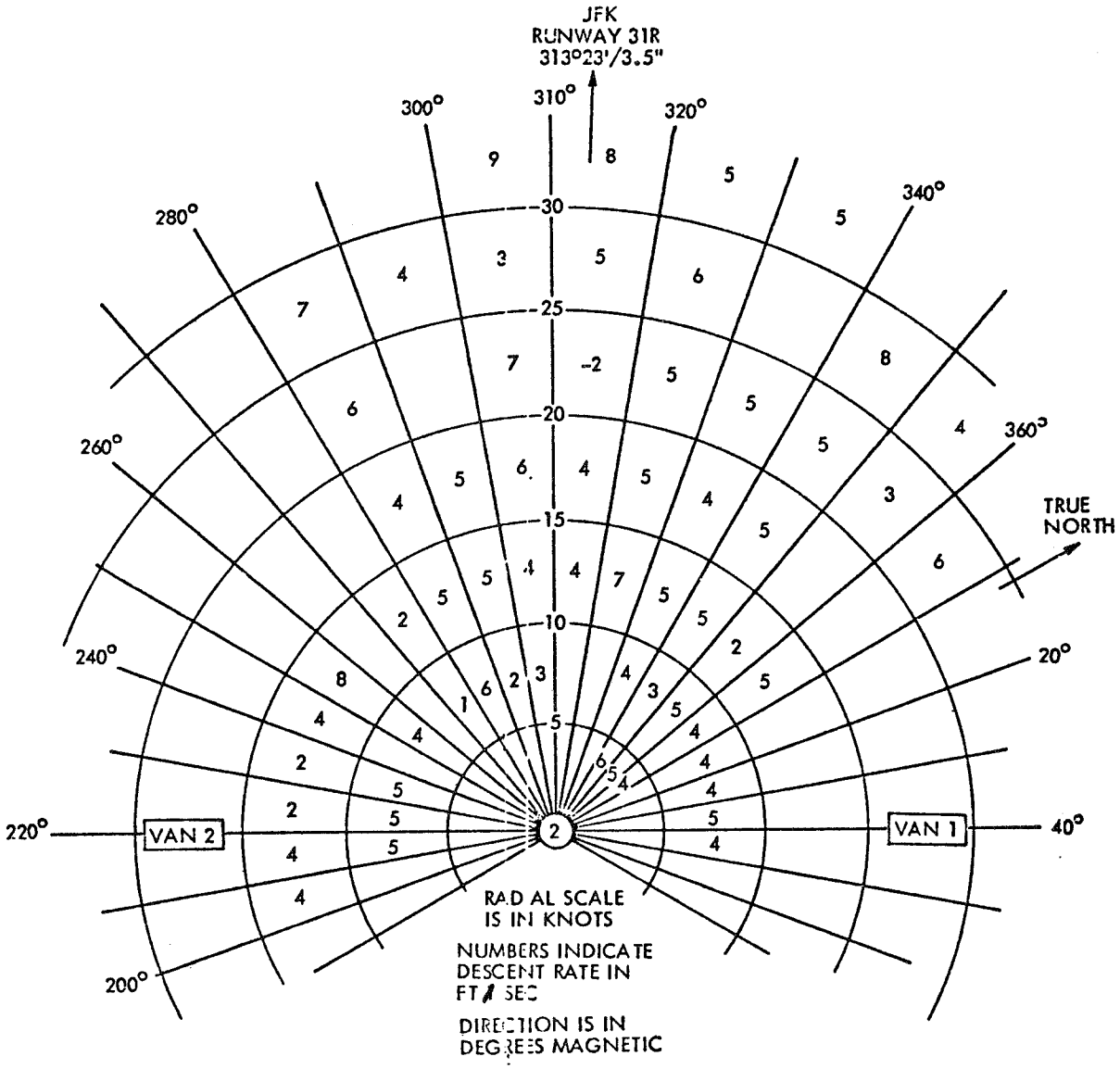

Figure 6-24. Descent rate versus wind speed and direction (all aircraft).

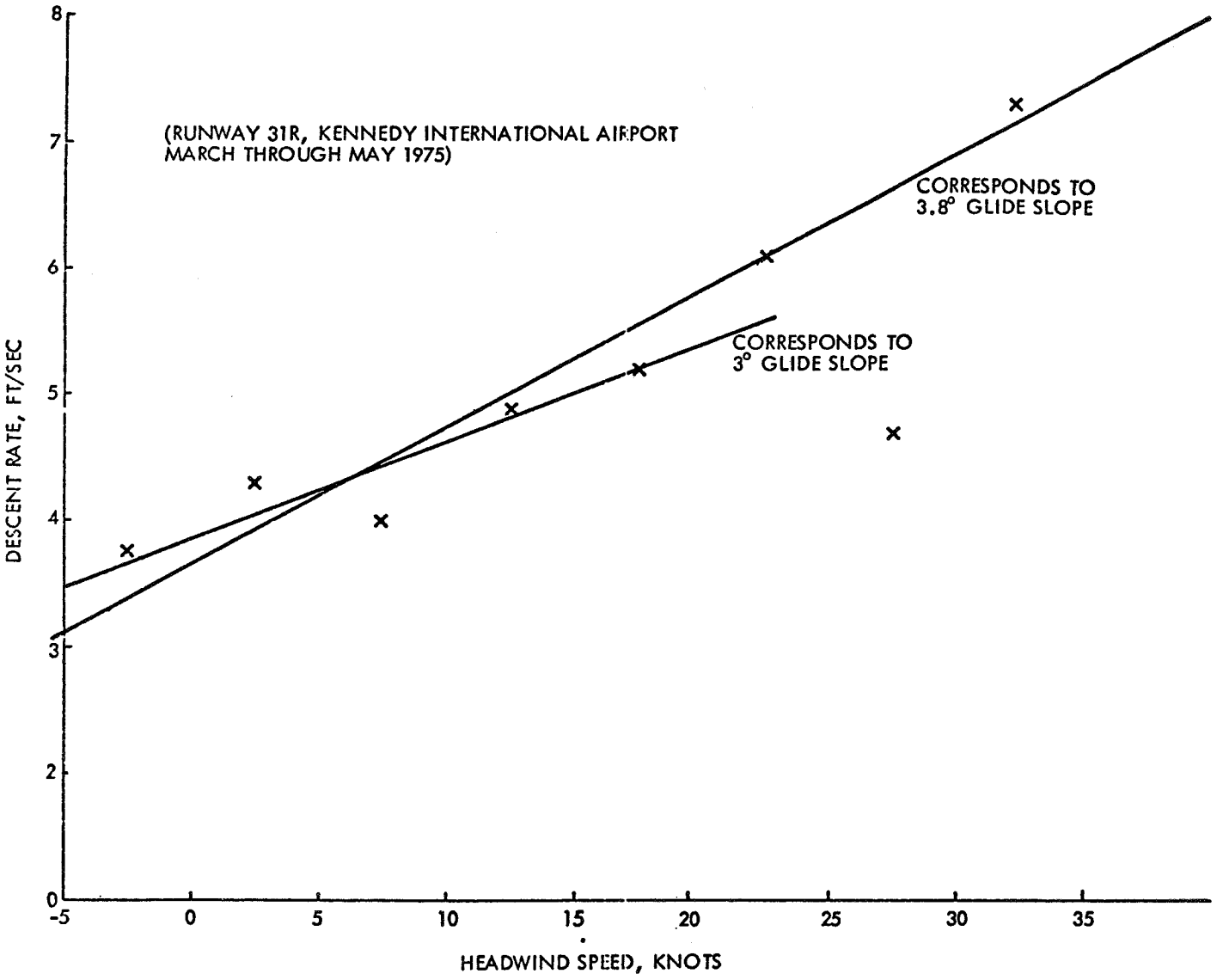

Figure 6-25. Average vortex descent rate versus headwind.

TABLE 6-12. DESCENT RATES OF VARIOUS VORTICES

	Descent Rate, ft/s				
	0 to 2	3 to 5	6 to 8	9 to 11	12 to 14
B-747	9	12	21	3	1
DC-10, L1011	6	9	9	9	
B-707, DC-8	34	76	45	2	
B-727	4	51	43	2	
DC-9, B-737	11	26	14	4	
All	64	174	132	12	1

Note: Numbers indicate number of landings of given aircraft with given descent rate.

made it possible to determine average transport velocities. The descent rates of the vortex pair were typically between 7 and 8 ft/sec (2 and 2.5 m/s), and the horizontal transport velocity was approximately equal to the ambient wind velocity. Also, analysis of the scatter plots indicated a significant size difference between the vortices. This was expected, based on visual observation of the aircraft exhaust during the flight. Vortex location was obtained in a limited number of cases by first looking for relative maxima in V_{pk} as a function of angle and then looking for relative maxima of I_{pk} as a function of range. This made it possible to locate the vortex cores quite accurately in angle and to make it possible to locate the vortex cores quite accurately in angle and to make estimates of the vortex range using the I_{pk} information. It is believed that an algorithm of this type would be suitable for further high altitude data analysis.

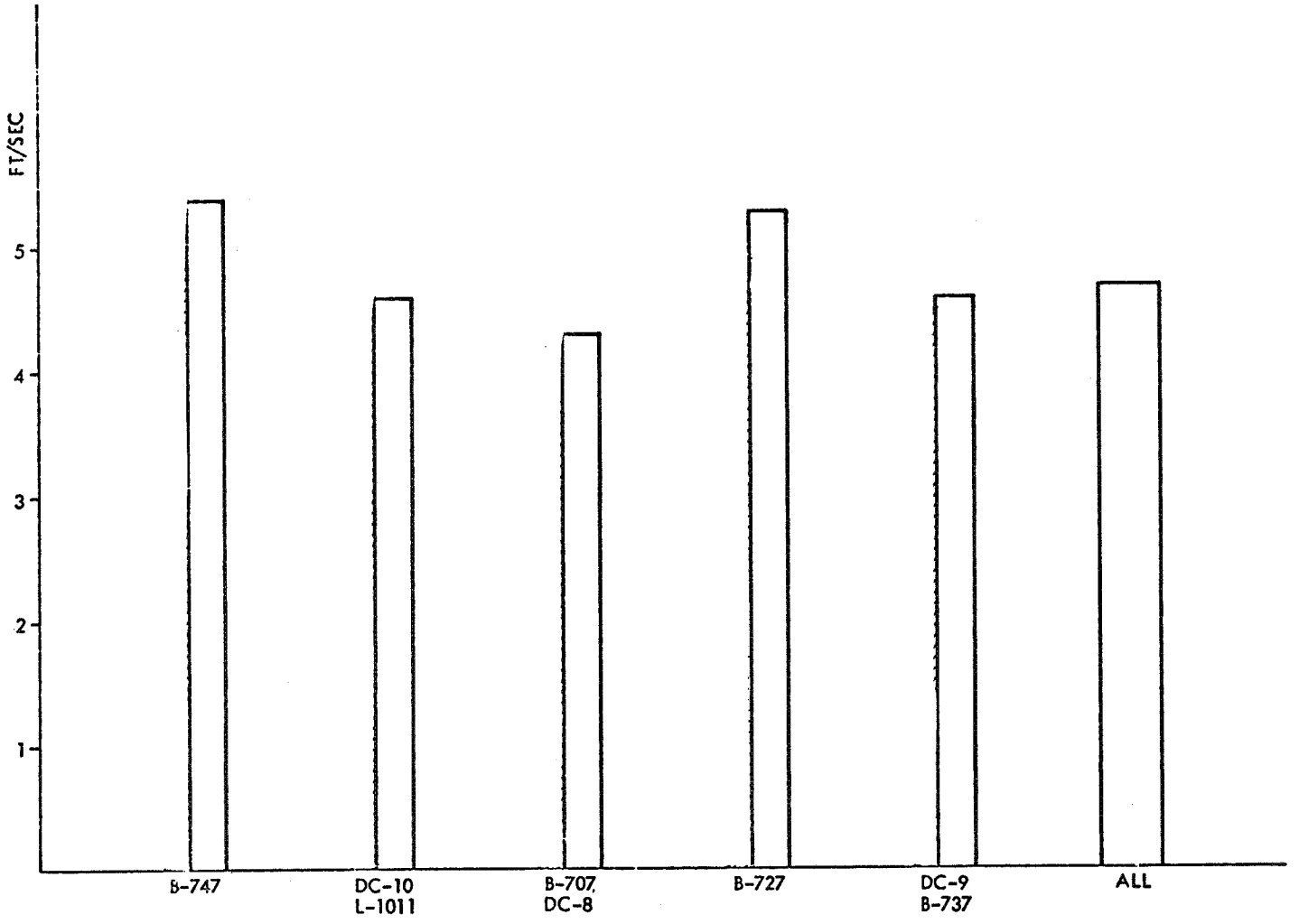

Figure 6-26. Average vortex descent rate.

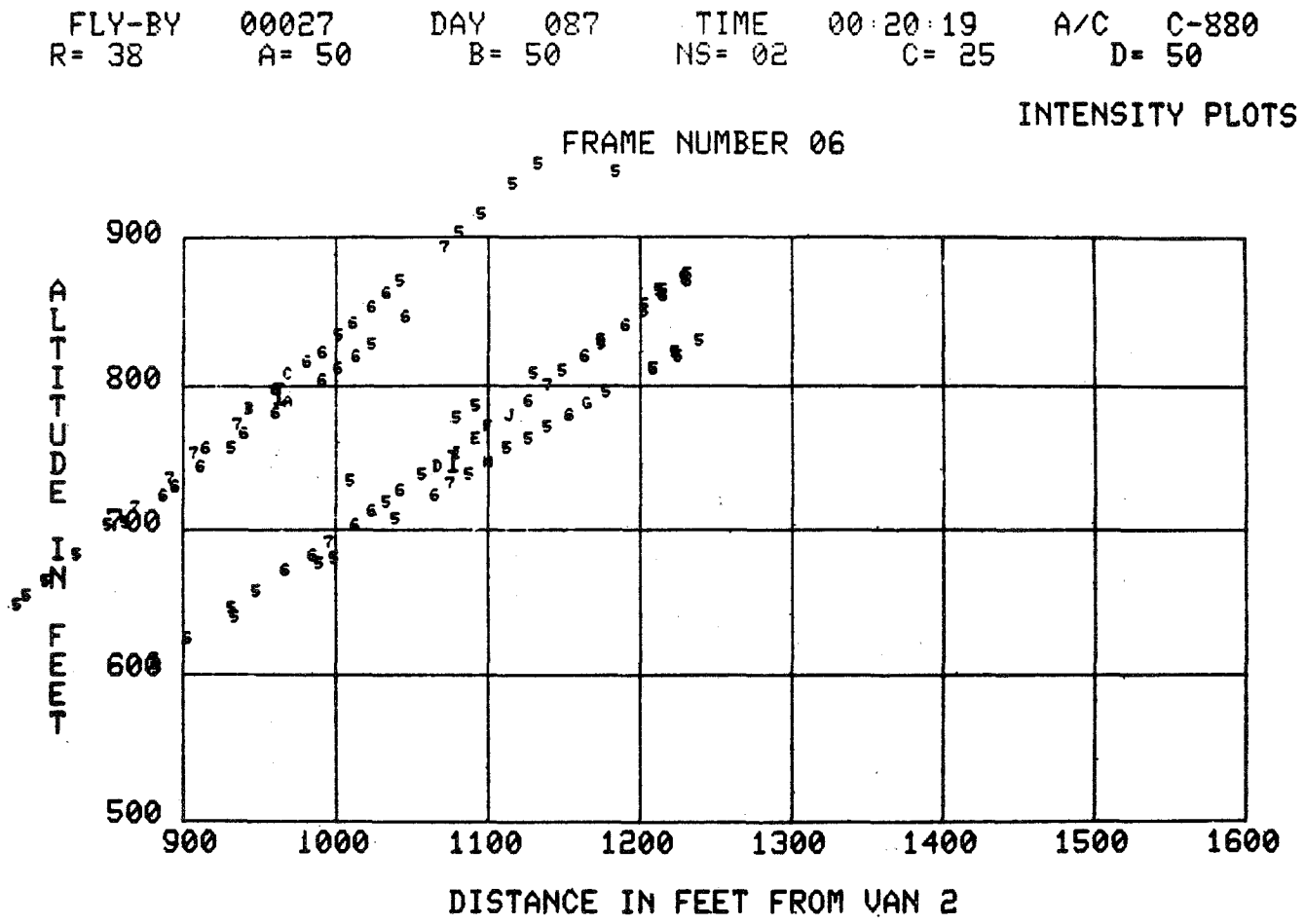

Figure 6-27. Intensity scatter plot for high altitude flyby.

7.0 RECOMMENDATIONS DIRECTED TOWARD MORE OPERATIONAL SLDV SYSTEMS

7.1 Introduction

The current SLDV System emphasizes versatility. There is a broad capability designed into the system because the exact signal characteristics of the vortex and atmosphere were not sufficiently known at the time of system design and development. Use of the system, in an operational mode, at the JFK Airport resulted in a considerable amount of data and operational experience upon which recommendations can be made for system improvement. Some features of the current system can be eliminated thereby reducing size, operating requirements, and cost, making the system more effective for the vortex application. Improvements in the system will be directed toward two types of systems. The first system will be a research oriented system for the purpose of studying the details of vortex transport and flow fields to develop a more complete understanding of vortex behavior. The second system that will be considered is an airport monitor system which could be used to detect and monitor the presence of vortices in the landing corridor. The research instrument would have most of the features of the present system to obtain a maximum of information. The monitoring system could be made considerably smaller, less expensive, and considerably more operational than the present system. A comparison of the two systems is given in Table 7-1.

7.2 Hardware Considerations

7.2.1 Laser

For the research instrument, high signal-to-noise ratios are important and the laser power should not be reduced below its present value. The present value is proven to be sufficient for accurate vortex location and flow field measurements, and a similar laser power and short term stability should be employed in any future design of a research instrument. However, for the monitoring system, the system requirements would be less severe and would make possible the reduction of laser power to approximately 5 W. This reduction of laser power will result in a significant saving in space requirements. The laser, in research and monitoring systems, should have a long lifetime and be relatively maintenance free.

TABLE 7-1. SYSTEM COMPARISON

	Present	Research	Monitoring
Laser	20 W Water Cooled	20 W Water Cooled	Approximately 5 W Air Cooled
Telescope	12 in. (30.48 cm)	12 in. (30.48 cm)	6 in. (19.68 cm)
Interferometer	Modified Mach Zehnder	Same or smaller depending on requirement for translator	Smaller size modified Mach Zehnder
Processor		Reduced functions	Reduced functions. Incorporate mirco-processor
Scanner	Wide range of scan limits and frequencies	4 - 6 preset scan configurations possible	3 present scan configurations
Software	Location algorithm with diagnostic aids	Location algorithm adaptive thresholds, tracking, circulation calculation statistical analysis	Use of microprocessor to aid in tracking, displays
Configuration	2 systems side-looking 400 ft (122 m) from extended centerline	1 system with side-looking and upward looking capability	1 system - upward looking

The present system requires approximately 1 hr of warm-up time before the laser becomes stable. Improvements should be made in the laser for the research and monitoring systems to have the capability of immediate stability when turned on. This can be achieved by laser mode-locking techniques.

7.2.2 Optics

The 12 in. (30.48 cm) optics size for the telescope should be retained for the research system. It may be possible to reduce the optics size for the monitoring system.

The present design of the optical system is basically sound but there are several variations and replacement of components that are suggested for the research and monitoring systems. The output telescope is of a Cassegrainian design which incorporates a secondary mirror in the optical axis of the 6 mm diameter beam. The backscatter along the optical axis is too intense to efficiently use the detector for heterodyne measurements with the translator in the system. One solution to the problem is to use an off-axis parabolic telescope. The present solution to the backscatter problem is to filter the unwanted signal in the early phase of signal amplification.

Most of the optical components in the interferometer are made of Germanium. Since this material does not transmit in the visible, it is not possible to use an auxiliary visible laser to aid in system alignment. There are now available optical components — mirrors, beamsplitters, lenses, etc. — that are excellent 10.6 μ optics and also transmit in the visible. The Germanium transmitting optics should be replaced with zinc selenide (ZeSe) or cadmium sulfide (CdS) optics.

The modified Mach Zehnder interferometer is considered essential to both systems because it minimizes the loss in signal-to-noise ratio in the interferometer. However, since translation of the local oscillator frequency is not a requirement for the monitoring system, a smaller interferometer with less adjustments required could easily be desirable. It may be advisable to use a solid block interferometer design in which adjustments are eliminated completely. The interferometer used in the present system can also be reduced in size to increase the compactness of the system.

7.2.3 Detector

The basic HgCdTe detector has provided acceptable operation during the JFK Airport testing. There are, however, some improvements which would considerably improve the ease of operation and reliability. These improvements would be necessary in a monitoring system but not necessarily in the research system:

a. A self-contained cooling system should be incorporated. This can either be of the thermoelectric cooler type or a mechanical cryorefrigeration unit. This would eliminate the need for constant attention to liquid nitrogen coolant monitoring.

b. A method of automatic self-biasing should be incorporated into the detector-amplifier circuitry, which would automatically optimize the detectors operating point.

7.2.4 Scanner

In either the research or monitoring system, a considerable reduction in versatility of the scanner is possible. The large number of different scan frequencies available on the present scanner could be reduced to approximately three each of typical arc scan and finger scan frequencies. The scan extremes should still be variable but should be set by limits from the computer rather than manual controls in normal operation. This will allow vortex tracking to be performed by the computer.

For the monitoring system, a microcomputer control of the scanning system elements should be incorporated. The utilization of a microprocessor-based control system for an automated remote Laser Doppler Vortex System offers several significant advantages:

a. Overall simplification of hardware required for implementation of multiaxis control system. The simplification is inherent in such a microprocessor system due to the overall lower parts count and commonality of chip types which eases service and troubleshooting. In addition, increased reliability should result due to this simplification and lower power dissipation.

b. Automated operation and the flexibility of scan program changes are other advantages of such a system concept. Programs for fixed scan geometry may be stored in the system, or changes to an automated program may be easily implemented by the operator.

c. Calibration and self-checkout are features which will be necessary for any automated system. These concepts may be easily implemented in a microprocessor-based system and further lend to the high degree of flexibility of such a system.

d. The display of the scanning geometry of the Laser Doppler Vortex System has, in the past, led to somewhat complicated program changes. With a dedicated microcomputer scan controller, such options as display format could be easily accommodated even for a multiaxis system.

The design of future scanning systems should encompass several considerations: (a) reliability, (b) ease of service and troubleshooting, (c) ease of calibration and alignment, (d) flexibility for system changes, and (e) economy.

Several design changes to the existing hardware could more fully meet these design requirements: (a) use of full rotation dc torque motors for scan mirror operation, (b) the use of resolver (with digital conversion) angular sensors with potentiometer backup, and (c) utilization of a suspended, voice coil driven, secondary mirror system with Linear Variable Differential Transformer positioning pickoff.

7.2.5 Signal Processor

The signal processing system, as presently designed, has performed quite well and leaves only slight areas for improvement. Some features of the processor can be eliminated for the specific vortex application. The processor for either system may be simplified by eliminating the density mode, width integration, analog outputs, and the CFAR mode without loss of versatility. The data format to produce the PCM data may be eliminated in the monitor system but should not be eliminated in the research system.

7.2.6 Data Reduction

The current capability of the SLDV System allows a very elaborate and detailed data analysis to be performed from the PCM format data. The digital output of the data algorithm processor utilizing a PDP-1135 reduces the data to the critical velocity spatial and time information. This slow speed digital data can be reduced in a postflight analysis mode with the onsite PDP-11. Several software changes could be incorporated to process the data to obtain particular vortex information that would be required when operating for the research and monitoring systems.

7.3 Software

The software requirements for the research system would be basically the same as those of the present system. Key additions might include adaptive thresholding and tracking. The tracking function would be necessary for a monitoring system and could be accomplished using a least-square-fit to a specified number of previous scans. After 3 or 4 scans through the vortex to establish the location accurately, tracking could begin based on the assumption that the vortex would move in the horizontal and vertical directions with the velocities obtained for the least-square-fit over the previous scans. This would automatically result in an increased data density as the system began to track more and more accurately. Consideration should be given to developing software which would obtain vortex circulation in real time.

8.0 CONCLUSION

The SLDV System, developed by MSFC, was deployed for 6 months of field operations at JFK Airport to detect, track, and measure aircraft wake vortices. The SLDV operated reliably throughout the test period under a variety of adverse environmental conditions including rain, snow, temperature extremes, acoustic vibrations, and high EMI concentrations from airport radars. Of these conditions, temperatures in excess of 90°F had the only significant adverse effect on the operation of the system. This problem can be alleviated to a great extent by increasing the air conditioning available to the electronic hardware.

During the JFK Airport operations, information was collected on more than 1600 aircraft landings. This information was stored on magnetic tape from three different data processing points in the system for analysis. This included velocity and position on the flow field of the entire scan plane, the flow field of the vortex, and the track of the vortex centers. In addition, information on vortex centers was obtained on hard copy and can be found in microfiche form in the appendices of this report.

Analysis of the JFK Airport data indicates that vortex locations to within 10 ft (3 m) were achieved and that vortices were tracked to a range of 1500 ft (457 m) and for a duration in excess of 80 s. Vertical and horizontal transport of the vortices as well as vortex circulation information were also obtained. In addition, the system was also used to successfully calculate vertical and horizontal wind profiles.

Based on the data obtained, the SLDV performed within 3 dB of the theoretical value, fully meeting, and in many cases exceeding, the original objectives of the development program.

The experience and information gained indicate a number of potential improvements in operation and reliability of the system. Implementation of these improvements depends, to a great extent, upon the future application of the system.

9.0 REFERENCES

1. Huffaker, R.; Jeffreys, H.; Weaver, E.; Bilbro, J.; et al.: Development of a Laser Doppler System for the Detection, Tracking, and Measurement of Aircraft Wake Vortices. Final Report, FAA-RD-74-213, March 1975.

2. Bierach, Karl F.: Wake Vortex Sensing, Processing and Display. Journal of the ISA Transactions, vol. 13, no. 2, 1974, p. 149.

3. Verstynen, Harry A., Jr.: NASA Flight Research on Aircraft Wake Vortices and Minimization Concepts. AIAA 6th Aircraft Design, Flight and Operations Meeting, Los Angeles, Calif., Aug. 12, 1974.

4. Harris, C.: Development of Frequency Translator for Use With Laser Doppler System. Final Report, Contract No. NAS8-29706, Equipment Division, Equipment Development Laboratories, Raytheon Company, Sudbury, Massachusetts, Sept. 1974.

5. Edwards, B. and Coffey, E.: Development and Testing of Laser Doppler System Components for Wake Vortex Monitoring, Vol. II, Scanner Operations Manual. Contract NAS8-29824, Huntsville Research and Engineering Center, Lockheed Missiles and Space Company, Inc., Huntsville, Alabama, Aug. 1974.

6. Signal Processing and Display Interface Studies. Final Report, Contract NAS8-29822, Advanced Development Laboratory, Equipment Development Laboratories, Raytheon Company, Wayland, Massachusetts, Sept. 1975.

7. Conway, R.; Matuck, G.; Roe, J.; Taylor, J.; and Turner, A.: Vortex Information Display System (VIDS) Program Description Manual. Final Report, Contract NAS8-31330, M&S Computing, Inc., Huntsville, Alabama, Dec. 1975.

8. Sonnenschein, C.; DiMarzio, C.; Clippinger, D.; and Toomey, D.: Aviation Safety Research and Technology/ Hazard Avoidance and Elimination. Interim Report, Contract NAS8-30795, Advanced Development Laboratory, Equipment Development Laboratories, Raytheon Company, Sudbury, Massachusetts, Nov. 1975.

9. Description Manual for Two-Dimensional Curve Fit and Display Software. M&S Computing, Inc., Report No. 75-0012, Contract No. NAS8-31305, April 1, 1975.

10. Hallock, J.: Wake Vortex Decay Near the Ground. AIAA Paper No. 75-882, AIAA 8th Fluid and Plasma Dynamics Conferences, Hartford, Connecticut, June 1975.

APPROVAL

LASER DOPPLER VELOCIMETER WAKE VORTEX TESTS

By J. W. Bilbro, H. B. Jeffreys, E. A. Weaver, R. M. Huffaker, G. D. Craig, R. W. George, and P. J. Marrero

The information in this report has been reviewed for security classification. The report, in its entirety, has been determined to be unclassified and contains no information concerning the Department of Defense or Atomic Energy Commission programs.

This document has also been reviewed and approved for technical accuracy.

F. W. WAGNON
Acting Chief, Optics Branch

JOSEPH L. RANDALL
Chief, Optical and R. F. Systems Division

F. BROOKS MOORE
Director, Electronics and Control Laboratory

☆U.S. GOVERNMENT PRINTING OFFICE 1976--640-255/292 REGION NO.4